SCIENTIFIC COMMITTEE
NINETEENTH REGULAR SESSION

Koror, Palau
16 – 24 August 2023

Project 90 update: Better data on fish weights and lengths for scientific analyses

WCPFC-SC19-2023/ST-IP-04

1 August 2023

Jed Macdonald[1], Peter Williams[1], Francois Roupsard[1], Caroline Sanchez[1], Lui Bell[1], Shui-Kai Chang[2], Rosanna Bernadette B. Contreras[3], Marc Ghergariu[1], Malo Hosken[1], Simon Hoyle[4], Stephanie Nguyen Cuu[1], Tim Park[1], Joanne Potts[1], Emmanuel Schneiter[1], Simon Nicol[1]

[1] Oceanic Fisheries Programme (OFP), Pacific Community (SPC), Nouméa, New Caledonia
[2] National Sun Yat-sen University, Kaohsiung City, Taiwan
[3] SOCSKSARGEN Federation of Fishing & Allied Industries, Inc.
[4] External Consultant

EXECUTIVE SUMMARY

Project 90 arose from discussions at SC13 around the need for accurate 'conversion factor' (CF) data for target and bycatch fish species captured across the western and central Pacific Ocean (WCPO). The project is now in its fourth year, and in conjunction with CF data collected since 2015 through other sampling programmes, has returned a total of 42,295 CF measurements on skipjack tuna, 31,723 measurements on yellowfin, 7,934 on bigeye, 374,787 on albacore and 3,121 measurements on billfish and bycatch species caught by WCPO tuna fisheries.

While Project 90's original objectives were to design and co-ordinate the systematic collection of representative, high quality length measurements for bycatch species, and length-length (L-L), length-weight (L-W) and weight-weight (W-W) conversion factors for tunas, billfish and bycatch species, the project's scope has since expanded to incorporate analyses of these data, particularly in the context of developing and updating CF relationships for WCPO tuna stock assessments as new data comes to hand. This Information Paper updates SC19 on Project 90 activities undertaken since SC18 and outlines planned actions for 2023-2024.

Efforts to obtain conversion factor data continued across the region and focussed largely on filling the longstanding data gap for the gilled-and-gutted weight (GG) to whole weight (WW) conversion for large bigeye and yellowfin tuna. Our longstanding collaboration with SFFAII and BFAR in General Santos, Philippines, proved crucial in this regard. Through this partnership, we were able to obtain 43 new coupled GG and WW measurements for bigeye and 787 new measurements for yellowfin captured in the Philippines' handline fishery in the 12 months to 28 July 2023, in addition to 112 and 1428 new coupled fork length (UF) and WW measurements on bigeye and yellowfin, respectively, over the same period.

These new data allowed us to update the GG-WW CF relationships for WCPO bigeye and yellowfin for use in the 2023 stock assessments presented in Day et al. (2023) and Magnusson et al. (2023) – the first such update of these relationships since Langley et al. (2006). The new relationships between GG and WW for each species follow power functions of the form $WW = a \times GG^b$ with parameter estimates as follows:

$\text{Bigeye}_{\text{GG-WW}}$ a = 1.1617 (95% CIs: 1.1275, 1.1969); b = 0.9817 (95% CIs: 0.9739, 0.9895)
so, $WW = 1.1617 \times GG^{0.9817}$ (Eq. 1)

$\text{Yellowfin}_{\text{GG-WW}}$ a = 1.1821 (95% CIs: 1.1747, 1.1895); b = 0.9755 (95% CIs: 0.9737, 0.9773)
so, $WW = 1.1821 \times GG^{0.9755}$ (Eq. 2)

The mean predictions from these models were found to be very similar to those derived by Langley et al. (2006).

The length-weight relationships (LWRs) for bigeye and yellowfin were also revised for this year's stock assessments. This analysis made use of all available coupled length and weight measurements from port sampling and observer records across the region, including the updated WW estimates from GG fish derived using Eq. 1 and 2. We created a pipeline in R for data extraction, screening, filtering and modelling of these LWRs that is repeatable and can be applied consistently in future updates as new data comes to hand. The new relationships between UF and WW for each species follow power functions of the form $WW = a \times UF^b$ with parameter estimates as follows:

$\text{Bigeye}_{\text{LWR}}$ a = 3.0634e-05 (95% CIs: 3.0494e-05, 3.0774e-05); b = 2.9324 (95% CIs: 2.9314, 2.9333)
so, $WW = 3.0634\text{e-}05 \times UF^{2.9324}$ (Eq. 3)

$\text{Yellowfin}_{\text{LWR}}$ a = 1.9865e-05 (95% CIs: 1.9775e-05, 1.9955e-05); b = 2.9908 (95% CIs: 2.9898, 2.9917)
so, $WW = 1.9865\text{e-}05 \times UF^{2.9908}$ (Eq. 4)

In a related analysis, we have also completed modelling to explore spatial and temporal variability in bigeye tuna LWRs across the WCPO. This project commenced in 2021 and has involved the compilation and analysis of all coupled bigeye length and weight measurements from SPC port and observer records and Taiwanese observer data holdings through 2021. The final report is available in Appendix 1. Results focus on the

Taiwanese dataset which was used to develop and refine the modelling approach for later application to the combined SPC-Taiwanese dataset.

SPC has recently prepared Letters of Agreement (LOAs) with Samoa, Tonga and Fiji detailing work on biological sample and CF data collection. In relation to Project 90 tasks, these LOAs focus on alternative protocols for collecting much-needed GG and WW measurements from the central Pacific, in addition to boosting numbers of L-L CF measurements.

Work has continued on the electronic monitoring (EM) versus observer length comparison project in French Polynesia, involving SPC, Direction des Resources Maritimes (DRM), The Nature Conservancy (TNC) and Satlink/DOS. Analysis of new data from a full longline trip revealed that length measurements of tunas, billfish and common bycatch species made with EM were consistently lower than length measurement made by the observer for that trip, with larger fish underestimated at a much greater rate by EM than smaller fish. That said, consistent positive relationships between EM and observer lengths were seen for all species, suggesting that simple improvements in length calibration on board and/or corrections during image and statistical analysis could increase the accuracy and reliability of EM length measurements in the near term.

With the return to more normal travel conditions across the region and the resumption of observer deployments, opportunities to collect new length and weight data at sea and in port are now increasing. Project 90 work over the coming 12 months will focus on 1) boosting numbers of CF measurements outside of the Philippines, across the broadest possible spatial area possible; 2) filling key data gaps, such as W-W conversion factors for large bigeye tuna landed at central Pacific ports; and 3) progressing the EM/observer length comparison analysis as data from more longline trips on different vessels filter in. This workplan will be implemented through a variety of initiatives as detailed in this paper.

We invite SC19 to:

1. review and comment on the progress made on Project 90 activities at this stage;
2. note that Project 90 has been selected for inclusion in the *Online Discussion Forum* at SC19, and SPC looks to that forum to table and define the priority activities proposed in this paper; and
3. consider Project 90 as an ongoing project of the WCPFC, with indicative 2024 and 2025 budgets of USD 20,000 per annum to cover ongoing and new work focussing on alternative approaches for collecting coupled GG and WW measurements and L-L CF data on longline-caught yellowfin and bigeye in the central Pacific.

1. BACKGROUND

WCPFC Project 90 developed from discussions at SC13 in 2017 regarding regional estimates of purse seine and longline bycatch (Peatman et al. 2017; 2018a,b), and the need for accurate 'conversion factor' (CF) data for targeted and bycatch species.

Following these discussions, SC13 recommended that the WCPFC Scientific Services Provider (SPC) be tasked with:

a) designing and co-ordinating the systematic collection of representative length measurements for bycatch species; and
b) designing and co-ordinating the systematic collection of length-length (L-L), length-weight (L-W) and weight-weight (W-W) CF data on all species.

These recommendations have shaped the evolution of tasks undertaken within Project 90 since its commencement in 2019 (see Williams and Smith 2018; SPC-OFP 2019; Macdonald et al. 2020, 2021, 2022) for details and annual updates to the SC). That said, the project's scope has now expanded to incorporate analyses and modelling of the length and weight data where needed, particularly for the purposes of updating key CF relationships for WCPO tuna stock assessments, as documented below in this Information Paper.

Project 90 was not discussed substantively at SC16, SC17 or SC18, due to these meetings being held online as a result of COVID-19 related travel restrictions. However, we note that Project 90 was included in the *Online Discussion Forum* at all three meetings, and is again slated for inclusion at SC19. We look to this forum as a useful platform for commentary on this Information Paper which provides an update on Project 90 activities in the 12 months since SC18, and outlines planned activities for the coming year.

2. PROJECT 90 WORK TO DATE

2.1 Overview - in brief

The work conducted in Project 90 to date has included:

i) The establishment, refinement and regular updating of the CF database and associated tables, and the incorporation of new CFs as they are developed and/or published.
ii) Scoping and gap analysis to determine the priority areas for collecting CF data under Project 90.
iii) Engagement with CCMs regarding data requirements for generating accurate CFs.
iv) Development and refinement of a web-based tool for accessing SPC's CF database, available with login at: www.spc.int/ofp/preview/login.php?redirect=species_conv_factor.php or through the Tufman2 database portal accessible here.
v) Initiation and continuation of port sampling activities in the Philippines from 2019 onwards targeted towards the systematic collection of L-L, L-W and W-W CF data, biological samples and tag recovery information for key tuna species under *Activity 3.2*, Table A1 in Macdonald et al. (2021). These data have contributed importantly to the CF database for tropical tunas (i.e. skipjack, yellowfin, bigeye), augmenting other CF data collected across the region (including for albacore) (see Tables 1, 2, and 3).
vi) Purchase of a 'WPL Industries' motion-compensated scales to augment collection of gilled-and-gutted (GG) to whole weight (WW) CF data across the region.
vii) Establishment of a dialogue with the Solomon Islands Ministry of Fisheries and Marine Resources (MFMR) and the Solomon Islands National Observers programme (SBOB) in response to a June 2021 request to SPC regarding alternative employment opportunities for Solomon Islands' observers unable to work due to COVID-19 related travel restrictions.
viii) Development of a sampling plan to address the request outlined in **vii)**. The draft plan was circulated in 2021 and adapted to include onboard-observer and port-based collection of GG-WW CF data and other biological samples for yellowfin and bigeye tuna in the Solomon Islands. This plan has since been parked, as an analysis of recent catch composition revealed that Solomons purse seiners were not capturing the size classes relevant to the current GG-WW data gap in the numbers required.

ix) Preparation, in early 2023, of Letters of Agreement (LOA) with Samoa, Fiji and Tonga regarding the pursuit of alternative approaches for collecting coupled GG and WW measurements and L-L CF data on longline-caught yellowfin and bigeye in the central Pacific.

x) An update of **a.** the GG-WW CF relationships and **b.** the LWRs (i.e., UF-WW relationships) for WCPO bigeye and yellowfin for input into the 2023 stock assessment models. We created a pipeline in R for data extraction, screening, filtering and modelling of these LWRs that is repeatable and can be applied consistently in future updates as new data comes to hand.

xi) Creation of processes and R code for the exchange of length and weight data with WCPFC members and other international fisheries agencies through LOA, noting also the recent establishment of the WCPFC public domain size data (https://www.wcpfc.int/public-size-data).

xii) Commencement in 2022 and completion in 2023 of modelling to explore spatial and temporal variability in the bigeye tuna LWR across the WCPO using Taiwanese observer data.

xiii) Commencement in 2022 and continuation in 2023 of a comparative study of length measurements recorded by EM, onboard observers and port samplers for tunas and billfish captured by longliners in French Polynesia.

xiv) Efforts to improve links between the data collected as part of Project 90 and other SPC-OFP projects (i.e. Project 35b, Project 42, Ecosystem and Climate Indicators).

2.2 Progress since SC18 - in detail

i) - iv) Following the major updates made to SPC's CF database entries during 2020 and 2021, work related to points **i) - iv)** over the past 12 months has focused on acquiring new data to improve existing CFs and developing training materials to enhance biological sampling skills and the accuracy of length and weight measurements taken by observers at sea and samplers in port.

Recent additions of CF data for tropical tunas have come primarily from the ongoing collaboration with SOCSKSARGEN Federation of Fishing & Allied Industries (SFFAII) and the Bureau of Fisheries and Aquatic Resources ministry (BFAR) in General Santos, Philippines [discussed further under point **v)** below].

Training material released over the past year and relevant to Project 90 tasks includes a revised biological sampling manual entitled 'Biological Sampling Manual – Guide for samplers at sea and at port' (Sanchez et al. 2023) (available here) and a series of 19 training videos (available on SPC's YouTube channel here). Together, these materials demonstrate techniques for best-practice biological sampling and collection of length and weight data on tunas, mahi mahi, wahoo and billfish. The materials are designed for scientists, observers, fisheries officers, fishing captains, crew and port samplers, and as teaching tools for high school and university students.

V) Port sampling activities continue in partnership with SFFAII and BFAR in the Philippines. Through the contributions of L-W, L-L and W-W measurements at General Santos Port in addition to other CF data collected across the region, as at 28 July 2023, we have now amassed 42,295 CF measurements on skipjack, 31,723 measurements on yellowfin, 7,934 on bigeye, 374,787 on albacore (all L-W measurements, coming mostly from Fiji) and 3,121 measurements on other bycatch species over the past nine years (see Tables 1-3 for breakdowns by CF type).

The opportunity to obtain L-L and L-W CFs on very small tunas (< 25 cm fork length) captured by the small-scale purse seine and ringnet fisheries, and W-W CFs from large, handline-caught yellowfin and bigeye landed fresh and whole in port, is unique to the Philippines, highlighting the importance of this continued collaboration.

The recent signing of a 4-year preferred supplier agreement with SFFAII that allows some year-to-year flexibility in project deliverables is an important step in ensuring that port sampling efforts in General Santos can be adapted to collect the most relevant CF data (under Project 90), biological samples (under Project 35b) and tag recovery information (under Project 42) needed for each tuna stock assessment.

Table 1. Numbers of individual tuna length-length (L-L) CF measurements collected between 2019 and 2023, by species.

Number of L-L CF measurements					
Year	Skipjack	Yellowfin	Bigeye	Albacore	Others
2019	4	17	0	0	0
2020	0	2,192	431	0	0
2021	0	2,362	267	0	0
2022	0	2,101	136	0	0
2023	0	341	49	0	0

Notes
1. Where length is upper jaw to caudal fork (UF) and other CF length measurements have been taken.
2. Source: Port sampling.

Table 2. Numbers of individual tuna length-weight (L-W) CF measurements collected between 2015 and 2023, by species.

Number of L-W CF measurements					
Year	Skipjack	Yellowfin	Bigeye	Albacore	Others
2015	44	5	10	27,678	158
2016	1,754	50	2	56,914	113
2017	5,379	5,750	4,976	48,333	55
2018	864	8	0	17,042	50
2019	3,593	317	50	78,735	1,003
2020	13,241	6,811	780	45,556	1,015
2021	10,571	4,621	598	55,570	325
2022	6,079	4,104	416	34,622	312
2023	762	639	94	10,337	90

Notes
1. Where length is upper jaw to caudal fork (UF) and weight is whole weight only (WW).
2. Source: Port sampling.
3. Port sampling under Project 90 has allowed the sampling of very small tunas (< 25 cm UF) previously unavailable.

Table 3. Numbers of individual fish weight-weight (W-W) CF measurements collected between 2019 and 2023, by species.

Number of W-W CF measurements					
Year	Skipjack	Yellowfin	Bigeye	Albacore	Others
2019	4	17	0	0	0
2020	0	20	0	0	0
2021	0	840	54	0	0
2022	0	1,406	65	0	0
2023	0	122	6	0	0

Notes
1. Where weight is whole weight (WW) and other CF processed weights have been taken.
2. Source: Port sampling.

vi) In 2021 SPC purchased a set of 'WPL Industries' motion-compensated scales as part of a plan to facilitate the at-sea collection of accurate W-W CF data for tunas and bycatch species across the region. This plan addressed work scheduled under *Activity 3.2 iv)* in the 2020-2021 work plan (see Table A1 in Macdonald et al. 2021 for details). The scales arrived in Nouméa in late 2021, but were not calibrated correctly, and were subsequently sent back to the manufacturer for re-calibration in 2022. Despite being re-calibrated and returned to Nouméa, substantial issues remain in terms of setup and operation that have precluded field

testing. Therefore, a decision was made in early 2023 to return this scale to WPL Industries and we are currently exploring options for a replacement scale from another supplier.

vii-viii) In response to a June 2021 enquiry from the Solomon Islands MFMR and SBOB regarding the possibility of alternative work opportunities for Solomon Island fisheries observers, SPC drafted a sampling plan for at-sea and in-port collection of W-W CF measurements on yellowfin and bigeye. An analysis conducted last year (see Figure 1 in Macdonald et al. 2022) showed that sufficient yellowfin and bigeye in the 80+ cm UF range are sometimes available in the domestic purse seine catches to justify rollout of the plan. However, a reanalysis of recent catch composition conducted in early 2023 revealed that Solomons purse seiners were not capturing the size classes needed to fill the longstanding GG-WW data gap for bigeye in the numbers or with the regularity required to pursue the sampling plan at this stage. Opportunities may still exist to collect relevant data onboard longline vessels, but this is contingent upon the availability of a functioning motion-compensating scale. As outlined in **vi)**, we are still pursuing these opportunities.

ix) The recently prepared LOAs with Samoa, Fiji and Tonga are exciting in that they provide an alternative pathway towards filling the GG-WW CF data gap for large, longline-caught bigeye from the central Pacific, augmenting data already collected from the Philippines' handline fishery. Under these LOAs, observers placed on longline and/or purse seine vessels operating out of Samoa, Fiji and Tonga are asked, for each captured bigeye > 70 cm UF, to:

<u>On board</u>

- Measure the fish's length. Record three length measurements (i.e., UF, US - upper jaw to 2nd dorsal fin, and PS - anterior base of pectoral fin to 2nd dorsal to the nearest lowest cm) on the 'GEN-4' form.
- Remove the gills and guts.
- Place gills and guts inside a sealable plastic bag with a unique label number, and store under the same conditions as the fish is stored (e.g., blast frozen, on ice).
- Place a cable-tie coded with the same label number through the jaw of the fish.
- Record the label numbers on the GEN-4 form. This allows association of the bagged gills and guts with the relevant fish at port.

<u>At port</u>

- If fish are brought to port GG and frozen:
    1) record the weight of the frozen gills and guts (to nearest 0.01 kg),
    2) record the weight of the frozen GG fish from which they came (to nearest 0.01 kg) identified by the same label number.
- If fish are brought to port whole and fresh:
    1) record fresh WW weight (to nearest 0.01 kg),
    2) remove gills and guts and record fresh GG weight (to nearest 0.01 kg),
    3) measure the fresh weight of the gills and guts (to nearest 0.01 kg),
    4) freeze these,
    5) measure frozen weight of the gills and guts (to nearest 0.01 kg).
- If fish are brought to port whole and frozen:
    1) record frozen WW weight (to nearest 0.01 kg),
    2) remove gills and guts and record frozen GG weight (to nearest 0.01 kg) (noting that this may be logistically challenging in some instances).
- Note down any special comments in the 'COMMENTS' section on the 'GEN-4' form.

The LOAs encourage collection of these measurements for as many bigeye as possible without setting strict targets for numbers. If this protocol proves workable during trials in Samoa, Fiji and Tonga later in 2023, roll out to other member countries and territories is envisaged into 2024.

x_a.) ***Update of the GG-WW CF for WCPO yellowfin and bigeye***

The new CF data sourced from the Philippines' port sampling collaboration over the past four years provided an opportunity to update of the GG-WW CF for bigeye and yellowfin for the 2023 stock assessments. This is the first update of these relationships since Langley et al. (2006). Fully annotated R code is available here that

sets out the analytical pipeline used for data extraction, filtering and modelling and allows for reproduction of the analysis. We summarise the steps taken below.

Data extraction, checking and filtering

Available coupled GG and WW records for bigeye and yellowfin were extracted from SPC's Tufman2 database and were compiled, checked and filtered. For bigeye, n = 125, and for yellowfin, n = 2431. We used exploratory plots to visualise trends in the data for each species and to check for outliers. We identified any extreme weight records – i.e., those outside the realm of biological plausibility – and made the GG weight for these records = NA. We then fit an exploratory linear model of WW ~ GG for each species, and searched for remaining outliers by i) using the 'simulateResiduals' function in the 'DHARMa' R package (Hartig 2022) that creates quantile (i.e. scaled) residuals by simulating from the fitted model in combination with the 'testOutliers' function which tests if the number of observations outside the simulation envelope is larger or smaller than expected; and ii) identifying records with absolute standardised residual values > 3. All flagged values from i) and ii) were considered potential outliers and investigated further.

Based on these checks, no outliers were present in the bigeye dataset, and 16 outliers were identified in the yellowfin dataset. Each yellowfin outlier was confirmed to be a recording error made either at port, or during copying onto the datasheets sent to SPC. We wanted to make use of these records if possible, rather than removing them from the analysis. As the datasets contained information on each fish's 'OC' weight (i.e., weight of gills and guts only), we were able to subtract the OC weight from WW to obtain an estimate of the GG weight. We could use this approach for identified outliers (above) and for the fish with GG weights that we coded as NA, but first we checked if this introduced any bias across the distribution of weights for each species.

Plots of WW against OC weight show a consistent increase in OC weight with WW, and a large spread of possible OC weights for a given WW – this spread increasing with WW for yellowfin (Figure 1). These plots indicate that OC weight for bigeye and yellowfin is generally measured and recorded accurately at General Santos Port.

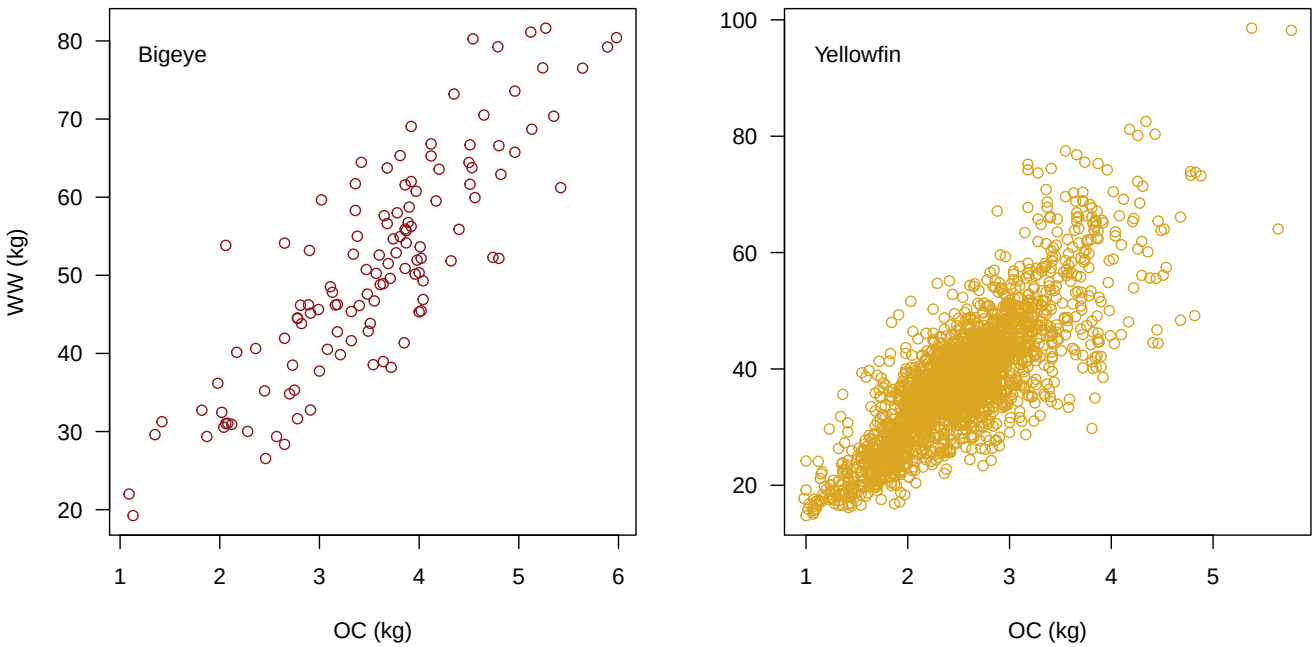

Figure 1. Plots of whole weight (WW) against the weight of the gills and guts (OC) for bigeye and yellowfin measured at General Santos Port between 2019 and 2023.

We next subtracted the OC weight from WW for each fish (hereafter WW-OC) and checked for any bias across the weight distribution by plotting the GG weight against WW-OC by species, using only records for which we have complete WW, GG and OC weight data (Figure 2).

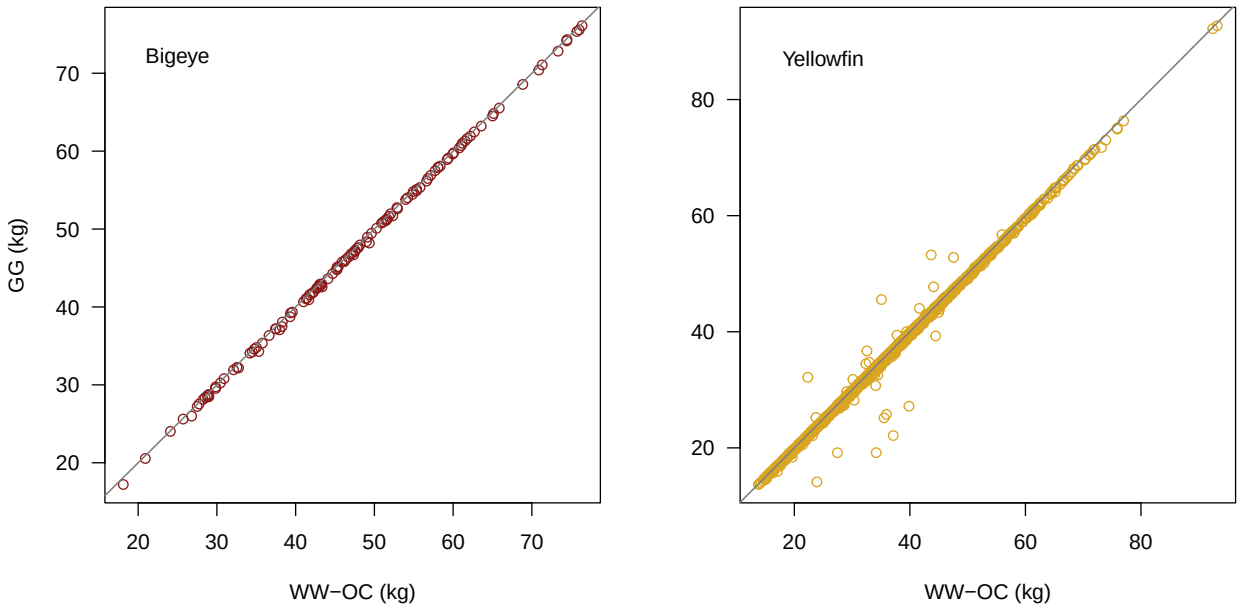

Figure 2. Plots of gilled and gutted weight (GG) against the whole weight minus the weight of the gills and guts (WW-OC) for bigeye and yellowfin measured at General Santos Port between 2019 and 2023. The grey line on each panel is the 1:1 line.

No bias was detected for bigeye, but we see a slight tendency for the WW-OC values to overestimate GG weight compared with measured GG weight in the largest yellowfin (Figure 2, right panel). This underestimation lessens in smaller individuals - individuals that fall within the weight range of the outliers identified earlier. Hence, we felt confident in taking the WW-OC weight as the estimated GG weight for identified outliers and for fish with GG weights we had coded as NA.

Modelling

With these data filtering steps complete, we then searched for plausible models for the GG-WW CF for each species. Our exploratory plots showed that the relationships between GG weight and WW were approximately linear for both species. However, in light of Langley et al.'s results and previous work (Anon. 2001) that indicated that a size specific conversion factor may be more appropriate, we explored both linear models of the form $WW = a + b \times GG$ and non-linear power models of the form $WW = a \times GG^b$ for each species, where a and b are parameters to be estimated. Standard visual checks were used to assess model adequacy, including plots of standardised and quantile residuals against the fitted values and GG weights. We extracted the model parameter estimates and their 95% confidence intervals (CIs) and generated predicted values of WW from each model across the full range of GG weights together with 95% CIs and 95% prediction intervals (PIs) around the mean prediction. We bias-corrected the mean prediction of the power models on the original scale, assuming normal errors. Lastly, we compared the fits of the linear and power models by calculating the R^2 of the predicted versus the observed values on the original scale. All models were fitted using the 'lm' function in the 'stats' package, with quantile residuals generated in the 'DHARMa' package in R version 4.2.3 (R Core Team 2023).

For bigeye, both the linear and power models fitted the data well with close agreement between observed and predicted values (power model R^2 = 0.99818, linear model R^2 = 0.99816). No evidence of model misspecification was found for either model; however, some minor deviations from uniformity were detected in the quantile residuals for the linear model that were absent for the power model. For this reason, the power model was preferred for the updated bigeye GG-WW CF for 2023 which has the following parameter estimates:

$\text{Bigeye}_{\text{GG-WW}}$ a = 1.1617 (95% CIs: 1.1275, 1.1969); b = 0.9817 (95% CIs: 0.9739, 0.9895)
so, $WW = 1.1617 \times GG^{0.9817}$ (Eq. 1)

This model was very similar to the GG-WW CF relationship derived by Langley et al. (2006) for bigeye which was used to convert GG weight to WW in the 2020 bigeye assessment (Figure 3).

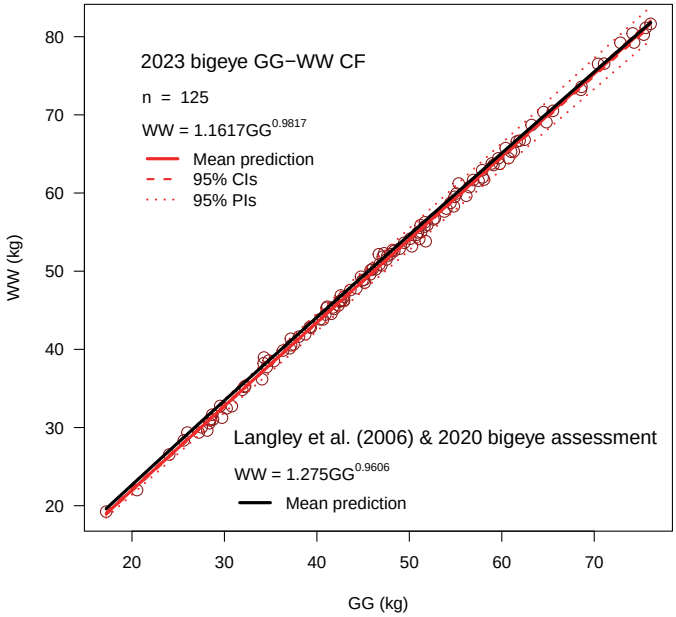

Figure 3. Updated GG-WW CF for bigeye for the 2023 stock assessment, comparing the mean prediction of the 2023 model (red lines) to the Langley et al. (2006) model (black line) which was used in the 2020 assessment. Red circles are the 125 coupled GG and WW measurements used to fit the 2023 model.

For yellowfin, again both the linear and power models fitted the data well (power model $R^2 = 0.99816$, linear model $R^2 = 0.99814$). The quantile residuals for both models showed some minor deviations from uniformity likely driven by small number of data points that fell outside the range of simulated values. These data points were checked and deemed to represent plausible weight measurements, so were retained in the models. As residual deviations for the power model were less pronounced than the linear model, the power model was preferred for the updated yellowfin GG-WW CF for 2023 which has the following parameter estimates:

$\text{Yellowfin}_{\text{GG-WW}}$ $a = 1.1821$ (95% CIs: 1.1747, 1.1895); $b = 0.9755$ (95% CIs: 0.9737, 0.9773)
so, $WW = 1.1821 \times GG^{0.9755}$ (Eq. 2)

This model for yellowfin was very similar to that derived by Langley et al. (2006) for yellowfin which was used to convert GG weight to WW in the 2020 yellowfin assessment (Figure 4).

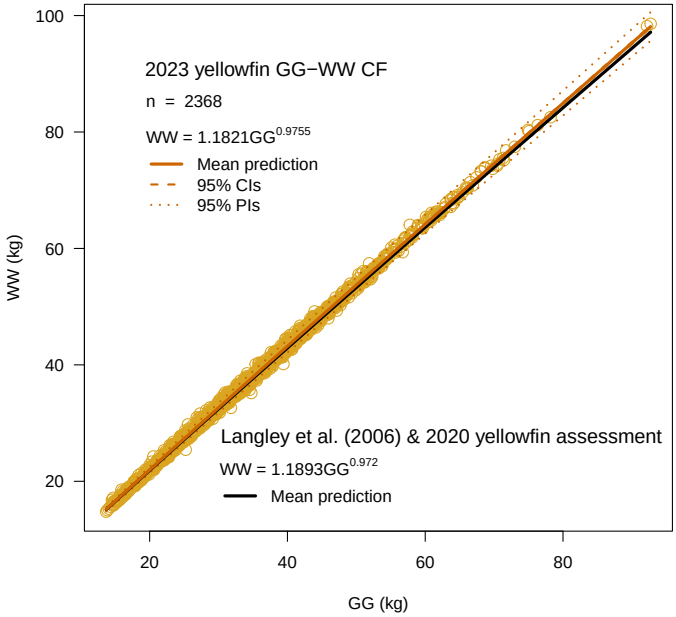

Figure 4. Updated GG-WW CF for yellowfin for the 2023 stock assessment, comparing the mean prediction of the 2023 model (gold lines) to the Langley et al. (2006) model (black line) which was used in the 2020 assessment. Gold circles are the 2368 coupled GG and WW measurements used to fit the 2023 model.

x_b.) *Update of the LWRs for WCPO yellowfin and bigeye*

The LWRs for bigeye and yellowfin were also revised for this year's stock assessments. This analysis made use of all available coupled length and weight measurements from port sampling and observer records across the region, including the updated WW estimates from GG fish derived using Eq. 1 and 2. Fully annotated R code is available here that sets out the analytical pipeline used for data extraction, filtering and modelling and allows reproduction of the analysis. We summarise the key steps below.

Data extraction, checking and filtering

We expand on the analysis conducted for the 2020 assessments by using data from five sources:

1. bio_LW: BioDaSys is our biological sampling database. This houses L-W records taken from individual fish sampled by either observers or port samplers, for which other biological material (e.g., otoliths, gonads, liver, dorsal spine, stomachs) was also collected. (Drawn from the 'BioDaSys' database)
2. obsv_LW: Includes L-W records from individual fish measured by at-sea observers on longline vessels. (Drawn from the 'OBSV_MASTER' database)
3. port1_LW: Includes L-W records for fish measured at port prior to 2015. (Drawn from the 'FISH_MASTER_WORK' database)
4. port2_LW: As for 3, but includes L-W records for fish measured at port after 2015. (Drawn from the 'Tufman2' database)
5. SFFAII_LW: Port sampling L-W records from handline and purse-seine caught bigeye and yellowfin landed whole in General Santos Port, collected from 2019 onwards. (Drawn from the 'Tufman2' database)

Weights recorded for many individual fish in these datasets were processed weights (i.e., weight codes: GG, GX, GT, GH, GO – see Macdonald et al. 2020 Table A4 for code definitions) rather than WW, and we converted these to WW using the preferred species-specific CF equations available from the CF database housed within the Tufman2 database. For converting GG weights to WW, we made use of the updated GG-WW CFs in Eq. 1 and 2.

Focussing on each of the five datasets separately, we followed a similar approach to the identification and treatments of outliers as used for the GG-WW CF update, with some modifications. First, we split each dataset by species and then removed extreme outliers – i.e., those clearly outside the realm of biological plausibility. Second, we fitted an exploratory power model of the form $WW = a \times UF^b$ to the data and then predicted the mean WW-at-UF from this model across the full range of UF in that dataset. Third, we applied a filtering step to define weight outliers as any value more than 70% heavier or 70% lighter than the predicted mean WW at UF. These values likely arise from recording errors made at port or in the SPC databases and were removed as they are not deemed biologically plausible. Fourth, we refit the power model and flagged remaining outliers by i) using the DHARMa 'simulateResiduals' and 'testOutliers' functions, and ii) identifying records with absolute standardised residual values > 3. All flagged values from i) and ii) were considered potential outliers and investigated further. Decisions on whether to keep or exclude these records were based on the balance of biological reasoning and the sensitivity of the final model parameter estimates to inclusion or exclusion.

Modelling

Following these filtering steps, we next fitted species-specific models to each dataset separately, and finally, an overall model for each species fitted to all five datasets combined. For each of these models, residual checks, extraction of parameter estimates and generation of predictions followed the same procedures outlined in the GG-WW CF update. All models were fitted using the 'lm' function in the 'stats' package, with quantile residuals generated in the 'DHARMa' package.

For bigeye, models for the different datasets had similar mean predictions of WW-at-UF, though the range of observed UF values and the spread of the observed WW values at a given length varied markedly across datasets (Figure 5). The overall model was based on a total of 1,358,097 records sourced from across the five datasets. Plots of quantile residuals indicated an adequate fit to the data with no systematic deviations from uniformity. The model exhibited strong predictive performance, with good agreement found between observed and predicted values ($R^2 = 0.9567$), and has the following parameter estimates:

Bigeye $_{LWR}$ a = 3.0634e-05 (95% CIs: 3.0494e-05, 3.0774e-05); b = 2.9324 (95% CIs: 2.9314, 2.9333)
so, $WW = 3.0634e\text{-}05 \times UF^{2.9324}$ (Eq. 3)

The mean predicted WW-at-UF from the 2023 model for bigeye aligned closely with the mean curve used in the 2020 assessment for fish up to ~150 cm UF but predicted heavier WW-at-UF for fish larger than this (Figure 5).

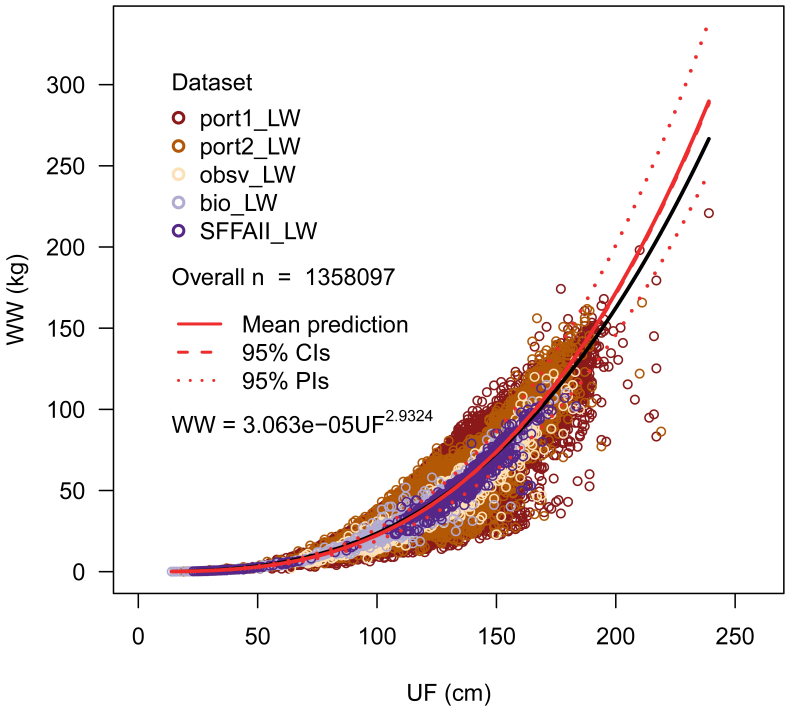

Figure 5. Overall LWR for WCPO bigeye updated for the 2023 stock assessment. Different colour circles represent coupled UF and WW measurements from the five different datasets used to fit the model. Red lines are predictions from the 2023 model; the black line is the mean prediction from the model used in the 2020 bigeye assessment, given by $WW = 6.48e\text{-}05 \times UF^{2.781}$ (Vincent et al. 2020).

For yellowfin, like bigeye, we again see differences among datasets in the range of UF values represented and the spread of the observed WW values at a given length (Figure 6). The total number of records in the overall model for yellowfin exceeded 1.5 million, a number dominated by port sampled measurements from the port1_LW and port2_LW datasets. The quantile residual plots revealed no evidence of model misspecification, though there were a small number of data points that fell outside the range of simulated values. These data were checked, considered to represent plausible weight measurements, and retained in the model. Strong agreement was found between observed WW and those predicted from the model (R^2 = 0.9387). The 2023 LWR for yellowfin has following parameter estimates:

Yellowfin $_{LWR}$ a = 1.9865e-05 (95% CIs: 1.9775e-05, 1.9955e-05); b = 2.9908 (95% CIs: 2.9898, 2.9917)
so, $WW = 1.9865e\text{-}05 \times UF^{2.9908}$ (Eq. 4)

The mean predicted WW-at-UF from the 2023 model for yellowfin aligned closely with the mean curve used in the 2020 assessment throughout the full UF range (Figure 6).

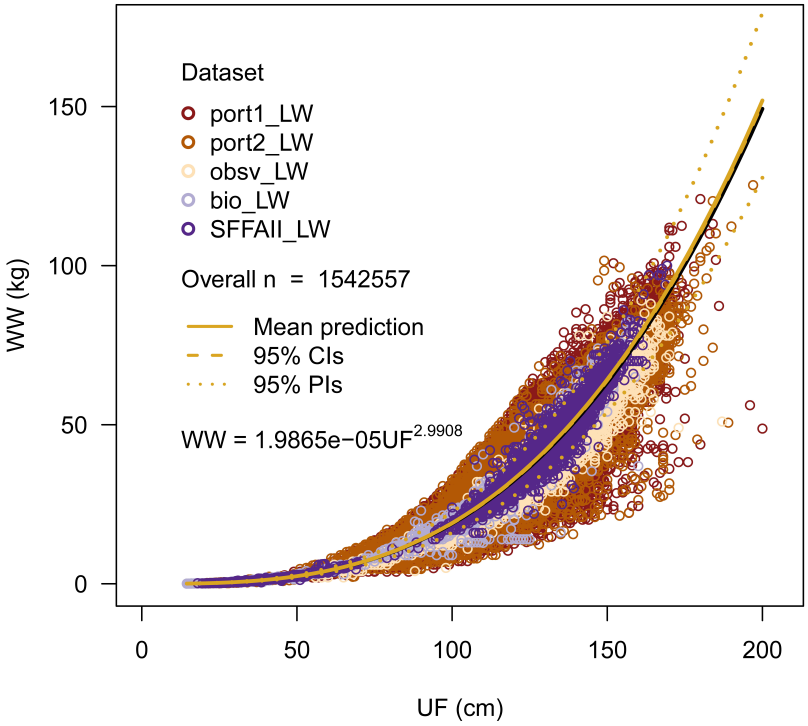

Figure 6. Overall LWR for WCPO yellowfin updated for the 2023 stock assessment. Different colour circles represent coupled UF and WW measurements from the five different datasets used to fit the model. Gold lines are predictions from the 2023 model; the black line is the mean prediction from the model used in the 2020 yellowfin assessment, given by WW = 2.01e-05× $UF^{2.986}$ (Vincent et al. 2020).

xi-xii) In January 2021, SPC and colleagues at the National Sun Yat-sen University, Taiwan (NSYSU) entered into an agreement regarding an exchange of bigeye length and weight measurements covering all SPC and Taiwanese data holdings across the WCPO through to 2021, and the subsequent collaboration on the statistical analyses of these data (see Macdonald et al. 2021 for details). A primary objective of this work was to explore spatial and temporal variability in bigeye tuna growth parameters across the WCPO, thereby addressing a key recommendation of the 2020 bigeye tuna stock assessment (Ducharme-Barth et al. 2020).

The data were successfully compiled and partly exchanged under a LOA arrangement between SPC and NSYSU in early 2021, with preliminary modelling results presented by Eric Chang at the 2021 Pre-Assessment Workshop (PAW). Following this, SPC released a 'Request for Quotation' for services to build on the initial modelling work, specifically with regard to improving our understanding of data reliability and how biological factors, the environment, the sampling location, year, season, and vessel- and gear-related effects can influence relationships between bigeye length and weight across the region. A contract was successfully awarded, and the modelling exercise completed in May 2023, with a presentation of the key results given by Simon Hoyle at this year's PAW. The analysis focussed on the Taiwanese dataset with the view to develop and refine the modelling approach for later application to the combined SPC-Taiwanese dataset. A full report detailing the methods used and results is available in Appendix 1. In brief, a series of generalised additive models (GAMs) were fitted to the bigeye length and weight data, which exposed considerable variation in the bigeye LWR associated with location and season. The results highlight the importance of considering factors such as the lack of independence of individuals captured in the same set, rounding issues, and observer and gear effects when estimating LWRs, as well as exploring different error distributions. The report concludes with a useful set of recommendations that will help guide model development for the combined SPC-Taiwanese datasets - work tabled for the 2023-2024 reporting period.

xiii) Progress continues on the EM versus observer length comparison project in French Polynesia. Building on the first results presented in Macdonald et al. (2022), we recently analysed new data from a full longline trip comprising length measurements made on individual fish by EM and an onboard observer for all 16 sets. For this trip, a total of 385 albacore, bigeye and yellowfin were measured (see Figure 7), together with lower numbers of billfish and common bycatch species.

Our analysis revealed that length measurements of individual tunas (and billfish and common bycatch species – results not shown) collected by EM were consistently lower than the length measurement made by the observer for that trip (Figure 7). Larger fish were underestimated at a much greater rate by EM than smaller fish across all species. That said, consistent positive relationships between EM and observer lengths were evident for all species, suggesting that easily implemented improvements in length calibration on board and/or corrections during image and statistical analysis could increase the accuracy and reliability of EM length measurements in the near term. Indeed, length data collected using the EM digital tool in past projects (e.g., in the Marshall Islands) was shown to be accurate, so we do have confidence that EM systems have the capacity collect reliable length data. As new data continues to roll in, our analysis is expanding to test for any vessel, set, observer and EM analyst-level effects on the nature of the relationships between EM and observer length measurements.

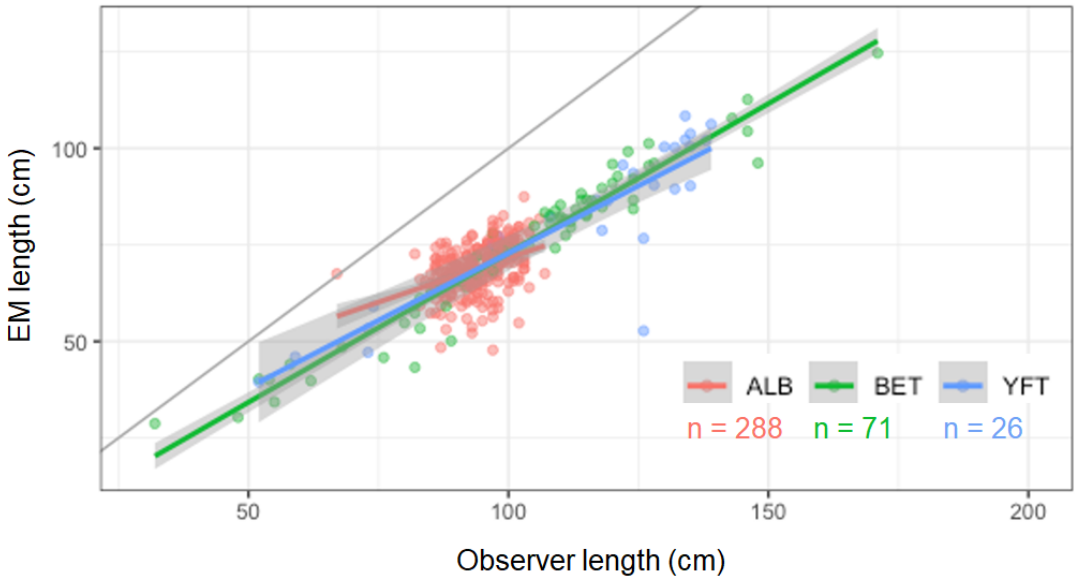

Figure 7. Comparison of EM versus observer length measurements. Data points represent coupled EM and observer length measurements made on the same fish, colour coded by species. Length measurements made by the EM digital measuring tool are on the y-axis, and physical length measurements made by observers are on the x-axis, with the 1:1 line shown in grey. Thick lines and grey shading are mean predictions from linear models and 95% CIs, respectively, colour coded by species.

xiv) Over the past 12 months, we have continued to forge stronger links between Project 90 and a range of SPC-OFP projects. These include:

- **a.** the work undertaken as part of the EM length measurement comparison, outlined in **xiii)** above;
- **b.** ongoing work on developing candidate ecosystem and climate indicators for the WCPO (SPC-OFP 2021, 2022a, 2023a);
- **c.** biological data and sample collection for the WCPFC Pacific Marine Specimen Bank (PMSB) conducted as part of WCPFC Project 35b (SPC-OFP 2022b, 2023b);
- **d.** tag recovery activities undertaken as part of WCPFC Project 42 (SPC-OFP 2022c, 2023c); and
- **e.** publication of the revised biological sampling manual entitled 'Biological Sampling Manual – Guide for samplers at sea and at port' (Sanchez et al. 2023) (available here) and a series of 19 biological sampling and data collection training videos (available here).

3. SUMMARY AND WORK PLAN FOR 2023-2024

Whilst solid progress has been made in relation to Project 90 work over the past 12 months, SPC notes that:

1. The updating and enhancement of the CF database is an ongoing priority.
2. Efforts to collect high-priority GG-WW CF data on bigeye will continue across the region through new initiatives in Samoa, Fiji and Tonga, and the continuation of the port sampling programme in General Santos under the new 2023 SFFAII contract.
3. Application of the modelling framework established for bigeye length and weight on the Taiwanese data (see Appendix 1) to the combined SPC-Taiwanese datasets is a priority item.
4. Analyses for the EM length comparison study in French Polynesia continues as new data come to hand.
5. The importance of accurate CF data was highlighted during discussions at the 2022 FAO Coordinating Working Party on Fisheries Statistics (CWP), and a suggestion was put forward of developing some global CF data standards. Work conducted to date within Project 90 for WCPO species was mentioned, and the other tuna RFMOs (particularly IOTC) were interested and had in fact started to undertake some similar work.
6. Developing a web-based tool for plotting CF relationships for selected species that links to SPC's CF database and is accessible on the WCPFC web site is an ongoing work item for 2023-2024.
7. That with the return to more normal travel conditions across the region and the resumption of the observer deployments, opportunities to collect new length and weight data at sea and in port are now increasing. Project 90 work over the coming 12 months will focus on boosting numbers of CF measurements outside of the Philippines, across the broadest possible spatial area possible, and filling key data gaps, such as W-W conversion factors for large bigeye tuna landed at central Pacific ports.

4. RECOMMENDATIONS

We invite SC19 to:

1. review and comment on the progress made on Project 90 activities at this stage;
2. note that Project 90 has been selected for inclusion in the *Online Discussion Forum* at SC19, and SPC looks to that forum to table and define the priority activities proposed in this paper; and
3. consider Project 90 as an ongoing project of the WCPFC, with indicative 2024 and 2025 budgets of USD 20,000 per annum to cover ongoing and new work focussing on alternative approaches for collecting coupled GG and WW measurements and L-L CF data on longline-caught yellowfin and bigeye in the central Pacific.

5. ACKNOWLEDGEMENTS

We thank Joanna Mae E. Padua (SOCSKSARGEN Federation of Fishing & Allied Industries, Inc.) for her ongoing interest and support for this work. Thank you also to the data entry team in SPC, Nouméa, for their continued tireless efforts on compiling and quality checking the data feeding into SPC's conversion factor database.

6. REFERENCES

Anon. 2001. Report of the Fourteenth Meeting of the Standing Committee on Tuna and Billfish (SCTB14). Noumea, New Caledonia, 9-16 August 2001.

Day, J. et al. 2023. Stock assessment of bigeye tuna in the western and central Pacific Ocean. SC19/SA-WP-05. Nineteenth Regular Session of the Scientific Committee of the Western and Central Pacific Fisheries Commission Koror, Palau, 16-24 August 2023.

Ducharme-Barth, N., Vincent, M., Hampton, J., Hamer, P., Williams, P. and Pilling, G. 2020. Stock assessment of bigeye tuna in the western and central Pacific Ocean. SC16/SA-WP-03. Sixteenth Regular Session of the Scientific Committee of the Western and Central Pacific Fisheries Commission. Online meeting, 11-20 August 2020.

Hartig, F. 2022. DHARMa: Residual Diagnostics for Hierarchical (Multi-Level / Mixed) Regression Models. R package version 0.4.5. https://CRAN.R-project.org/package=DHARMa

Langley, A. Okamoto, H., Williams, P., Miyabe, N. and Bigelow, K. 2006. A summary of the data available for the estimation of conversion factors (processed to whole fish weights) for yellowfin and bigeye tuna. SC2/ME-IP-3. Second Regular Session of the Scientific Committee of the Western and Central Pacific Fisheries Commission. Manila, Philippines, 7-18 August 2006.

Macdonald, J., Williams, P., Sanchez, C., Schneiter, E., Ghergariu, M., Hosken, M., Panizza, A. and Park, T. 2020. Project 90 update: Better data on fish weights and lengths for scientific analyses. SC16/ST-IP-06. Sixteenth Regular Session of the Scientific Committee of the Western and Central Pacific Fisheries Commission. Online meeting, 11-20 August 2020.

Macdonald, J., Williams, P., Sanchez, C., Schneiter, E., Prasad, S., Ghergariu, M., Hosken, M., Panizza, A., Park, T., Chang, S.K. and Nicol, S. 2021. Project 90 update: Better data on fish weights and lengths for scientific analyses. SC17/ST-IP-05. Seventeenth Regular Session of the Scientific Committee of the Western and Central Pacific Fisheries Commission. Online meeting, 11-19 August 2021.

Macdonald, J., Williams, P., Sanchez, C., Schneiter, E., Prasad, S., Ghergariu, M., Hosken, M., Panizza, A., Park, T., Guillou, A. and Nicol, S. 2022. Project 90 update: Better data on fish weights and lengths for scientific analyses. SC18/ST-IP-04. Eighteenth Regular Session of the Scientific Committee of the Western and Central Pacific Fisheries Commission. Online meeting, 10-18 August 2022.

Magnusson, A. et al. 2023. Stock assessment of yellowfin tuna in the western and central Pacific Ocean. SC19/SA-WP-04. Nineteenth Regular Session of the Scientific Committee of the Western and Central Pacific Fisheries Commission Koror, Palau, 16-24 August 2023

Peatman, T., Allain, V., Caillot, S., Williams, P. and Smith, N. 2017. Summary of purse seine fishery bycatch at a regional scale, 2003-2016. SC13/ST-WP-05. Thirteenth Regular Session of the Scientific Committee of the Western and Central Pacific Fisheries Commission. Rarotonga, Cook Islands, 9-17 August 2017.

Peatman, T., Allain, V., Caillot, S., Park, T., Williams, P., Tuiloma, I., Panizza, A., Fukofuka, S. and Smith, N. 2018a. Summary of purse seine fishery bycatch at a regional scale, 2003-2017. SC13/ST-IP-04. Fourteenth regular session of the Scientific Committee of the Western and Central Pacific Fisheries Commission. Busan, Republic of Korea, 8-16 August 2018.

Peatman, T., Bell, L., Allain, V., Caillot, S., Williams, P., Tuiloma, I., Panizza, A., Tremblay-Boyer, L., Fukofuka, S. and Smith, N. 2018b. Summary of longline fishery bycatch at a regional scale, 2003-2017. SC13/ST-WP-02. Fourteenth regular session of the Scientific Committee of the Western and Central Pacific Fisheries Commission. Busan, Republic of Korea, 8-16 August 2018.

R Core Team 2023. R: A language and environment for statistical computing. R Foundation for Statistical Computing, Vienna, Austria. URL https://www.R-project.org/.

Sanchez, C., Anderson, G. and Macdonald, J.I. 2023. Biological Sampling Manual – Guide for samplers at sea and at port. Technical report, SPC, Nouméa, New Caledonia.

SPC-OFP 2019. Project 90 update: Better data on fish weights and lengths for scientific analyses. SC15/ST-WP-03. Fifteenth Regular Session of the Scientific Committee of the Western and Central Pacific Fisheries Commission. Pohnpei, Federated States of Micronesia, 12-20 August 2019.

SPC-OFP 2021. WCPO ecosystem and climate indicators from 2000 to 2020. SC17/EB-IP-09. Seventeenth Regular Session of the Scientific Committee of the Western and Central Pacific Fisheries Commission. Online meeting, 11-19 August 2021.

SPC-OFP 2022a. Ecosystem and climate indicators. SC18/EB-WP-01. Eighteenth Regular Session of the Scientific Committee of the Western and Central Pacific Fisheries Commission. Online meeting, 10-18 August 2022.

SPC-OFP 2022b. Project 35b: WCPFC Pacific Marine Specimen Bank. SC18/RP-P35b-01. Eighteenth Regular Session of the Scientific Committee of the Western and Central Pacific Fisheries Commission. Online meeting, 10-18 August 2022.

SPC-OFP 2022c. Project 42: Pacific Tuna Tagging Project report and work-plan for 2022-2025. SC18/RP-PTTP-01. Eighteenth Regular Session of the Scientific Committee of the Western and Central Pacific Fisheries Commission. Online meeting, 10-18 August 2022.

SPC-OFP 2023a. Ecosystem and climate indicators. SC19/EB-WP-01. Nineteenth Regular Session of the Scientific Committee of the Western and Central Pacific Fisheries Commission Koror, Palau, 16-24 August 2023.

SPC-OFP 2023b. Project 35b: WCPFC Pacific Marine Specimen Bank. SC19/RP-P35b-01. Nineteenth Regular Session of the Scientific Committee of the Western and Central Pacific Fisheries Commission Koror, Palau, 16-24 August 2023.

SPC-OFP 2023c. Project 42: Pacific Tuna Tagging Project report and work-plan for 2023-2026. SC19/RP-PTTP-01. Nineteenth Regular Session of the Scientific Committee of the Western and Central Pacific Fisheries Commission Koror, Palau, 16-24 August 2023.

Vincent, M. Ducharme-Barth, N. and Hamer, P. 2020. Background analyses for the 2020 stock assessments of bigeye and yellowfin tuna. SC16/SA-IP-06. SC16/ST-IP-06. Sixteenth Regular Session of the Scientific Committee of the Western and Central Pacific Fisheries Commission. Online meeting, 11-20 August 2020.

Williams, P.G. and Smith, N. 2018. Requirements for enhancing conversion factor information. SC14/ST-IP-05. Fourteenth Regular Session of the Scientific Committee of the Western and Central Pacific Fisheries Commission. Busan, Republic of Korea, 8-16 August 2018.

Appendix 1: Length-weight relationships for bigeye tuna based on Taiwanese observer data

Simon Hoyle, Shui-Kai Chang, Jed Macdonald

Introduction

Length-weight relationships (LWRs) are an important aspect of the study of tuna population biology and dynamics. The relationship between fish length and weight, also known as the weight-length relationship or the length-mass relationship, is a feature of a species' biology and life history (Finucci et al., 2019), associated with aspects such as the fish's shape, shape changes during growth, sexual dimorphism, and variation associated with food supply, energy balance, and the allocation of resources to reproduction (Froese, 2006; Fulton, 1904). Weight at length may also be related to competition, disease, and individual quality. Variation among individuals in the length-weight relationship can also be termed fish condition (Heincke, 1908).

Biology issues for Pacific bigeye tuna.

Length-weight relationships have a direct role in stock assessment. For example, bigeye stock assessments (Ducharme-Barth et al., 2020; Xu et al., 2020) implemented using the modeling platforms Stock Synthesis (Methot Jr and Wetzel, 2013) and Multifan-CL (Fournier et al., 1998; Kleiber et al., 2018) may accept catch data for different fisheries in either weight or numbers; the information informing the model may include both length frequency and weight frequency data; and fish growth is defined in terms of length at age. Using these diverse data types in the same model requires conversion between lengths and weights based on a defined length-weight relationship. Like most modelling platforms, Multifan-CL currently applies the same length-weight relationship across all years, locations, size classes and fisheries. However, data may also be converted outside the model, and there is potential to make software platforms more flexible if this is seen to be warranted.

Fishery and stock assessment issues for Pacific bigeye tunas.

SPC, on behalf of SPC members and the Western and Central Pacific Fisheries Commission (WCPFC), has been resourced under WCPFC Project 90 to assist in conversion factor data collection throughout the region and to undertake analyses of such data to help inform fishery management. Identifying the factors that drive LWRs across time and space is priority for the WCPFC Project 90 work programme.

This report describes work within Project 90 to develop statistical models to explore spatial and temporal variability in bigeye tuna (*Thunnus obesus*) LWRs across the WCPO. The project builds on a compilation and exchange of bigeye tuna length and weight measurements that occurred in 2021 under a 'Letter of Agreement' arrangement between SPC and National Sun Yat-sen University, Taiwan (NSYSU). The combined dataset covers all SPC and Taiwanese data holdings across the WCPO through to 2021. This report focuses on analysis of the Taiwanese dataset to develop and refine the modelling approach for later application to the combined SPC-Taiwanese dataset.

One concern about LWR estimates is that they vary between analyses and data sources, and the sources of the variation are not well understood. Carroceda and Colmenero (2016) reviewed LWRs for bigeye tuna in the Atlantic, and noted a variety of possible reasons for differences, including data quality (including potential confusion about the type of weight used), the treatment of outliers, sex differences, and the length range used in the study. Spatio-temporal variation in fish condition can be a factor, and such variation should be included in stock assessment calculations. For example, Cort et al. (2015) note that the different fattening stages of Atlantic bluefin tuna (ABFT), *Thunnus thynnus* (L.), throughout the year make it impractical to employ a single length-weight relationship. Some analyses have found variation between purse seine and longline-caught fish (Chassot et al., 2016; Parks et al., 1982). Sampling variation can also be

important, particularly with low sample sizes. Numerous length-weight relationships are available for bigeye tuna, based on both small-scale and large-scale studies (e.g., Ahmad et al., 2019; Anrose and Kar, 2010; Chang et al., 2008; Chantawong et al., 1999; Chassot et al., 2016; Choo, 1976; Chur and Krasovskaya, 1980; Cort, 1985; De Jaeger, 1963; Iversen, 1955; Kume and Shiohama, 1964; Lenarz, 1974; Liming et al., 2005; Morita, 1973; Nakamura and Uchiyama, 1966; Nguyen et al., 2022; Oliveira et al., 2005; Parks et al., 1982; Perera et al., 2013; Poreeyanond, 1994; Ronquillo, 1963; Sun et al., 2001; Tantivala, 2000; Thierry et al., 2021; Wang et al., 2002; Xu et al., 2006; Zhu et al., 2010).

The LWR applied in WCPO bigeye stock assessments prior to 2020 (Davies et al., 2011; Harley et al., 2014; McKechnie et al., 2017) was WW = 1.9729e – 5 * $L^{3.0247}$ (Morita, 1973). This was updated by Vincent et al. (2020) to WW = 6.481e − 5 * $L^{2.781}$, based on analysis of data provided to SPC from port sampling.

Most previous analyses of tuna length weight relationships have used relatively consistent methods, assuming that weight = a.length^b (Järvi, 1920). Analysts generally (and appropriately) fit a linear model to estimate log(weight) as a function of log(length) to allow for multiplicative errors. Few analyses include additional covariates, thereby assuming uniform length-weight relationships throughout the analysed dataset.

However, new methods allow more flexible and informative analysis. Ma et al. (2017) used linear mixed-effect models to compare LWRs for yellow croaker along the north coast of China and found interannual variation to be much larger than spatial variation. Finucci et al. (2019) fitted broken stick and variance shift models to data from deep sea fishes, to look for changes associated with life history, and found transitions that may have been associated with diet shifts and/or maturation. Generalized additive models (Wood, 2017) provide a flexible statistical platform to explore factors affecting the length-weight relationship, such as spatial and seasonal variation, using smoothers. These methods have previously been applied to length-weight relationships for lizardfish (Chang et al., 2022).

In the initial stages of an analysis, it is important to develop a full understanding of the dataset and the relationships among the variables. To that end, we explored and described the variables provided and relationships between them, using a combination of plots and statistical analyses. We examined issues associated with sampling, such as rounding, dependence within samples, and observer error. The main statistical tool used was generalized additive modeling (GAM) using the R package *mgcv* (Wood, 2011). Finally, we used GAMs to explore factors affecting the length-weight relationship, and to estimate the potential for bias from inaccurate LW relationships.

The steps involved were as follows:

1. Clean and prepare the Taiwanese longline observer data for analysis.
2. Carry out data exploration and characterisation to identify biological, environmental, longline fishery and observer catch sampling, and data collection and fish storage factors that may affect bigeye weight at length.
3. Develop statistical models to explore if (and how) these factors (in 2) are associated with variation in the bigeye LWR across the WCPO and through time.
4. Use predictions from these models (in 3) to generate aggregate LWRs for particular purposes such as stock assessments.
5. Work with SPC scientists to recommend analytical approaches for a combined analysis of SPC and Taiwanese data holdings.
6. Report on methods, results and recommendations in one written technical report, and at the 2023 WCPFC Pre-Assessment Workshop (PAW).

Issues of interest:

1. How to address non-independence of individuals within a set?
2. What error distributions are appropriate to deal with noisy data?
    a. Data recording errors
    b. Rounding. What is the nature of rounding?
3. GAM model structure: penalties on the smooth, optimizer (ML, REML, or gcv.ubre).
4. What is the pattern of nonlinearity in the LW relationship?
5. Does the length-weight relationship vary between sexes?
6. Spatial variation and seasonal variation and interactions.
7. Observer effects: are there significant differences between observers?
8. Other covariates – years, HBF, light sticks, hook course, weather, wave height.

Methods

Data preparation and cleaning

Data for this study was from the observer programs on Taiwanese distant-water longline vessels during 2008 to 2022. The data was managed by the OFDC and approved for this joint study by the Fisheries Agency of Chinese Taipei. The data includes the following fields:

Table 1: Fields provided.

Field	**Type**	**Description**
Trip ID	Character	Code identifying trip – 490 unique trips
Work date	Date	Date of set
Bait type	Character	Four types, well-reported since 2010
Process type	Character	Five types: OTH, RGG, RGT, RHG, RWW
Length	Real	Fork length in cm
Weight	Real	Weight in kg (affected by process type)
Sex	Character	F, M, I (imm), U (unknown), NA=966, most pre-2015
Wave scale	Character	Wave scale when retrieving hooks: 1 to 5+
Light stick	Logical	0/1.
HBF	Integer	1-32, and 351 NA in 2012
Observer ID	Character	192 observers, the field is anonymised
Weather	Character	Cloudy, rain, sunny, OTH
Hook course	Integer	1-4, Compass direction of hook deployment
Lon	Integer	Longitude
Lat	Integer	Latitude
Region	Integer	Based on lat and lon

*Work date*s were processed using the R package *lubridate* (Grolemund and Wickham, 2011) to determine the *year*, *month*, and *quarter*.

The fields *logwt* and *loglen* were calculated as the natural logarithms of the *weight* and *length* fields.

The fields *modwt5* and *modlen5* were calculated as the modulus (remainder) of *weight* and *length* after dividing by 5, to facilitate exploration of rounding to multiples of 5.

The field *Set ID* was created by combining the *Trip ID* and the *work date*, based on the assumption that vessels did one set per day.

The fields *moon phase* and *lunar illumination* were created based on the work date.

The field *cluster* was created based on the species composition caught in the set. [more detail needed].

Data cleaning

Only 133 samples were available in 2008, and these were removed. Data were sparse at lengths below 70 cm and above 200 cm, so these were excluded from analyses. HBF of 10 or below were excluded for the same reason. Samples from 3 observers who measured fewer than 10 fish were also excluded. Rows with missing values for any of the following variables were omitted: wave scale, light stick, weather, hook course, year, observer ID, longitude, latitude, HBF or work date. Since all analyses were applied by sex, any fish labelled as immature, unidentified, or NA were omitted.

Data characterization

Data were available in good numbers for the years 2009 to 2022, with a few samples from December 2008 (*Figure 1*). Although there was no trend in the number of samples per year, samples in earlier years were obtained from fewer sets, trips, and observers. From 2017, the number of unique sets, trips, and observers sampled per year were higher than in earlier years. Similarly, the number of samples per set declined through time.

The anonymised observer ids provided appeared to be unique. We checked for sharing of observer IDs by searching for sets on the same day by the same observer on different trips, but no such sets were identified.

Most fish were allocated to sex, recorded as U (unknown), F(female), M (male), or I (immature) (*Figure 2*).

Fish process types (*Figure 2*) were RWW (whole weight), RHG (head off, gutted), RGT (gutted and tailed), RGG (gilled and gutted), and OTH (other), with most fish recorded as RGG (2008-2014) or RGT (2015-2022). Comparing length frequency distributions by process type (*Figure 3*) showed that most OTH and RWW fish were small, with few RWW larger than 100 cm. RHG fish also tended to be smaller than RGT and RGG fish. RHG fish tended to be reported in locations near land (*Figure 4*), likely reflecting that this process type is used in coastal fisheries where fish are marketed fresh rather than frozen.

There did not appear to be temporal variation in reported weather, after discounting 2008 due to low sample sizes (*Figure 5*).

Wave scales suggested a higher proportion of samples during good conditions with smaller waves in the middle of the time series than at the beginning and end (*Figure 5*), perhaps due to changes through time in the proportions of samples in calmer equatorial areas.

Bait types trended through time. MAX declined from 65-80% in 2009-2010 to about 30% in 2022. Corresponding increases occurred in the proportions of PIL and SAP (*Figure 6*).

Most samples were allocated to species composition cluster 1 (bigeye-target), though in later years the proportions allocated to clusters 2 and 3 increased (*Figure 6*).

The average hooks between floats increased slightly though time, with the initial mean of 16 in 2009 increasing to over 20 by 2020 (*Figure 7*). There was distinct spatial patterning of HBFs, though the location of the highest HBF varied through time, in the tropical west during 2009-2014 (*Figure 8*) but occurring to the southeast from 2015-2022 (*Figure 9*).

Light sticks were rarely reported before 2014 due to the lack of a specific field to record their use. In April 2014 a new observer form was introduced which included a filed for light sticks. The reported numbers then increased, associated with between 30% and 40% of samples from 2019 (*Figure 7*)F.

After cleaning, the dataset of RGG (gilled and gutted) fish recorded from 2009-2014 included 22875 females in 6357 sets, and 35996 males in 7034 sets. The equivalent dataset for RGT (gilled, gutted, tailed) fish recorded from 2015-2022 included 29220 females in 11697 sets and 41335 males in 12981 sets.

Analytical methods

Models were fitted as generalized additive models using the *mgcv* package (Wood and Wood, 2020). The recommended gamma parameter setting of 1.4 was included in the GAM to reduce risk of overfitting the splines. Models were fitted using maximum likelihood (method = ML) rather than the default GCV.Cp, to reduce the likelihood of local minima as recommended by Wood (2017). ML was used rather than REML in order to compare models with different fixed effects. Models were compared using AIC.

Fish from the same set were caught at the same time and location and are not independent. Analyses may allow for this covariance by fitting a random effect for set (Gilman et al., 2018; Williams et al., 2014; Williams et al., 2012) to avoid wrongly identifying variables as statistically significant / important. We checked for within-set covariation by fitting a random effect to the set ID, in a model that included all covariates found to be significant in other analyses. Models with a set-level random effect could not be fitted to the full dataset in a reasonable time, so this test was done with a reduced dataset (years 2020-2022, month 2, process type RGT). To remove this source of covariation, we randomly selected one sample from each set to use in further analyses.

Analyses with response variables length and log weight were initially modelled using Gaussian errors. These resulted in models that met the required distributional assumptions (*Figure 10*), except when log length was included as an explanatory variable in the log weight analysis. The high explanatory power of log length turned measurement and rounding errors into large outliers, which made the distribution heavy-tailed. We therefore converted to using the scat (scaled t) family of error models (Wood et al., 2016), which is more appropriate for heavy-tailed data. The scat models took much longer to run than Gaussian models, so were restricted to use in final analyses.

Process type issue

Most samples in the dataset were reported as process type RGG (gilled and gutted) and RGT (gilled, gutted, tailed). No samples were reported as process type RGT before 2014. Thus, there was a transition from RGG to RGT during 2014 and 2015. Taiwanese data managers indicated that this transition was due to a change in the observer log sheet rather than a change in processing, and that all fish throughout the time series were measured after the removal of the tail (RGT). Process type RGG only occurs for non-frozen fish in the coastal fishery, and data from the coastal fishery were not included in this analysis.

We checked relationships between RGG and RGT by exploring the data, and comparing lengths, weights, and the relationship between length and weight in data collected during 2014 and 2015.

Most observers reported one process type or the other. Six observers reported both RGG and RGT, mostly on separate trips. Only one trip had a mixture of process types, with 342 RGG and 120 RGT reported.

We checked whether process type was associated with differences in size – fish processed as RGT would be expected to be shorter and lighter than RGG. Response variables length and weight were separately modelled as functions of continuous covariates location, month, HBF, and lunar illumination, and categorical variables (factors) year, process type, observer ID, and light stick use. Length was fitted without transformation and weight was log transformed to normalise residuals. Log length was also used as a covariate when fitting to log weight. Continuous variables with one dimension were fitted with the *mgcv* default thin plate regression splines (bs = ‘tp’). Interactions between location and month were explored by fitting a three-way interaction term using a tensor product of cubic splines (bs = ‘cr’), with month defined as a circular variable (bs = ‘cc’) to constrain estimates to be similar at the beginning and end of the year. The observer id was fitted as a random effect (bs = ‘re’).

The full model was:
Response ~ te(lat, lon, mon, k = c(10,10,4), bs = c("cr", "cr", "cc")) + yearf + s(obs_name, bs="re") + processtype + s(hbf) + lightstick + s(lunar_illumination).

Rounding issue

Frequency histograms of lengths and weights indicated peaks at multiples of 5 in both datasets (*Figure 13*), indicating that rounding had occurred for some samples but not others. Rounding of this type is commonly observed in fisheries size frequency data (e.g., Hoyle et al., 2017). Rounding appeared more prevalent for weights than for lengths, since the weight dataset had multiples of 5 that were higher relative to non-multiples of 5.

Rounding was explored by taking the remainder after division by 5 (modulus 5), which showed that weight rounding was greatest for fish of modulus 4 and important for modulus 1, but not substantial for modulus 2 and 3. Similarly, length rounding was greatest for moduli 1 and 4, and not substantial for modulus 2 and 3. Sea conditions (wave scale) did not appear strongly associated with rounding (*Figure 14*). However, there were large differences in rounding behaviour between observers (*Figure 15*), with one observer rounding almost every fish weight and length to multiples of 5.

Overall, for weights 31.5 % of fish were modulus 0, which was 11.5% above the expected level of 20%.

Length weight relationships

Given the large size of the dataset and the potential for differences between sexes, length-weight relationships were analysed separately for males and females. Analyses were also conducted separately for the process types RGG (2009 to 2014) and RGT (2015 to 2022), given uncertainty about whether the two process types were actually the same.

Models were run with log(weight) as the response variable. Covariates offered to the model were the same as in the process type analyses, except that year was offered as either a factor or continuous variable.

After initial fits of each analysis, all observations for observers identified as large outliers on the random effect q-q plot were removed before refitting. For the 2009-2014 RGG analyses, one outlying observer (the same individual) was removed for both females and males. For the 2015-2022 RGT analyses, 3 observers were removed for both females and males, with an additional 2 observers removed for males.

To explore the effect of allowing nonlinearity in the relationship between log(length) and log(weight), the best fitting model was refitted with the log(length) smoother constrained to be linear. Weight at length was then predicted from both models, and differences between models in predicted weight plotted against length.

Similarly, to explore the effect of separately modelling males and females, a further model was fitted that combined the male and female 2015-2022 datasets. Weights at length were then predicted from all three models, and differences between models in predicted weight plotted against length.

Purely additive models (logwt ~ a.length + b.cov1 +c.cov2) assume that covariates affect the intercept of the model but not the slope. This appears appropriate for temporary issues such as condition or seasonal effects, but Interactions between length and covariates are plausible for permanent or potentially long-term effects such as sex and location. Since we were already running separate models by sex, we ran additional analyses exploring interactions with length for effects associated with location. These models were applied only to the female 2015-2022 dataset.

To explore the effect on model results of assuming scaled t versus Gaussian residuals, we predicted weight at length from the best fitting models using each distributional assumption, for females 2009-2014, and compared them.

We estimated linear length-weight relationships using standard approaches, to explore how seasonal and spatial variation may affect length-weight relationships. We fitted a GAM with log(weight) as a linear function of log(length), a random effect term for the observers, and scaled-t distribution for residuals. This

obtains the average intercept value across all observers. No other terms were included. Separate models were fitted for the early and late periods, with combined data for both sexes.

Results

Process type issue

In analyses of data from 2014 and 2015 to check the effect of the changeover from process type RGG to RGT, process type was associated with small effects on length and weight.

The best model for length (*Table 2*) was :
length ~ te(lat, lon, mon, k = c(10, 10, 4), bs = c("cr", "cr", "cc")) + s(obs_name, bs = "re") + processtype + s(hbf) + lightstick + s(lunar_illumination) + sex.

Similarly, the best model for weight with loglen omitted (*Table 3*) was
logwt ~ te(lat, lon, mon, k = c(10, 10, 4), bs = c("cr", "cr", "cc")) + s(obs_name, bs = "re") + processtype + s(hbf) + lightstick + s(lunar_illumination) + sex.

Process type RGT was associated with 3 cm shorter length than RGG, and about 10% lighter weight.

The best model for weight with loglen included for the process type dataset (*Table 4*) was:
logwt ~ s(loglen) + te(lat, lon, mon, k = c(10, 10, 4), bs = c("cr", "cr", "cc")) + s(obs_name, bs = "re") + s(hbf).

Including loglen as a predictor in the model substantially improved the fit. Process type was not clearly supported as an explanatory variable once loglen was included. However, results were not entirely consistent, because although the model that included process type had less support than the model without that variable, the process type variable was statistically significant within the model. The process type parameter estimate, of -0.0364 (s.e.= 0.0100), indicated a 4% reduction in weight at length for process type RGT. The reason the model that included process type had less support (higher AIC) was because it used more degrees of freedom for the spatial-temporal smoother. We verified that this effect was not due to a local minimum by refitting the model with different starting values, which led to the same outcome. We concluded that imbalance during the overlap period in the spatial distributions of the two process types meant the model was unable to effectively test for an effect of process type on weight at length. Given the resulting uncertainty, and differences in reporting between periods linked to changes in the observer form, we subsequently analysed data from the two periods separately.

Error distributions

Models used to estimate length-weight relationships showed substantial lack of fit, with large outliers, when fitted with Gaussian distributions (*Figure 10*, lower left). However, they fitted well when error distributions were assumed to follow the scaled t distribution (*Figure 10*, lower right), with near linear q-q plots.

Within-set variation

Tests of within-set variability found set id to be statistically significant ($p < 2e\text{-}16$), though a smaller contributor to variation than factors such as observer ID, location, HBF, and year. This indicates that fish within a set were more similar than expected by chance, and not independent of one another. Due to this correlation within sets, only one randomly selected fish per set was included in each subsequent analysis.

Length-weight relationship models

A series of models was fitted to each of the four combinations of males and females, 2009-2014 and 2015 to 2022.

For females 2009-2014, the scat error distribution fitted the data well, with outliers addressed by the flexible scaled t distribution (*Figure 16*). Spatial patterns in weight at length were apparent with some

tendency for weights to be lower in the west and the tropics, and higher towards the northern and southern subtropical latitudes (*Figure 17*). However, uncertainty was higher outside the tropics in areas seasonally further from sampling (*Figure 18*). There was some variation associated with HBF, with higher weights at higher HBF (*Figure 19*). There was also a pattern of increasing weight through time (*Figure 19*). The relationship of log weight with log length was very close to linear (*Figure 19*), suggesting that assuming a linear relationship would provide adequate results. There was apparent variation in the results associated with different observers. After removing one outlier, observer distributions were approximately normal (*Figure 20*).

For males 2009-2014, the scat error distribution again fitted the data well, with outliers addressed by the flexible scaled t distribution (*Figure 21*). Spatial patterns in weight at length were stronger and more seasonally variable than for females, though with a similar tendency for weights to be lower in the west and higher in the southeast (*Figure 22*). Similarly, uncertainty was higher outside the tropics in areas seasonally further from sampling (*Figure 23*). There was some variation associated with HBF, again with higher weights at higher HBF, though with some variation at higher HBF (*Figure 24*). There was again a pattern of increasing weight through time (*Figure 24*). The relationship of log weight with log length was very close to linear (*Figure 24*), suggesting that assuming a linear relationship would provide adequate results. There was a considerable variation in the results associated with different observers. After removing one outlier, observer distributions were approximately normal (*Figure 25*), but with some lack of normality at the lower end.

For females 2015-2022, the scat error distribution again fitted the data well, with outliers addressed by the flexible scaled t distribution (*Figure 26*). Spatial patterns in weight at length differed from the earlier period, with weights lower in the northwest, the far east, and the far south, and generally higher in the tropics and the far north (*Figure 27*). Uncertainty was again higher outside the tropics in areas seasonally further from sampling (*Figure 28*). There was some variation associated with HBF, again with higher weights at higher HBF, though now with a suggestion of higher weights at low HBF (*Figure 29*). Weights were relatively stable through time (*Figure 29*). The relationship of log weight with log length was very close to linear (*Figure 29*), suggesting that assuming a linear relationship would provide adequate results. There was again considerable variation in the results associated with different observers. After removing three outliers, observer distributions were approximately normal (*Figure 30*).

For males 2015-2022, the scat error distribution again fitted the data well, with outliers addressed by the flexible scaled t distribution (*Figure 31*). Spatial patterns in weight at length were similar to females in the same period, with weights lower in the northwest and far east, though less so than females in the far south, and generally higher in the tropics and the far north (*Figure 32*, *Figure 27*). Uncertainty was again higher outside the tropics in areas seasonally further from sampling (*Figure 33*). There was some variation associated with HBF, again with higher weights at higher HBF, and without the suggestion of higher weights at low HBF seen in females (*Figure 34*). Weights varied a little through time but with no clear trend(*Figure 34*). The relationship of log weight with log length was very close to linear (*Figure 34*), suggesting that assuming a linear relationship would provide adequate results. There was again considerable variation in the results associated with different observers. After removing five outliers, observer distributions were approximately normal (*Figure 35*).

Non-linearity in the length-weight relationship

There was clear support for nonlinearity in the length weight relationship, with a dip below the linear at around the length of sexual maturity or 120 cm, a subsequent increase in weight at length at around 150 cm, followed by an ongoing decline about 170 cm (*Figure 36*). When assuming linear growth, the pattern slightly positively allometric. For females the beta (slope) of the length parameter was 3.066 with standard deviation of 5.5×10^{-3}. For males, the beta was 3.061 with standard deviation 5.1×10^{-3}.

Effect of distributional assumption

Patterns of weight at length, after accounting for other parameters, were quite similar for models using Gaussian and scaled t residuals. There was a slight tendency for the Gaussian model to predict higher weights at length, but the difference was less than 1kg until about 140 cm and always less than 2 kg (*Figure 37*, right).

Variation between sexes

Patterns of weight at length, after accounting for other variables, were similar for males and females (*Figure 37*, left).

Combined model across sexes

In a combined model fitted to data for males and females for the period 2015-2022, the scat error distribution again fitted the data well, with outliers addressed by the flexible scaled t distribution (*Figure 38*). Spatial patterns in weight at length were similar to females and males for the same period, with weights lower in the northwest and far east and generally higher in the tropics during the northern winter (*Figure 39*). Uncertainty was again higher outside the tropics in areas seasonally further from sampling (*Figure 40*). There was some variation associated with HBF, again with higher weights at higher HBF (*Figure 41*). Weights varied a little through time but with no clear trend (*Figure 41*). The relationship of log weight with log length was close to linear though some curvature was apparent (*Figure 41*), suggesting that assuming a linear relationship would provide adequate results. There was again considerable variation in the results associated with different observers. After removing outliers, observer distributions were approximately normal (*Figure 42*).

Spatial and seasonal covariates had moderately large effects on predicted weight at length (*Figure 43*), with larger effects at greater lengths, due to the additive form of the model which is linear after taking the logarithm of both length and weight. Plotting predictions on the scale of the model shows this (*Figure 44*).

Interactions between length and location

Including interactions between length and location improved the models' ability to predict weight, with delta AIC of 129. The formula for the best fitting model for females sampled 2015-2022 was:

```
logwt ~
ti(loglen, k=20) + yrf + ti(loglen, by = yrf) + s(observer, bs="re") +
ti(lat, k = 10) + ti(lon, k = 20) + ti(mon, k=8, bs="cc") +
ti(lat, lon, k = c(10,10)) + ti(lon, mon, k = c(10,6), bs=c("cr", "cc")) + ti(lat, mon, k = c(10,6), bs=c("cr", "cc")) +
ti(lat, lon, mon, k = c(10,10,4), bs =c("cr","cr","cc")) +
ti(lat, loglen, k = c(8,6)) + ti(lon, loglen, k = c(8,6)) + ti(lat, lon, loglen, k = c(8,8,6)) + s(hbf, bs = "cr")
```

See Tables 12 and 13 for the parametric and smooth terms. Predictions from this model (*Figure 45*) showed somewhat different patterns of variation at length from predictions from the model without these interactions. Compared to the model without these interactions, the variability at length tended to be reduced at larger sizes and increased at smaller sizes (*Figure 46*).

Standard models

Standard models were fitted to the early and late periods. The early and late models for the entire region provided estimates for the terms of the length-weight relationship that were similar, though with differences that were statistically significant (Table 14). Estimates by region are also provided (Table 15).

Discussion

Analyses of length-weight relationship for bigeye tuna showed statistically significant patterns that may be large enough to affect stock assessment results.

Lack of independence between individuals caught in a fishing set has the potential to affect estimated LWRs (Chang et al., 2022). Factors that may induce such similarity include similar times since feeding in the short term, similar histories of environmental conditions in the longer term, relatedness, and schooling by size. Randomly sampling a single individual from a set was an effective way to address this issue. An alternative approach that includes all the data is to fit a random effect for the set id. However, this approach was impractical with the current datasets since a model of this type ran for 12 hours on a fast machine (12th Gen Intel(R) Core(TM) i9-12900KF 3.19 GHz) without converging.

Rounding of measurements by observers was widespread, particularly for weights, and may have had quite a large impact for individual fish. For example, rounding an 18kg fish up to 20kg represents 10% of the fish's weight. Based on the proportions of fish recorded at each modulus of 5, weights ending in modulus 4 were rounded up about twice as often as those ending in modulus 1 were rounded down.

Rounding at these rates can have several effects on estimation of the LWR. First, it increases observation error, but with structure to the error that is different from other types of observation error. The additional error of up to 10% is likely to have contributed to the 'fat tails' in the error distributions. Second, the positive bias in rounding described above can bias the estimated LWR.

Observer effects are quite large, especially in the early years. Rounding variation between observers likely contributed to the large uncertainty associated with the observer random effect. However, other factors that may have contributed include variation in measurement techniques among observers, variation in fish preparation methods between vessels and trips, and spatial variation in length weight relationships that was absorbed by individual observer effects, since observer distribution varied spatially and through time. However, ignoring observer effects would likely affect predicted LW relationships and cause overdispersion in the data, which results in including too many variables in the models.

GAM analyses using the mgcv package ran considerably faster when assuming Gaussian residuals than when using the scaled t distribution. Model fit was much better based on the AIC, and model diagnostics were also considerably better. The same model was selected and fitted estimates were similar, suggesting that results would not have been unreasonable if we had assumed Gaussian distribution. Nevertheless, comparing delta AICs among the different models suggested that the approaches will not always select the same model. Moreover, data collected by observers from the same observer program may be less affected by error and fat tails than data in the SPC database, which come from a variety of sources.

There was considerable variation in the bigeye LWR associated with location and season. Such patterns have previously been found for bigeye caught by Korean longliners in the Indian Ocean (Hoyle et al., 2021). Spatial variation in LWRs occurs for other tuna species (Cort et al., 2015). Spatial variation cannot be ruled out as causing the differences between LWRs for purse seine and longline-caught bigeye (Chassot et al., 2016), since these fisheries often operate in different areas, but this issue requires further exploration.

Variation associated with HBF was found in analyses of all datasets, with heavier fish caught at the highest HBF. However, there was also spatial variation in the distribution of fishing with high HBF, so it is possible that these greater weights at higher HBF are due to confounding.

Other parameters (hook course, light stick, weather, wave scale) were not associated with statistically significant variation, which was encouraging for the credibility of the analysis. Hook course, for example, simply indicates the compass quadrant of vessel travel during setting. It is notable that this variable was statistically significant in some preliminary analyses that included all fish, indicating the potential for problems caused by covariation among fish in the same set.

The main factors contributing to observed variation between previous LWR analyses appear likely to be small sample sizes, limited numbers of observers, and limited spatial and temporal coverage.

Differences by sex were sufficiently small that the same LWR could reasonably be applied to both sexes. Predictions from a combined-sex model are provided in figures 43 and 44.

Variation in the LWR with length (nonlinearity) was statistically significant though it did not represent a large proportion of fish weight. Growth was initially close to the linear prediction, declining slightly until between 110-120 cm for both sexes. From this length, weight at length relative to linear began to increase, peaking at just over 140 cm. Above this length the trend changed again and began to decline, with fish above 160cm tending to weigh less than predicted by linear models.

Models that included interactions with the length effect fitted the data significantly better than models without such interactions. Predicted weights were somewhat different at larger sizes on the nominal scale, but notably at smaller sizes on the log scale. Predictions at local scale for models with length interactions fitted across the entire dataset may be unreliable for some combinations of length, location, and season, particularly for combinations not well represented in the dataset. The much better fits of the length interaction models indicate that the issue requires further investigation, but the current predictions from these models should be viewed with caution. Nevertheless, these patterns suggest that, given this potential for spatial and seasonal variation in both the intercept and the slope of the length weight relationship, the best estimates for an area may be obtained by analysing data from that area.

Recommendations for analyses of SPC database

1. Consider how the estimated LWR will be used and use an approach suitable for that purpose. Objectives may include:
    a. Understanding of the processes affecting the LWR.
    b. Development of a single LWR to use in a stock assessment.
    c. Transformation of size frequency data between weight and length formats.
2. Identify individuals who can provide background information about each source of data in the database. They may need to be contacted to resolve questions.
3. Explore data thoroughly using maps, plots and tables, to identify any obvious patterns in the LWRs, such as groups of fish prepared differently, or weighed / measured using different methods. When aiming for understanding, avoid jointly analysing data from fish prepared using different methods. When planning analyses, develop a set of hypotheses to test.
4. Analyses should be carried out using GAMs in mgcv with similar model structure to those applied in this paper. Consider using the bam() function rather than gam(), for faster runtimes.
5. Investigate factors not available in Taiwanese observer dataset, such as fish shrinkage due to measurement as frozen or fresh.
6. Reduce sample size and avoid covariation among fish within sets by taking one sample per set. For analyses of small datasets, use all data but fit a random effect for the set id.
7. Allow for variation associated with the identity of the measurer. Remove large outliers.
8. Investigate spatial, seasonal, and inter-annual variation. This can be allowed for when developing LWRs that are specific to fisheries or even more finely targeted, which may be useful for converting size frequency data between formats.
9. Include all data and use the scaled t distribution for fat tails, rather than applying an ad hoc approach to screen out outliers. Test whether scat and Gaussian errors give the same results, and if so use the much faster Gaussian for exploration and scaled-t for final estimates.

Acknowledgments

Work on this project was associated with WCPFC Project 90.

References

Ahmad, F.; Dewanti, L.P.; Arnenda, G.L.; Rizal, A. Length-weight relationship and catch size of bigeye tuna (Thunnus obesus) landed in Benoa, Bali, Indonesia. World News of Natural Sciences. 23:34-42; 2019.

Anrose, A.; Kar, A. Some aspects of the biology of Bigeye tuna (Thunnus obesus, Lowe 1839) in Andaman and Nicobar waters. IOTC-2010-WPTT-41; 2010

Carroceda, A.; Colmenero, C. Size-weight relationships of the bigeye tuna (Thunnus obesus) from North Atlantic areas using linear and non-linear fits. ICCAT Collective Volume of Scientific Papers. 72:472-484; 2016.

Chang, S.-K.; Chou, Y.-T.; Hoyle, S.D. Length-Weight Relationships and Otolith-Based Growth Curves for Brushtooth Lizardfish off Taiwan With Observations of Region and Aging–Material Effects on Global Growth Estimates. Frontiers in Marine Science:1098; 2022.

Chang, S.-K.; Hsu, C.C.; Liu, H.I. Preliminary estimation of length-weight relationship of Atlantic bigeye tuna from taiwanese observer data. Collect Vol Sci Pap, ICCAT. 62:480-484; 2008.

Chantawong, P.; Panjarat, S.; Singtongyam, W. Preliminary results on fisheries and biology of bigeye tuna (Thunnus obesus) in the Eastern Indian Ocean. IOTC Proceedings; 1999

Chassot, E.; Assan, C.; Esparon, J.; Tirant, A.; Delgado de Molina, A.; Dewals, P.; Augustin, E.; Bodin, N. Length-weight relationships for tropical tunas caught with purse seine in the Indian Ocean: update and lessons learned. IOTC-WPDCS12-INF05. . 12th Working Party on Data Collection and Statistics. Mahé, Seychelles: Indian Ocean Tuna Commission; 2016

Choo, W.I. Relationship between length and weight of yellowfin and bigeye tuna from eastern Atlantic Ocean. Collect Vol Sci Pap, ICCAT. 5:72-81; 1976.

Chur, V.; Krasovskaya, N. Dependence of the mass of bigeye tuna (Thunnus obesus) of the tropical part of the Atlantic Ocean on the length. Collect Vol Sci Pap, ICCAT. 9:291-293; 1980.

Cort, J. Data on tuna fishing by Spanish vessels in the western Indian Ocean. Expert Consultation on Stock Assessment of Tunas in the Indian Ocean, Colombo (Sri Lanka), 28 Nov-2 Dec 1985; 1985

Cort, J.L.; Estruch, V.D.; Neves Dos Santos, M.; Di Natale, A.; Abid, N.; de la Serna, J.M. On the variability of the length–weight relationship for atlantic Bluefin Tuna, Thunnus thynnus (L.). Reviews in Fisheries Science & Aquaculture. 23:23-38; 2015.

Davies, N.; Hoyle, S.D.; Harley, S.J.; Langley, A.D.; Kleiber, P.M.; Hampton, W.J. Stock assessment of bigeye tuna in the Western and Central Pacific Ocean. WCPFC Scientific Committee, 7th Regular Session. Pohnpei, Federated States of Micronesia: Western and Central Pacific Fisheries Commission; 2011

De Jaeger, B. Synopsis of biological data on blue fin tuna *Thunnus orientalis*, (Temminck and Schlegal 1842), Long fin tuna *Thunnus alalunga* (Bonnaterre 1788), Yellowfin tuna *Thunnus albacares* (Bonnaterre 1788) and Bigeye tuna *Thunnus obesus* (Lowe 1839) (South Africa). FAO Fisheries Report. 6:588-607; 1963.

Ducharme-Barth, N.; Vincent, M.; Hampton, J.; Hamer, P.; Williams, P.; Pilling, G. Stock assessment of bigeye tuna in the western and central Pacific Ocean. WCPFC-SC16-2020/SA-WP-03 (Rev. 01), 144; 2020

Finucci, B.; Dunn, M.R.; Arnold, R. Using length–mass relationships to estimate life history: an application to deep-sea fishes. Canadian Journal of Fisheries and Aquatic Sciences. 76:723-739; 2019.

Fournier, D.A.; Hampton, J.; Sibert, J.R. MULTIFAN-CL: a length-based, age-structured model for fisheries stock assessment, with application to South Pacific albacore, *Thunnus alalunga*. Canadian Journal of Fisheries and Aquatic Sciences. 55:2105-2116; 1998.

Froese, R. Cube law, condition factor and weight-length relationships: history, meta-analysis and recommendations. Journal of Applied Ichthyology. 22:241-253; 2006. 10.1111/j.1439-0426.2006.00805.x

Fulton, T.W. The rate of growth of fishes. Twenty-second annual report of the Fishery Board of Scotland 1904. 3:141-241; 1904.

Gilman, E.; Chaloupka, M.; Musyl, M. Effects of pelagic longline hook size on species-and size-selectivity and survival. Reviews in Fish Biology and Fisheries. 28:417-433; 2018.

Grolemund, G.; Wickham, H. Dates and times made easy with lubridate. Journal of statistical software. 40:1-25; 2011.

Harley, S.J.; Davies, N.; Hampton, J.; McKechnie, S. Stock Assessment Of Bigeye Tuna In The Western And Central Pacific Ocean. WCPFC Scientific Committee 10th Regular Session, Majuro, Republic of the Marshall Islands, 6-14 August 2014; 2014

Heincke, F. Bericht über die Untersuchungen der Biologischen Anstalt auf Helgoland zur Naturgeschichte der Nutzfische (1. April 1905 bis 1. Oktober 1907). Die Beteiligung Deutschlands an der Internationalen Meeresforschung 1908. 4/5:1-90; 1908.

Hoyle, S.D.; Chang, S.-T.; Fu, D.; Itoh, T.; Lee, S.I.; Lucas, J.; Matsumoto, T.; Yeh, Y.-M.; Wu, R.-F.; Lee, M.K. Review of size data from Indian Ocean longline fleets, and its utility for stock assessment. IOTC-2021-WPTT23-07. Working Party on Tropical Tunas. Online: Indian Ocean Tuna Commission; 2021

Hoyle, S.D.; Satoh, K.; Matsumoto, T. Exploration of Japanese size data and historical changes in data management. Indian Ocean Tuna Commission, WPM08. Victoria, Seychelles; 2017

Iversen, E.S. Size frequencies and growth of central and western Pacific bigeye tuna: US Department of the Interior, Fish and Wildlife Service; 1955

Järvi, T. Die kleine Marane (*Coregonus albula* L.) im Keitelesee, eine okologische und okonomische Studie, Serie A col. XIV, No. 1. Annales Academiae Scientiarum Fennicae, Helsinki; 1920

Kleiber, P.; Fournier, D.A.; Hampton, John; Davies, N.; Bouye, F.; Hoyle, S. MULTIFAN-CL User's Guide. 2018

Kume, S.; Shiohama, T. On the conversion between length and weight of bigeye tuna landings in the Pacific Ocean (Preliminary report). Rep Nankai Reg Fish Res Lab. 20:59-67; 1964.

Lenarz, W. LENGTH-WEIGHT RELATIONS FOR 5 EASTERN TROPICAL ATLANTIC SCOMBRIDS. NATL MARINE FISHERIES SERVICE SCIENTIFIC PUBL OFFICE 7600 SAND POINT WAY NE …; 1974

Liming, S.; Liuxiong, X.; Xinjun, C. Preliminary analysis of the Fork length-weight relationships and round weight-dressed weight relationships of bigeye tuna (Thunnus obesus) sampled from China tuna longlining fleet in Central Atlantic Ocean. Collect Vol Sci Pap, ICCAT. 58:283-291; 2005.

Ma, Q.; Jiao, Y.; Ren, Y. Linear mixed-effects models to describe length-weight relationships for yellow croaker (Larimichthys Polyactis) along the north coast of China. PLoS One. 12:e0171811; 2017.

McKechnie, S.; Pilling, G.; Hampton, J. Stock assessment of bigeye tuna in the western and central Pacific Ocean. WCPFC Scientific Committee, 13th Regular Session. Rarotonga, Cook Islands: Western and Central Pacific Fisheries Commission; 2017

Methot Jr, R.D.; Wetzel, C.R. Stock synthesis: A biological and statistical framework for fish stock assessment and fishery management. Fisheries Research. 142:86-99; 2013. https://doi.org/10.1016/j.fishres.2012.10.012

Morita, Y. Conversion factors for estimating live weight from gilled-and-gutted weight of bigeye and yellowfin tunas. Bull Far Seas Fish Res Lab. 9:109-121; 1973.

Nakamura, E.L.; Uchiyama, J.H. Length-weight relations of Pacific tunas. in: Manar T.A., ed. Proceedings of the Governor's Conference on Central Pacific Fishery Resources (28 February-12 March 1966). Honolulu and Hilo, Hawaii; 1966

Nguyen, K.Q.; Phan, H.T.; Tran, P.D.; Van Nguyen, B.; Van Do, T.; Nguyen, L.T.; Van To, P.; Vu, N.K. Length-length, Length–weight, and Weight-weight Relationships of Yellowfin (Thunnus Albacares) and Bigeye (Thunnus Obesus) Tuna Collected From the Commercial Handlines Fisheries in the South China Sea. Thalassas: An International Journal of Marine Sciences:1-7; 2022.

Oliveira, J.E.L.; Vasconcelos, J.A.; Travassos, P.; Garcia Jr, J.; Aldatz, J.P. Length-Weight relantionships and Length-Length conversions of tunas and swordfish in the Northeast of Brazil. Collect Vol Sci Pap ICCAT. 58:1724-1728; 2005.

Parks, W.; Bard, F.; Cayré, P.; Kume, S.; Guerra, A.S. LENGTH-WEIGHT RELATIONS FOR BIGEYE TUi~ A CAPTURED IN THE EASTERN ATLANTIC OCEAN. 1982.

Perera, H.; Haputhanthri, S.; Bandaranayake, K. A review on oceanic tuna fishery in Sri Lanka and estimation of the length-weight relationships for yellowfin tuna and bigeye tuna. IOTC-2013-WPTT15. 16:8; 2013.

Poreeyanond, D. Catch and size groups distribution of tunas caught by purse seining survey in the Arabian Sea, Western Indian Ocean, 1993. Expert Consultation on Indian Ocean Tunas Sess 5, Mahe (Seychelles), 4-8 Oct 1993; 1994

Ronquillo, I.A. A contribution to the biology of Philippine tunas. Proceedings of the World Scientific Meeting on the Biology of Tunas and Related Species; 1963

Sun, C.-L.; Huang, C.-L.; Yeh, S.-Z. Age and growth of the bigeye tuna, Thunnus obesus, in the western Pacific Ocean. Fishery Bulletin. 99:502-502; 2001.
Tantivala, C. Some biological study of yellowfin tuna (Thunnus albacares) and bigeye tuna (Thunnus obesus) in the Eastern Indian Ocean. Indian Ocean Tuna Commission Proceedings; 2000
Thierry, N.N.B.; Cheng, Z.; Achille, N.P.; Richard, K.; Xu, L. Catch per unit effort, condition factor and length-weight relationship of albacore tuna (Thunnus alalunga), yellowfin tuna (Thunnus albacares) and bigeye tuna (Thunnus obesus) in the longline tuna fishery in the eastern Pacific Ocean. Indian J Fish. 68:23-32; 2021.
Vincent, M.; Ducharme-Barth, N.; Hamer, P. Background analyses for the 2020 stock assessments of bigeye and yellowfin tuna, WCPFC-SC16-2020/SA-IP-06. Western and Central Pacific Fisheries Commission Scientific Committee, Sixteenth Regular Session, 11–20 August 2019. Online; 2020
Wang, S.-B.; Chang, F.-C.; Wang, S.-H.; Kuo, C.-L. Some biological parameters of bigeye and yellowfin tunas distributed in surrounding waters of Taiwan. 15th meeting of the Standing Committee on Tuna and Billfish (SCTB) Hawaii; 2002
Williams, A.J.; Allain, V.; Nicol, S.J.; Evans, K.J.; Hoyle, S.D.; Dupoux, C.; Vourey, E.; Dubosc, J. Vertical behavior and diet of albacore tuna (Thunnus alalunga) vary with latitude in the South Pacific Ocean. Deep Sea Research Part II: Topical Studies in Oceanography; 2014. 10.1016/j.dsr2.2014.03.010
Williams, A.J.; Farley, J.H.; Hoyle, S.D.; Davies, C.R.; Nicol, S.J. Spatial and sex-specific variation in growth of albacore tuna (Thunnus alalunga) across the South Pacific Ocean. PLoS One. 7:e39318; 2012. 10.1371/journal.pone.0039318
Wood, S.; Wood, M. Package 'mgcv'. R package version 1.8-32. 2020
Wood, S.N. Fast stable restricted maximum likelihood and marginal likelihood estimation of semiparametric generalized linear models. Journal of the Royal Statistical Society: Series B (Statistical Methodology). 73:3-36; 2011.
Wood, S.N. Generalized additive models: an introduction with R: Chapman and Hall/CRC; 2017
Wood, S.N.; Pya, N.; Säfken, B. Smoothing parameter and model selection for general smooth models. Journal of the American Statistical Association. 111:1548-1563; 2016.
Xu, H.; Maunder, M.N.; Minte-Vera, C.; Valero, J.L.; Lennert-Cody, C.; Aires-da-Silva, A. Bigeye tuna in the Eastern Pacific Ocean, 2019: benchmark assessment, Document SAC-11-06. IATTC Scientific Advisory Committee, 11th meeting. San Diego, California: Inter-American Tropical Tuna Commission; 2020
Xu, L.; Zhu, G.; Song, L.; Jiang, W. Preliminary analysis on biological characteristics of bigeye tuna, Thunnus obesus, based on observer's data available from the 2004-2005 survey in the Western Central Atlantic Ocean. Col Vol Sci Pap ICCAT. 59:555-563; 2006.
Zhu, G.; Xu, L.; Zhou, Y.; Song, L.; Dai, X. Length-weight relationships for bigeye tuna (Thunnus obesus), yellowfin tuna (Thunnus albacares) and albacore (Thunnus alalunga)(Perciformes: Scombrinae) in the Atlantic, Indian and Eastern Pacific Oceans. Collect Vol Sci Pap ICCAT. 65:717-724; 2010.

Tables

Table 2: Models to test whether RGG and RGT are the same: fit to length. The full model is: length ~ te(lat, lon, mon, k = c(10,10,4), bs = c("cr", "cr", "cc")) + yrf + s(obs_name, bs="re") + processstype + s(hbf) + lightstick + s(lunar_illumination).

	yrf	lat	lon	mon	obs ID	hbf	lunar	process type	light stick	sex	AIC	dAIC
1	1	1	1	0	0	0	0	1	0	0	26018.7	202.3
2	1	1	1	1	0	0	0	1	0	0	25928.7	112.2
3	1	1	1	1	0	0	0	1	0	0	25982.6	166.1
4	1	1	1	1	1	0	0	1	0	0	25853.2	36.8
5	1	1	1	1	1	1	0	1	0	0	25845.1	28.6
6	1	1	1	1	1	1	0	1	1	0	25843.2	26.7
7	1	1	1	1	1	1	1	1	1	0	25844.1	27.6
8	0	1	1	1	1	1	1	1	1	0	25842.4	25.9
9	0	1	1	1	1	1	1	0	1	0	25844.3	27.8
10	0	1	1	1	1	0	1	0	1	0	25846.9	30.4
11	**0**	**1**	**1**	**1**	**1**	**1**	**1**	**1**	**1**	**1**	**25816.5**	**0.0**

Table 3: Models to test whether RGG and RGT are the same: fit to weight. The full model is: logwt ~ te(lat, lon, mon, k = c(10,10,4), bs = c("cr", "cr", "cc")) + yrf + s(obs_name, bs="re") + processtype + s(hbf) + lightstick + s(lunar_illumination).

	yrf	lat	lon	mon	obs ID	hbf	lunar	process type	light stick	sex	AIC	dAIC
1	1	1	1	0	0	0	0	1	0	0	4327.1	226.1
2	1	1	1	1	0	0	0	1	0	0	4198.7	97.7
3	1	1	1	1	0	0	0	1	0	0	4271.7	170.6
4	1	1	1	1	1	0	0	1	0	0	4116.9	15.9
5	1	1	1	1	1	1	0	1	0	0	4115.1	14.1
6	1	1	1	1	1	1	0	1	1	0	4111.8	10.8
7	1	1	1	1	1	1	1	1	1	0	4112.4	11.3
8	0	1	1	1	1	1	1	1	1	0	4111.5	10.4
9	0	1	1	1	1	1	1	0	1	0	4113.9	12.8
10	0	1	1	1	1	0	1	0	1	0	4114.3	13.2
11	**0**	**1**	**1**	**1**	**1**	**1**	**1**	**1**	**1**	**1**	**4101.1**	**0.0**

Table 4: Models to test whether RGG and RGT are the same: fit to LW using scat family. The full model is: logwt ~ s(loglen) + te(lat, lon, mon, k = c(10,10,4), bs = c("cr", "cr", "cc")) + yrf + s(obs_name, bs="re") + processtype + s(hbf) + lightstick + s(lunar_illumination).

	yrf	log len	lat	lon	mon	obs ID	hbf	lunar	process type	light stick	Sex	AIC	dAIC
1	1	1	1	1	0	0	0	0	1	0	0	-4234.3	1113.8
2	1	1	1	1	1	0	0	0	1	0	0	-4582.0	766.1
3	1	1	1	1	1	0	0	0	1	0	0	-4255.9	1092.1
4	1	1	1	1	1	1	0	0	1	0	0	-5289.3	58.8
5	1	1	1	1	1	1	1	0	1	0	0	-5335.7	12.4
6	1	1	1	1	1	1	1	0	1	1	0	-5333.3	14.8
7	1	1	1	1	1	1	1	1	1	1	0	-5332.8	15.3
8	0	1	1	1	1	1	1	1	1	1	0	-5333.4	14.7
9	0	1	1	1	1	1	1	1	0	1	0	-5345.6	2.5
10	0	1	1	1	1	1	0	1	0	1	0	-5276.3	71.7
11	0	1	1	1	1	1	1	0	1	1	0	-5333.9	14.2
12	0	1	1	1	1	1	1	0	0	1	0	-5346.0	2.1
13	**0**	**1**	**1**	**1**	**1**	**1**	**1**	**0**	**0**	**0**	**0**	**-5348.1**	**0.0**
14	0	1	1	1	1	1	1	1	0	0	0	-5347.6	0.5
15	0	1	1	1	1	1	1	0	0	1	1	-5331.4	16.7

Table 5: Comparison of models for females 2009-2014, based on optimisation using maximum likelihood, and modelling errors with the Gaussian distribution.

Model	AIC	dAIC	Change in terms
mod5rgfx_ml	-9281.3	9.1	
mod4rgfx_ml	-9287.4	3.1	- hook course
mod6rgfx_ml	-9287.2	3.2	- light stick
mod9rgfx_ml	-9288.7	1.7	- weather
mod9rgfxy_ml	-9287.7	2.7	- year factor, + s(year)
mod10rgfxy_ml	-9290.4	0	- wave scale

Table 6: Models for females 2009-2014, based on optimisation using maximum likelihood, and modelling errors with the scaled t distribution.

Model	AIC	dAIC	Change in terms
mod5rgfx_scat	-11331.6	11.3	
mod4rgfx_scat	-11336.1	6.8	- hook course
mod6rgfx_scat	-11337.7	5.2	- light stick
mod9rgfx_scat	-11340.9	2.0	- weather
mod9rgfxy_scat	-11341.8	1.2	- year factor, +s(year)
mod10rgfxy_scat	-11342.9	0.0	- wave scale
mod10rgfx_scat	-11342.0	0.9	+ year factor, -s(year)

Table 7: Models for males 2009-2014, based on optimisation using maximum likelihood, and modelling errors with the scaled t distribution.

Model	AIC	dAIC	Change in terms
mod5rgmx_ml_scat	-11688.3	0.9	
mod4rgmx_ml_scat	-11689.3	0.0	- hook course
mod6rgmx_ml_scat	-11688.3	1.0	- light stick
mod9rgmx_ml_scat	-11684.8	4.4	- weather
mod9rgmxy_ml_scat	-11684.7	4.6	- year factor, +s(year)
mod10rgmxy_ml_scat	-11687.1	2.2	- wave scale

Table 8: Models for females 2015-2022, based on optimisation using maximum likelihood, and modelling errors with the scaled t distribution.

Model	AIC	dAIC	Change in terms
mod5rgtfx_ml_scat	-22046.7	11.6	
mod4rgtfx_ml_scat	-22048.9	9.3	- hook course
mod6rgtfx_ml_scat	-22049.3	8.9	- light stick
mod9rgtfx_ml_scat	-22050.8	7.4	- weather
mod9rgtfxy_ml_scat	-22042.4	15.8	- year factor, +s(year)
mod10rgtfxy_ml_scat	-22050.0	8.2	- wave scale
mod10rgtfx_ml_scat	-22058.2	0.0	+ year factor, -s(year)

Table 9: Models for males 2015-2022, based on optimisation using maximum likelihood, and modelling errors with the scaled t distribution.

Model	AIC	dAIC	Change in terms
mod5rgtmx_ml_scat	-23267.0	15.1	
mod4rgtmx_ml_scat	-23270.6	11.4	- hook course
mod6rgtmx_ml_scat	-23272.4	9.7	- light stick
mod9rgtmx_ml_scat	-23275.6	6.4	- weather
mod9rgtmxy_ml_scat	-23272.3	9.7	- year factor, +s(year)
mod10rgtmxy_ml_scat	-23278.5	3.5	- wave scale
mod10rgtmx_ml_scat	-23282.0	0.0	+ year factor, -s(year)

Table 10: Parametric coefficients for best model for females, 2015-2022.

	Estimate	Std. Error	z value	Pr(>|z|)	
(Intercept)	3.52300	0.00754	467.068	<2e-16	***
yrf2016	-0.00003	0.00517	-0.006	0.9951	
yrf2017	-0.00035	0.00598	-0.059	0.9532	
yrf2018	0.01361	0.00624	2.18	0.0292	*
yrf2019	-0.00353	0.00612	-0.577	0.5639	
yrf2020	0.00552	0.00642	0.86	0.3898	
yrf2021	0.00218	0.00580	0.376	0.7071	
yrf2022	0.00379	0.00640	0.593	0.5533	

Table 11: Smooth terms of best model for females, 2015-2022.

	edf	Ref.df	Chi.sq	p-value	
s(loglen)	8.042	10.0	314621.2	<2e-16	***
s(obs_name)	114.769	119.0	6625.9	<2e-16	***
te(lon,lat,mon)	50.278	68.3	238.7	<2e-16	***
s(hbf)	6.498	7.6	59.8	<2e-16	***

Table 12: Parametric coefficients of the best model with interaction terms based on data for both sexes, 2015-2022.

	Estimate	Std. Error	z value	Pr(>|z|)	
(Intercept	3.50E+03	6.35E-03	551.928	< 2e-16	***
yrf2016	-3.59E-03	3.79E-03	-0.946	0.34413	
yrf2017	5.36E-03	4.32E-03	1.241	0.2147	
yrf2018	1.45E-02	4.56E-03	3.166	0.00154	**
yrf2019	-5.20E-05	4.48E-03	-0.012	0.99074	
yrf2020	2.25E-03	4.68E-03	0.481	0.63053	
yrf2021	8.83E-03	4.30E-03	2.054	0.04002	*
yrf2022	1.59E-03	4.71E-03	0.337	0.73599	

Table 13: Smooth terms of the best model with interaction terms based on data for both sexes, 2015-2022.

	edf	Ref.df	Chi.sq	p-value	
ti(loglen)	9.4	11.5	253.1	< 2e-16	***
s(obs_name)	113.8	117.0	9216.3	< 2e-16	***
ti(lat)	6.1	6.8	31.0	4.39E-05	***
ti(lon)	9.2	11.2	64.3	< 2e-16	***
ti(mon)	3.7	6.0	41.4	< 2e-16	***
ti(lat,lon)	7.8	77.0	32.7	2.92E-05	***
ti(lon,mon)	12.1	36.0	112.7	< 2e-16	***
ti(lat,mon)	13.6	36.0	81.3	< 2e-16	***
ti(lat,lon,mon)	36.8	162.0	394.6	< 2e-16	***
ti(lat,loglen)	5.7	7.6	9.9	0.231	
ti(lon,loglen)	16.6	19.8	130.3	< 2e-16	***
ti(lat,lon,loglen)	40.6	54.4	219.0	< 2e-16	***
ti(loglen):yrf2015	2.6	3.1	31157.4	< 2e-16	***
ti(loglen):yrf2016	1.4	1.7	26590.0	< 2e-16	***
ti(loglen):yrf2017	3.7	4.0	34703.8	< 2e-16	***
ti(loglen):yrf2018	1.0	1.0	32520.1	< 2e-16	***
ti(loglen):yrf2019	1.0	1.0	33544.7	< 2e-16	***
ti(loglen):yrf2020	1.8	2.3	30741.3	< 2e-16	***
ti(loglen):yrf2021	1.0	1.0	31013.1	< 2e-16	***
ti(loglen):yrf2022	1.0	1.0	30161.3	< 2e-16	***
s(hbf)	7.3	8.3	101.1	< 2e-16	***

Table 14: Parameter estimates for length weight relationships by period across all locations and seasons, based on standard methods that assume weight = a.length^b, but account for observer effects.

Period	Parameter	Value	CV	R^2	N
2009-2014	A	1.108e-5	0.025	0.950	13210
	B	3.087	0.0015		
2015-2022	A	1.274e-5	0.018	0.960	24116
	B	3.058	0.0012		

Table 15: Parameter estimates for length weight relationships by region and period, based on standard methods that assume weight = a.length^b, but account for observer effects.

Period	Region	a	a.cv	b	b.cv	R^2	n
2009-2014	2	1.44E-05	0.101	3.037	6.80E-03	0.967	735
	3	9.98E-06	0.098	3.109	6.55E-03	0.934	1030
	4	1.01E-05	0.039	3.107	2.14E-03	0.959	6237
	5	8.57E-06	0.136	3.135	8.90E-03	0.909	736
	6	1.11E-05	0.127	3.086	8.48E-03	0.943	451
	10	1.11E-05	0.042	3.093	2.67E-03	0.947	3400
	11	2.16E-05	0.154	2.948	1.08E-02	0.963	392
2015-2022	1	1.66E-05	0.121	3.001	8.44E-03	0.962	573
	2	1.10E-05	0.053	3.090	3.50E-03	0.961	3023
	3	1.26E-05	0.043	3.062	2.87E-03	0.947	4477
	4	1.01E-05	0.040	3.104	2.60E-03	0.948	6266
	6	1.22E-05	0.067	3.065	4.48E-03	0.958	1616
	10	1.07E-05	0.029	3.090	1.87E-03	0.970	7368
	11	2.39E-05	0.137	2.931	9.76E-03	0.969	337

Figures

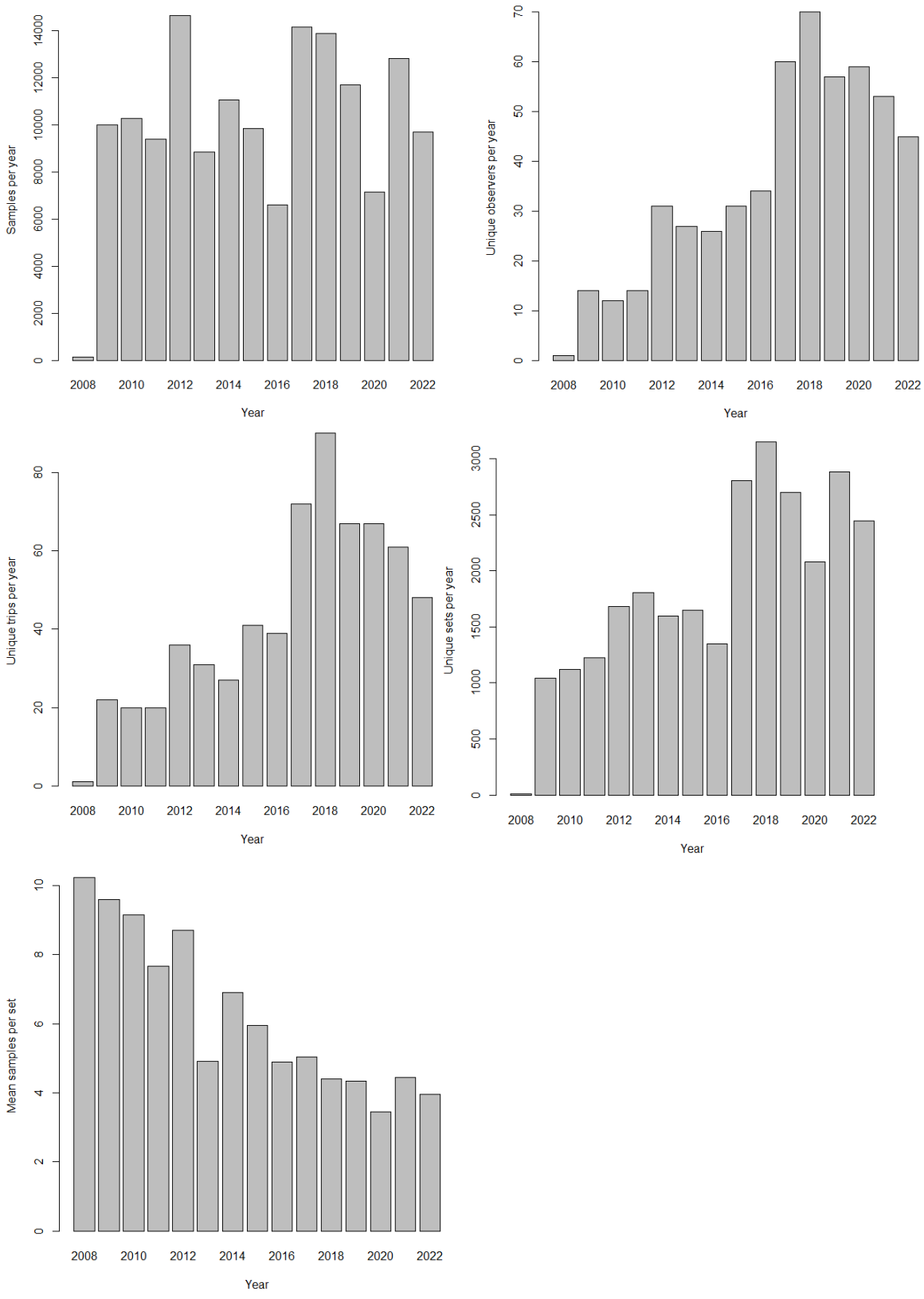

Figure 1: Unique observers per year (top left), trips per year (top right), sampled sets per year (mid left), samples per set per year (mid right), and total samples per year (lower left).

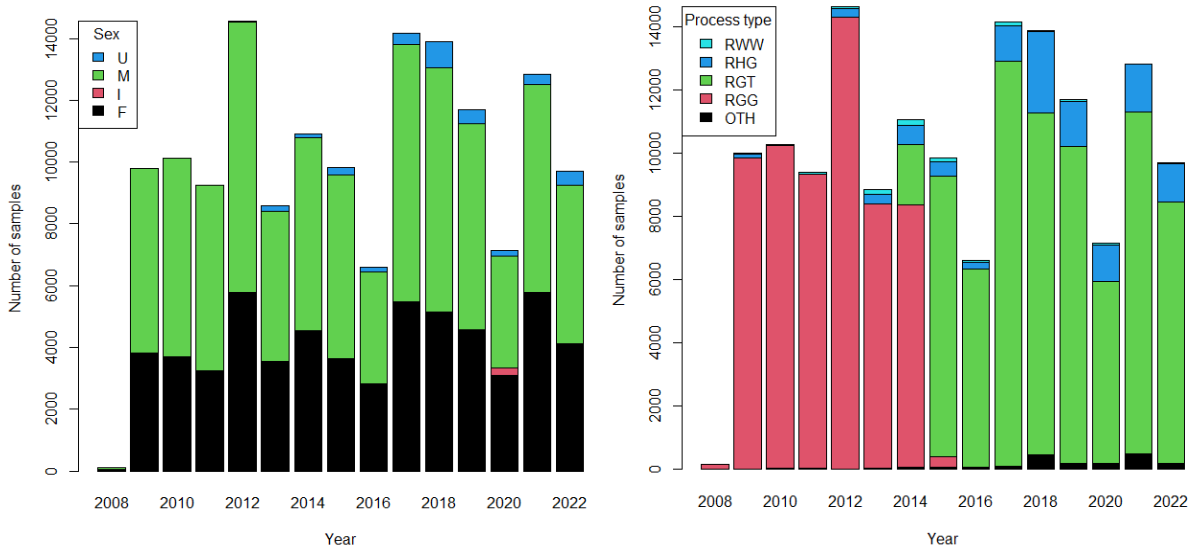

Figure 2: Samples of each sex (left) and process type (right) per year.

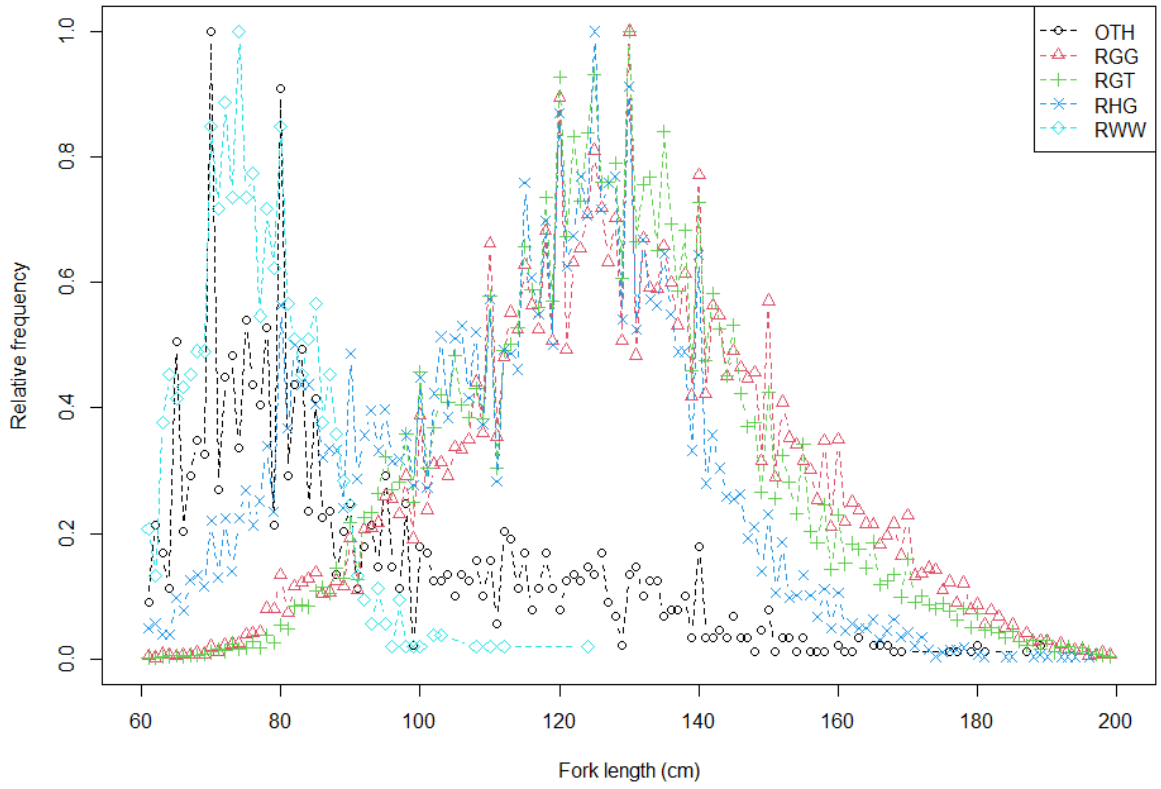

Figure 3: Length frequency distribution by process type.

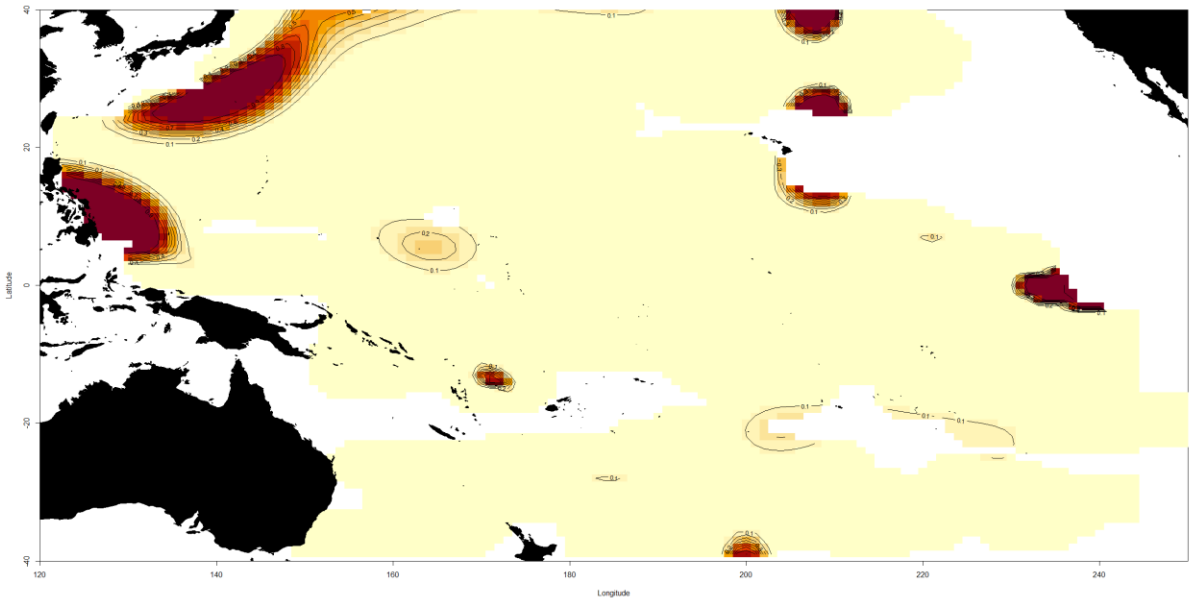

Figure 4: Map showing the spatial distribution of the predicted proportions of fish reported as process type RHG. The majority of such fish are reported close to coastal areas.

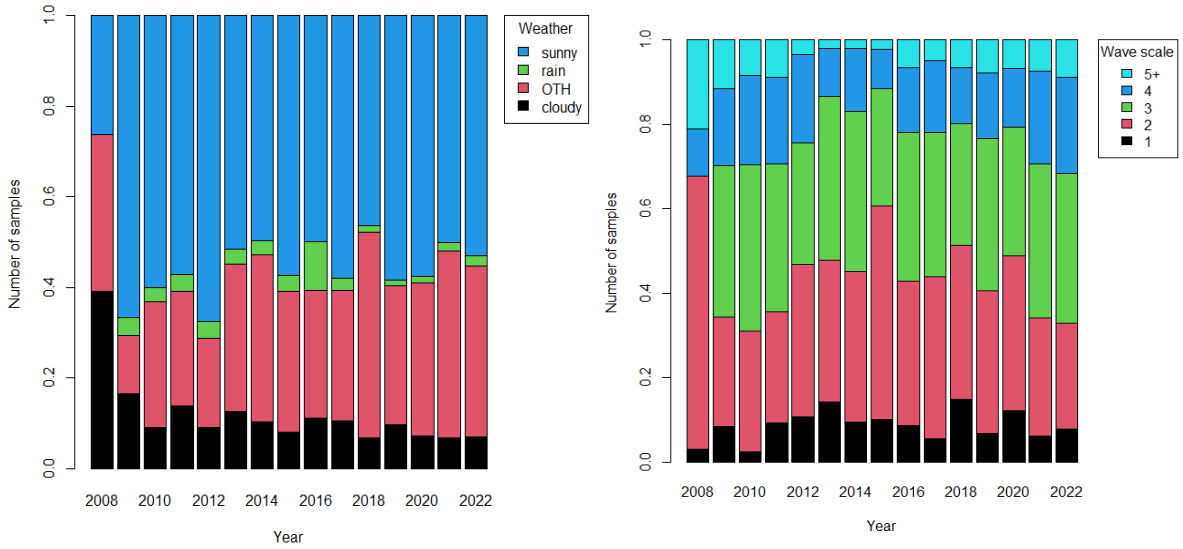

Figure 5: Proportions of samples by reported weather (left) and wave scale (right) per year.

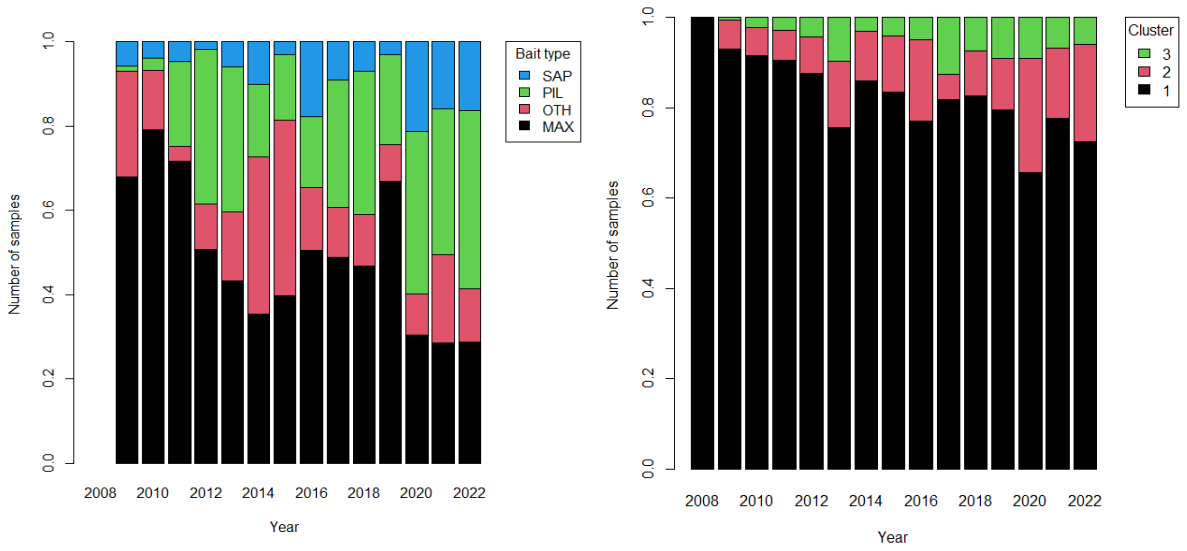

Figure 6: Proportions of samples by reported bait type (left) and allocated cluster (right) per year.

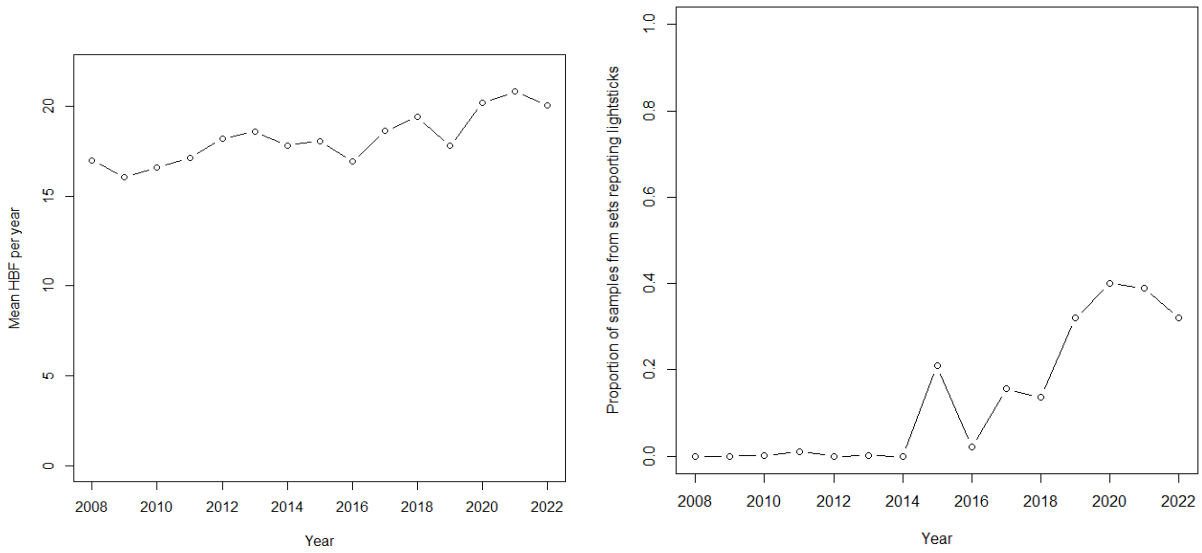

Figure 7: Mean HBF across all samples per year (left) and proportions of samples associated with sets reporting light sticks (right).

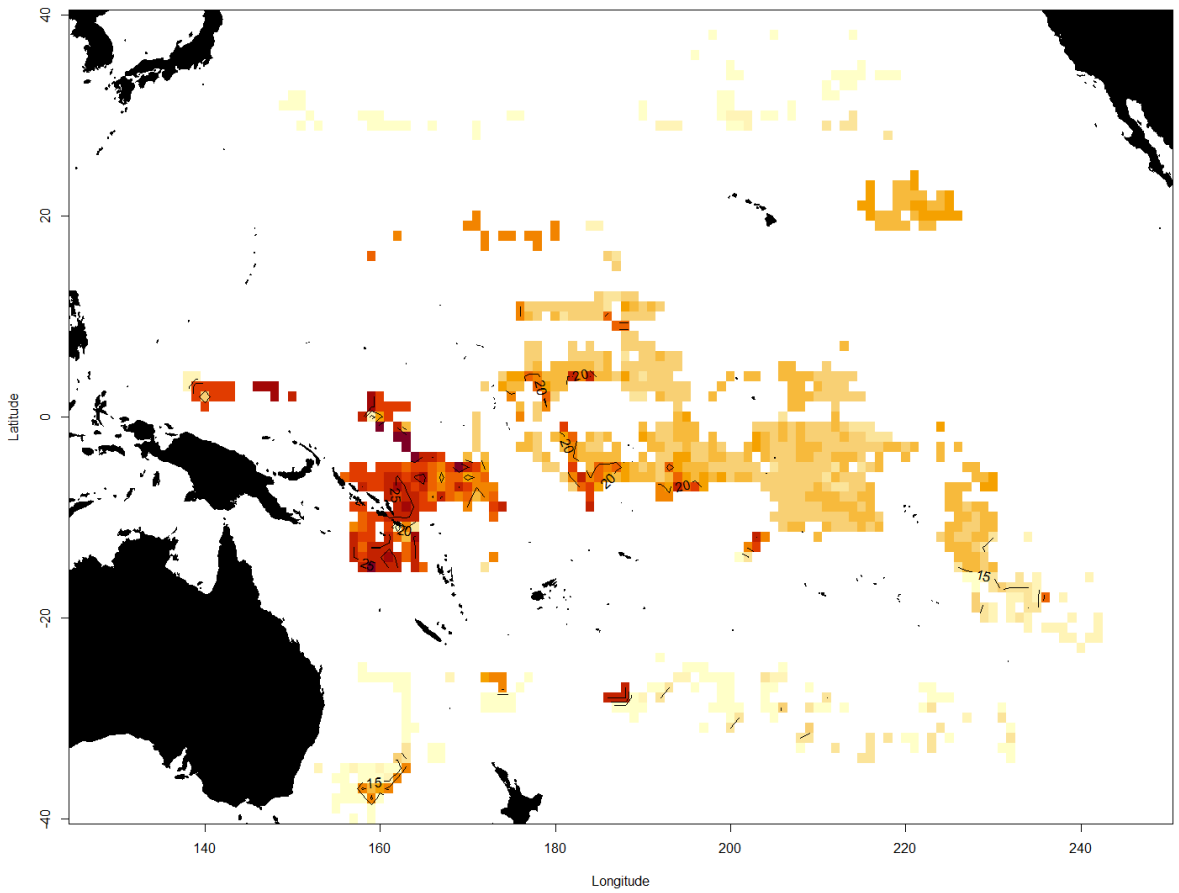

Figure 8: Map of the distribution of mean HBF during the period 2009-2014, showing spatial patterns and higher HBF in the west.

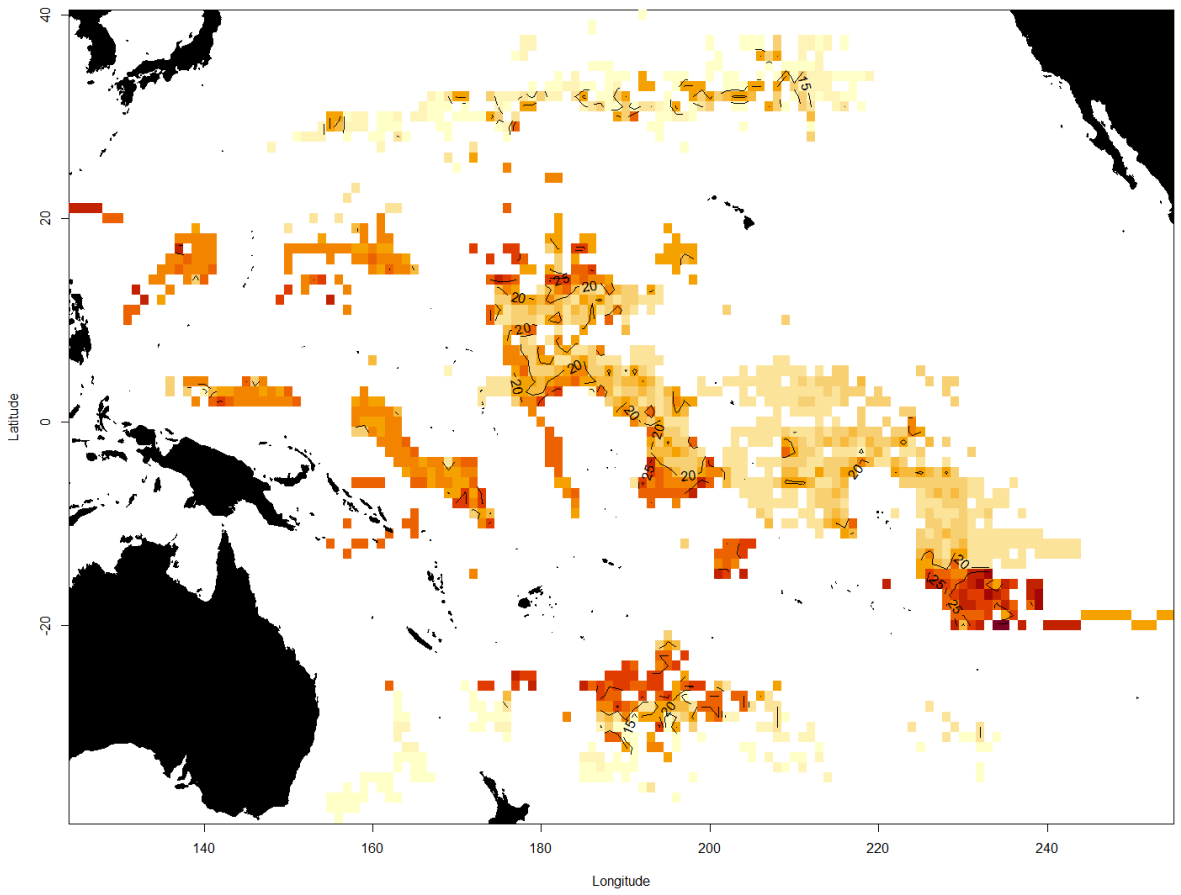

Figure 9: Map of the distribution of mean HBF during the period 2015-2022, showing spatial patterns and higher HBF in the southeast.

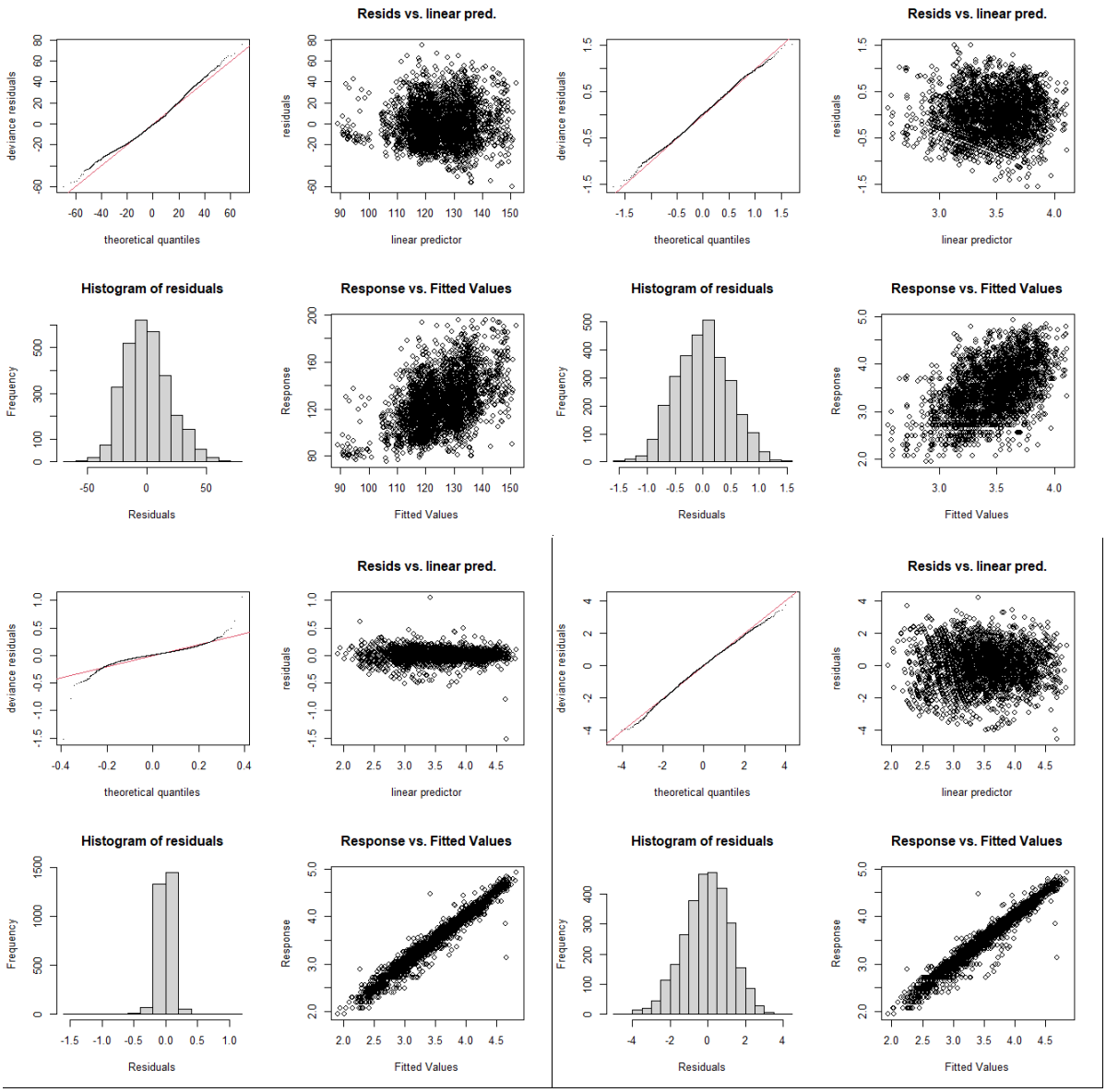

Figure 10: Residual distribution plots for four models, with four plots for each model. Residuals are plotted for the model of length with Gaussian residuals (top left), log weight with Gaussian residuals (top right), log weight ~ log length with Gaussian residuals (lower left), and log weight ~ log length with scaled t-distribution residuals (lower right).

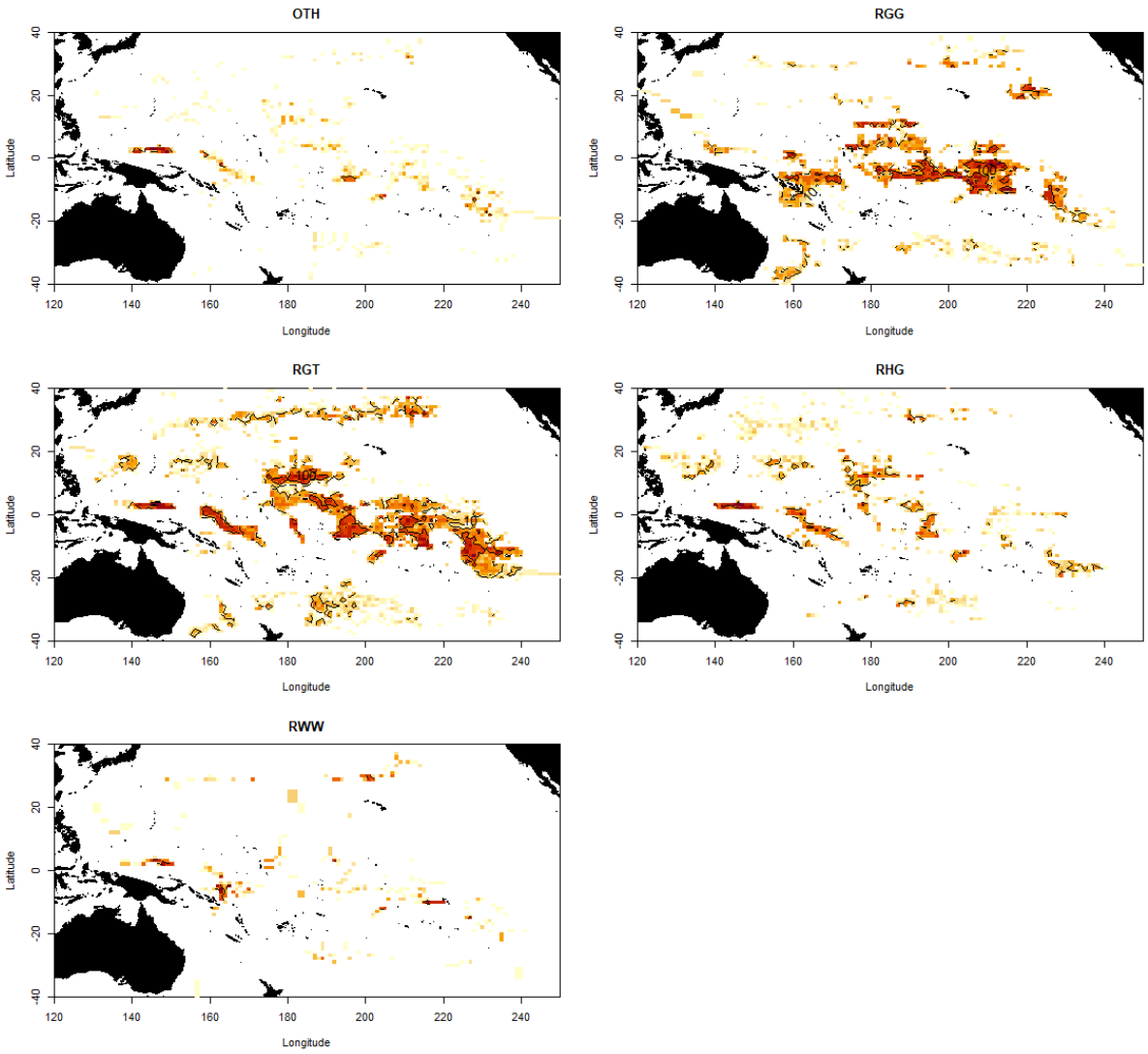

Figure 11: Sampling location maps by process type.

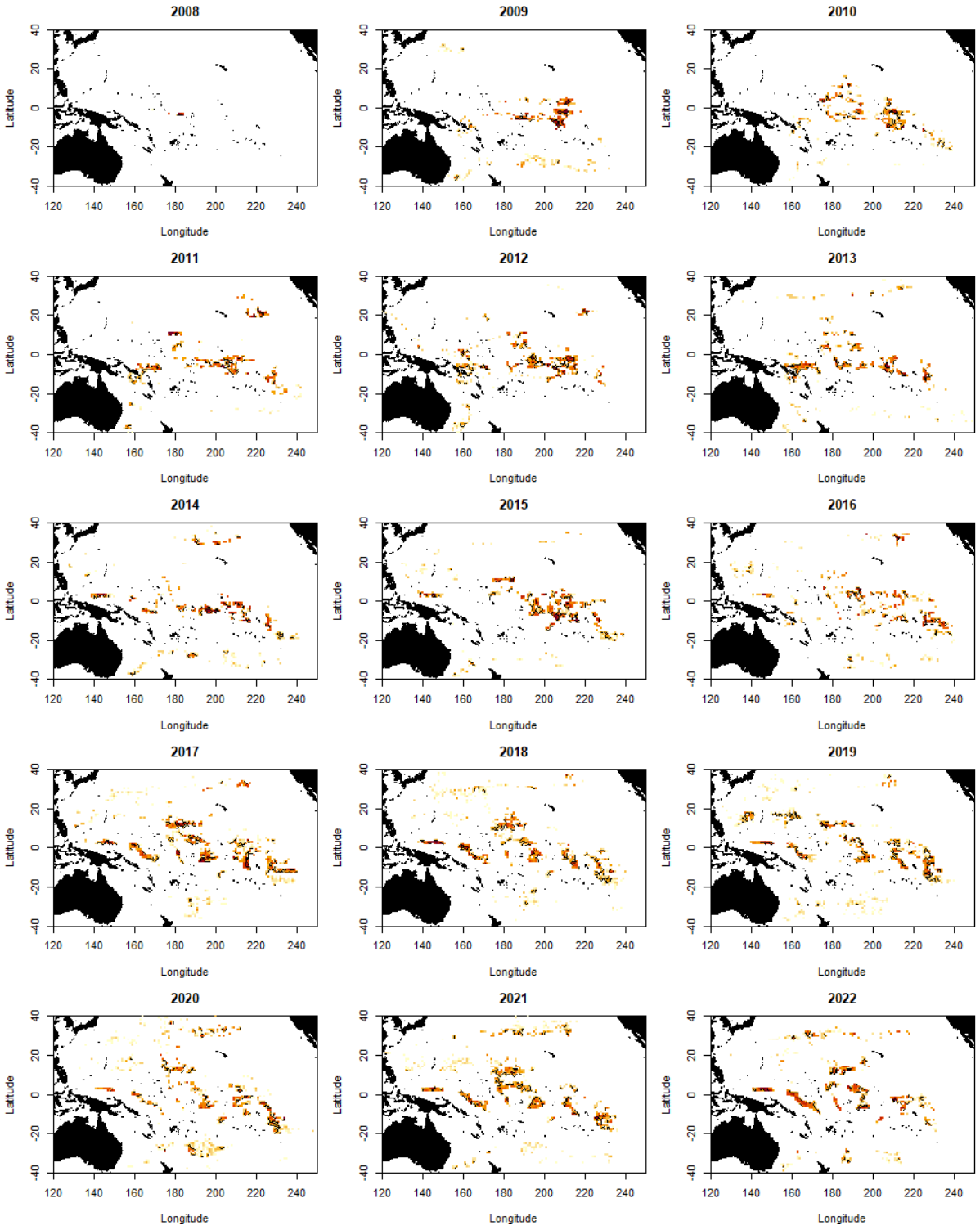

Figure 12: Maps of sample locations by year.

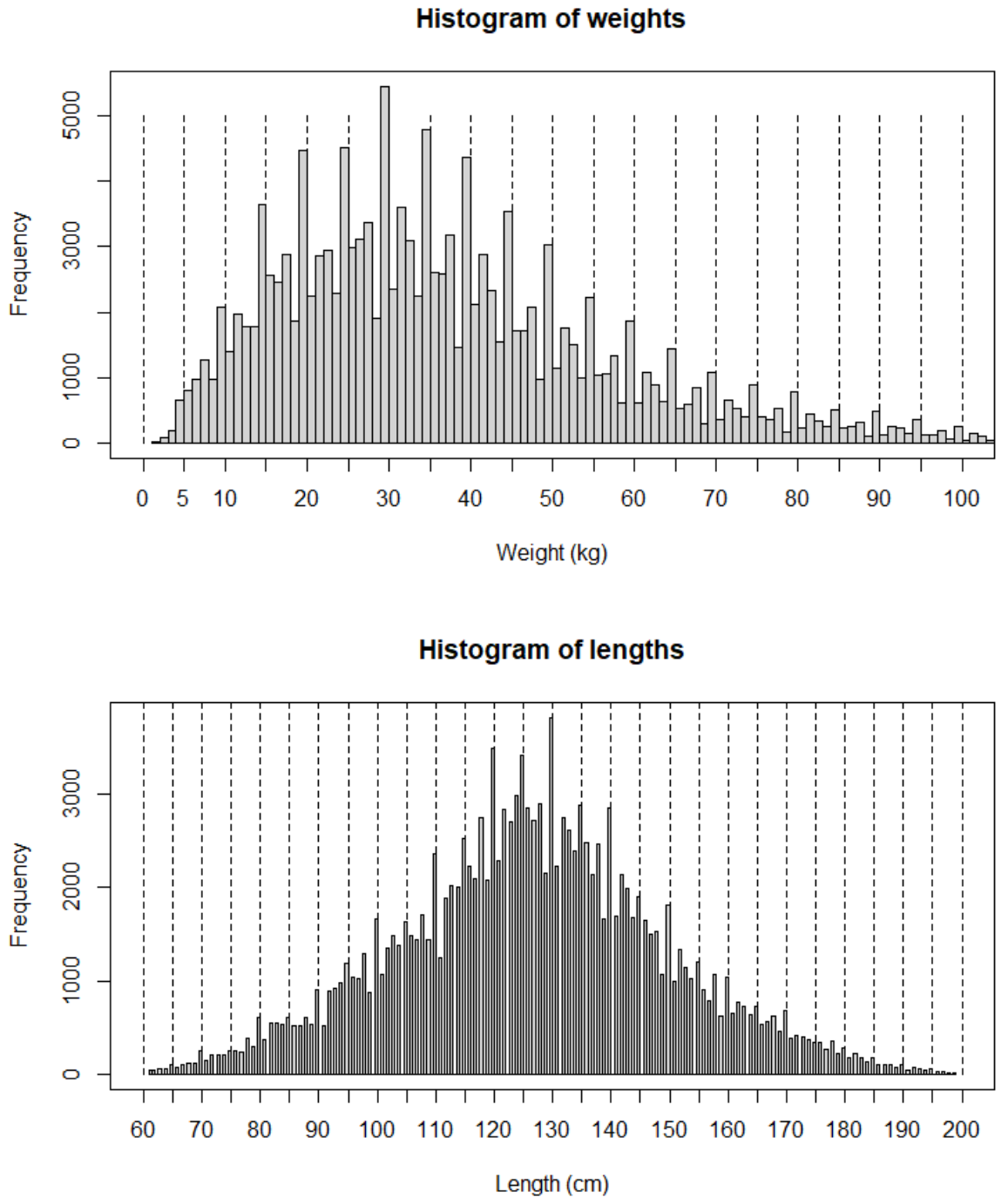

Figure 13:: Size frequency histograms for weight (above) and length (below) data. Lines have been added at intervals of 5 kg and 5 cm, to highlight the peaks that occur due to rounding.

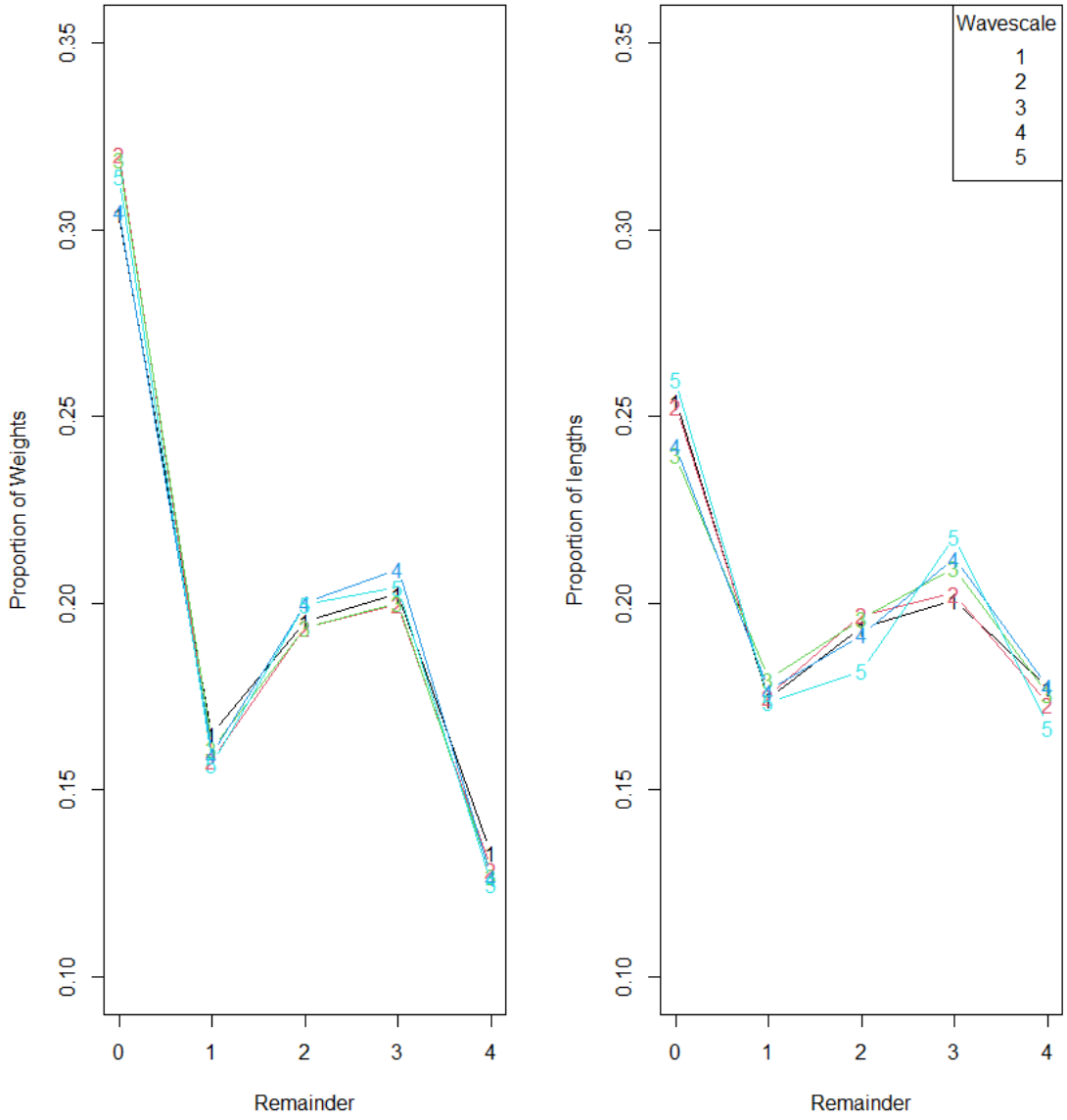

Figure 14: Rounding patterns by reported wave scale. Without rounding, 20% of samples would be expected for each value of the remainder.

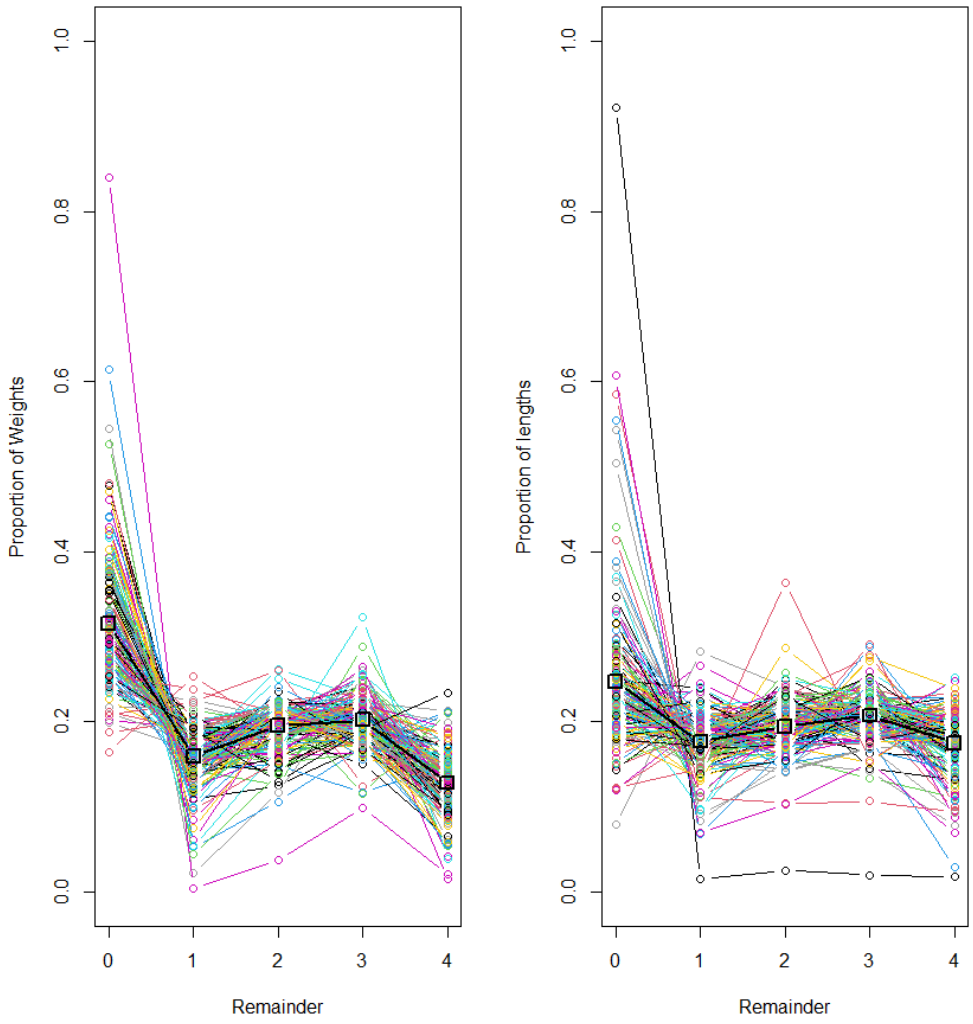

Figure 15: Measurement rounding by observer, for observers with at least 200 samples. The proportion of all samples in each rounding class is highlighted in black with square markers. Without rounding, 20% of samples would be expected for each value of the remainder.

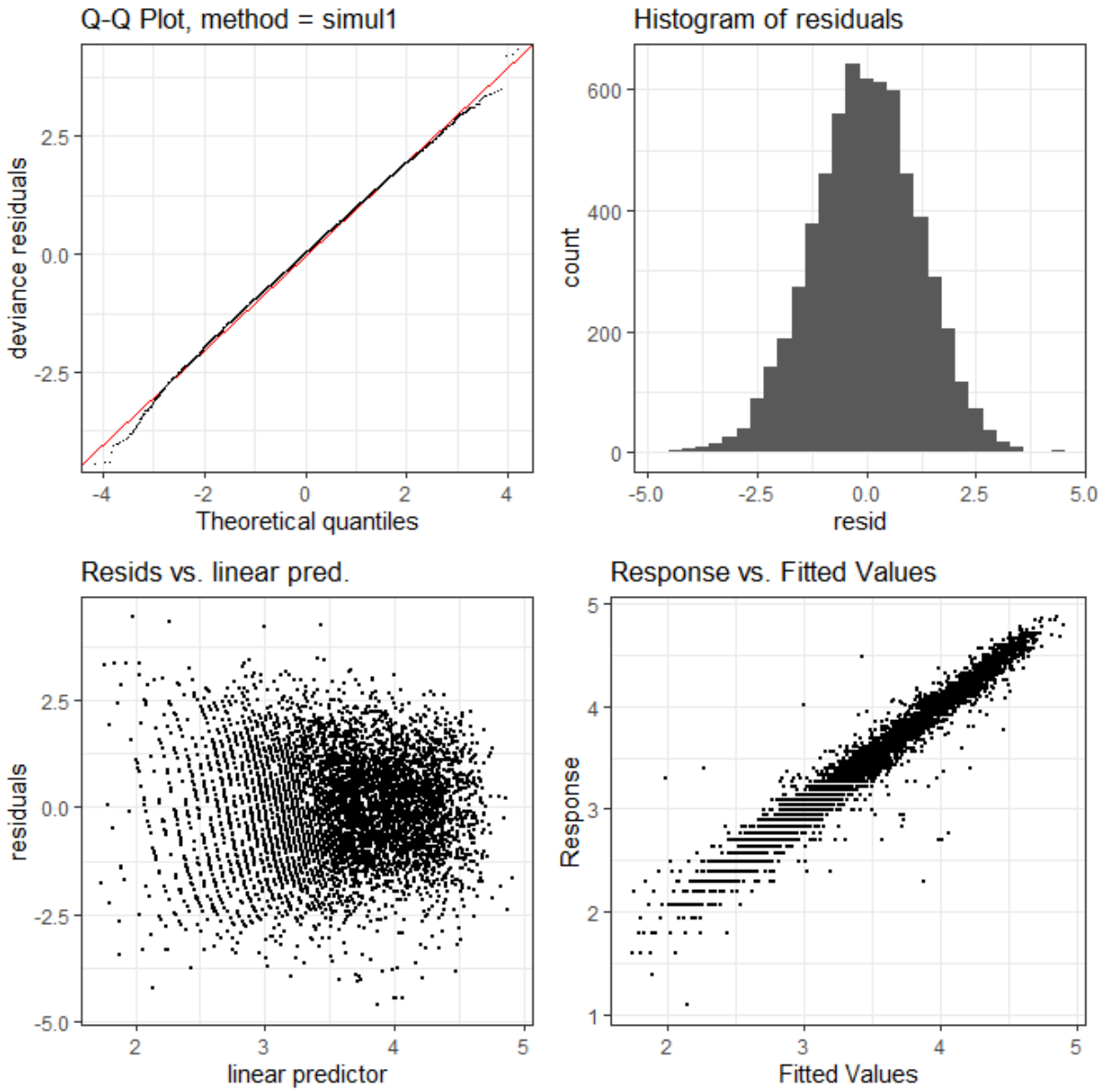

Figure 16: Diagnostic plots for best model of LW for females reported as process type RGG from 2009-2014.

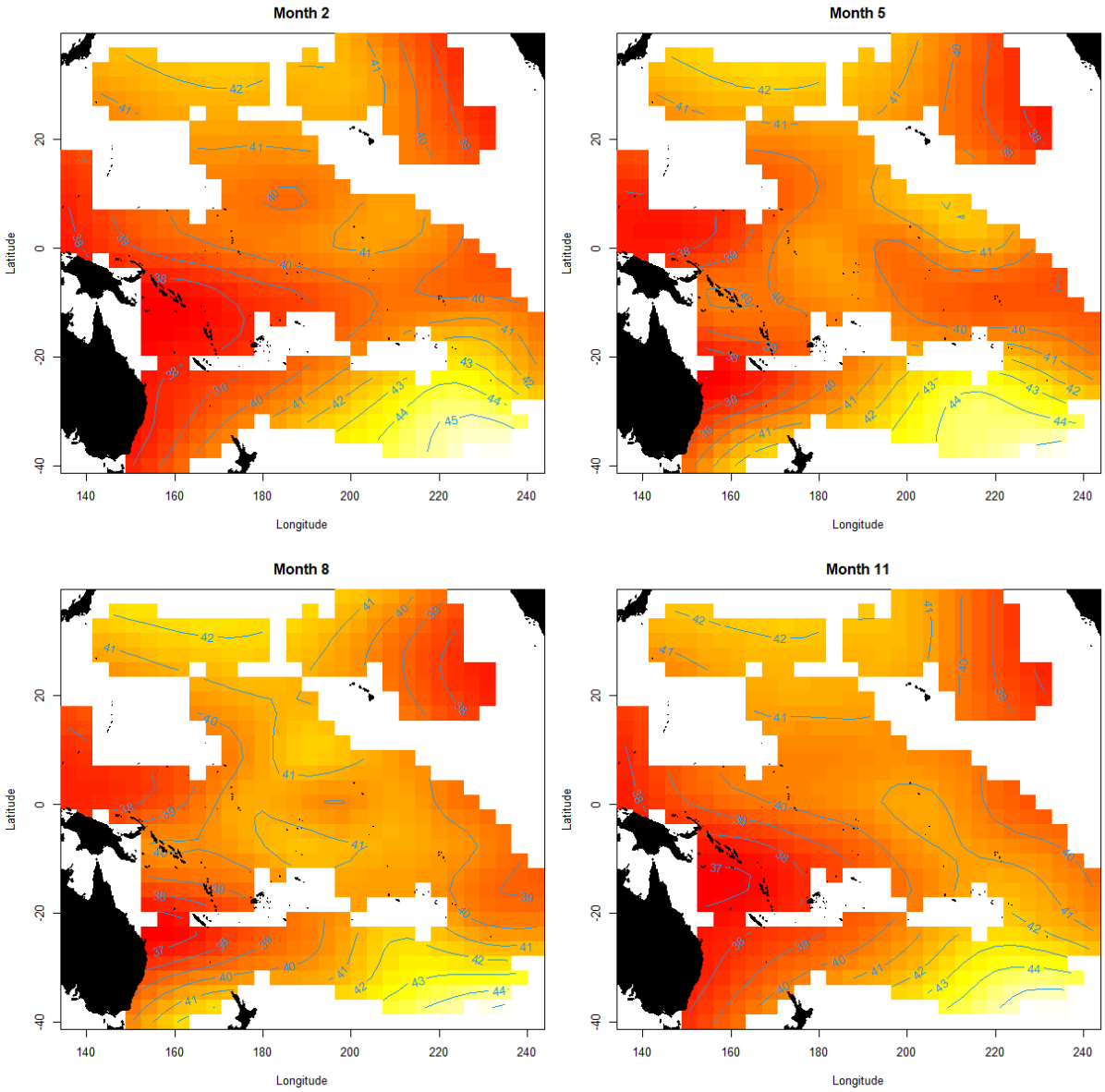

Figure 17: Predicted weight by location and month for length 130 cm caught using HBF of 20 at wave scale 2 in 2012, based on the best fitting model of data for females from 2009-2014.

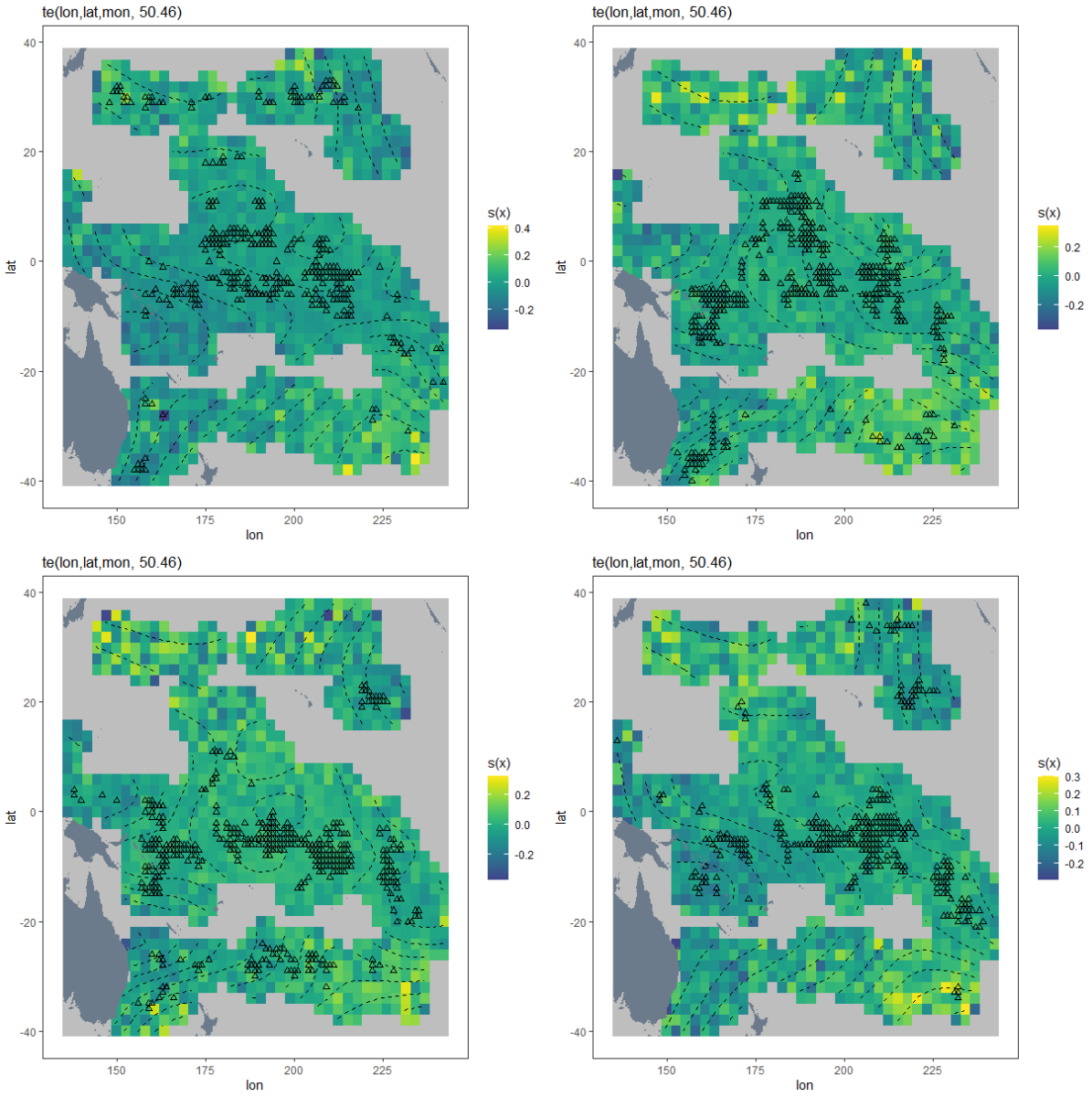

Figure 18: Effect plot by location and month (2, 5, 8, and 11) from the best fitting model of data for females from 2009-2014. The fitted effect is perturbed at each location by adding a random variable based on the local variance. Thus areas with more uncertainty appear more noisy. The triangles represent locations of observations closest to the month addressed by the plot.

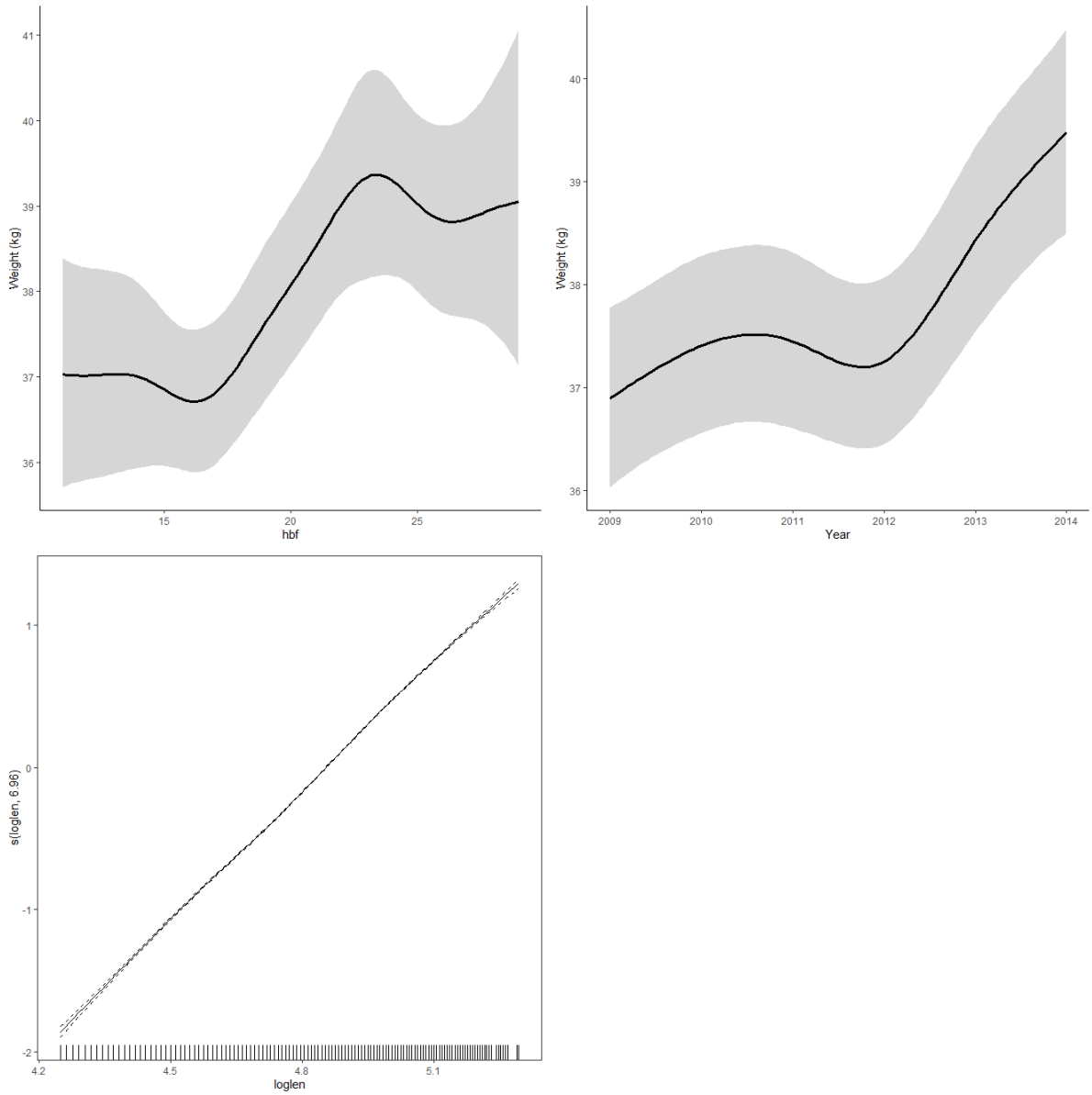

Figure 19: Predicted mean weight at length 130 cm by HBF (top left) and year (top right), based on the best fitting model of data for females from 2009-2014. In each case the variables latitude, longitude, month, and either hbf or year were excluded from the prediction, which resulted in the average effect being applied for these smooths. The partial effect of the log length smoother is shown at lower left.

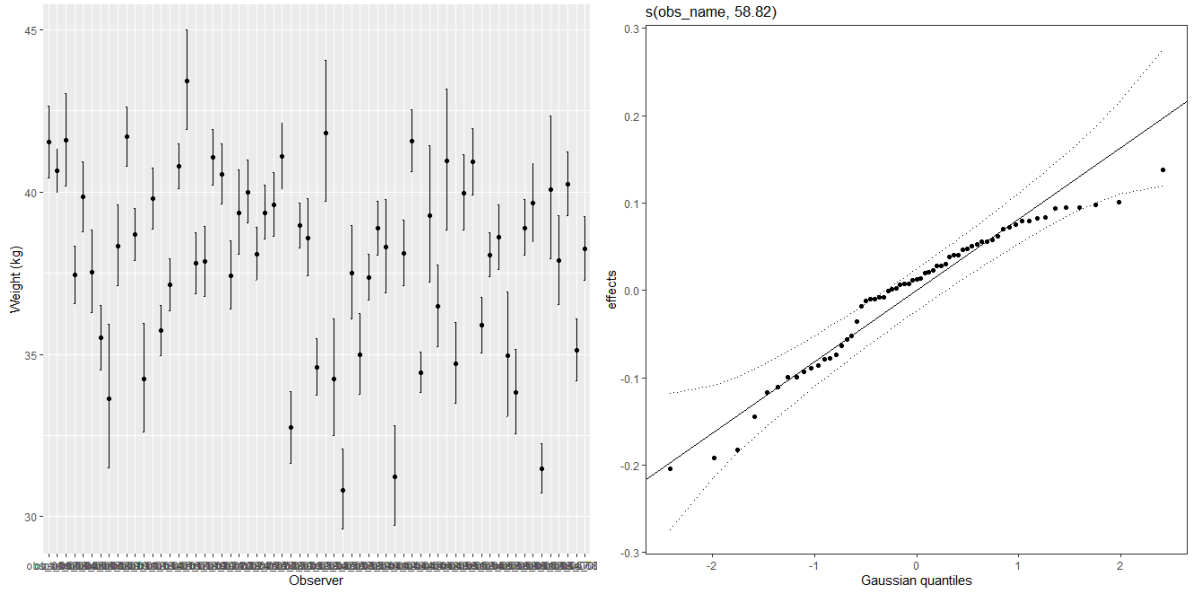

Figure 20: Predicted mean weight at length 130 cm by observer (left), based on the best fitting model of data for females from 2009-2014. In each case the variables latitude, longitude, month, hbf, and year were excluded from the prediction, which resulted in the average effect being applied for these smooths. The qq plot (right) shows the degree to which observer effects are normally distributed.

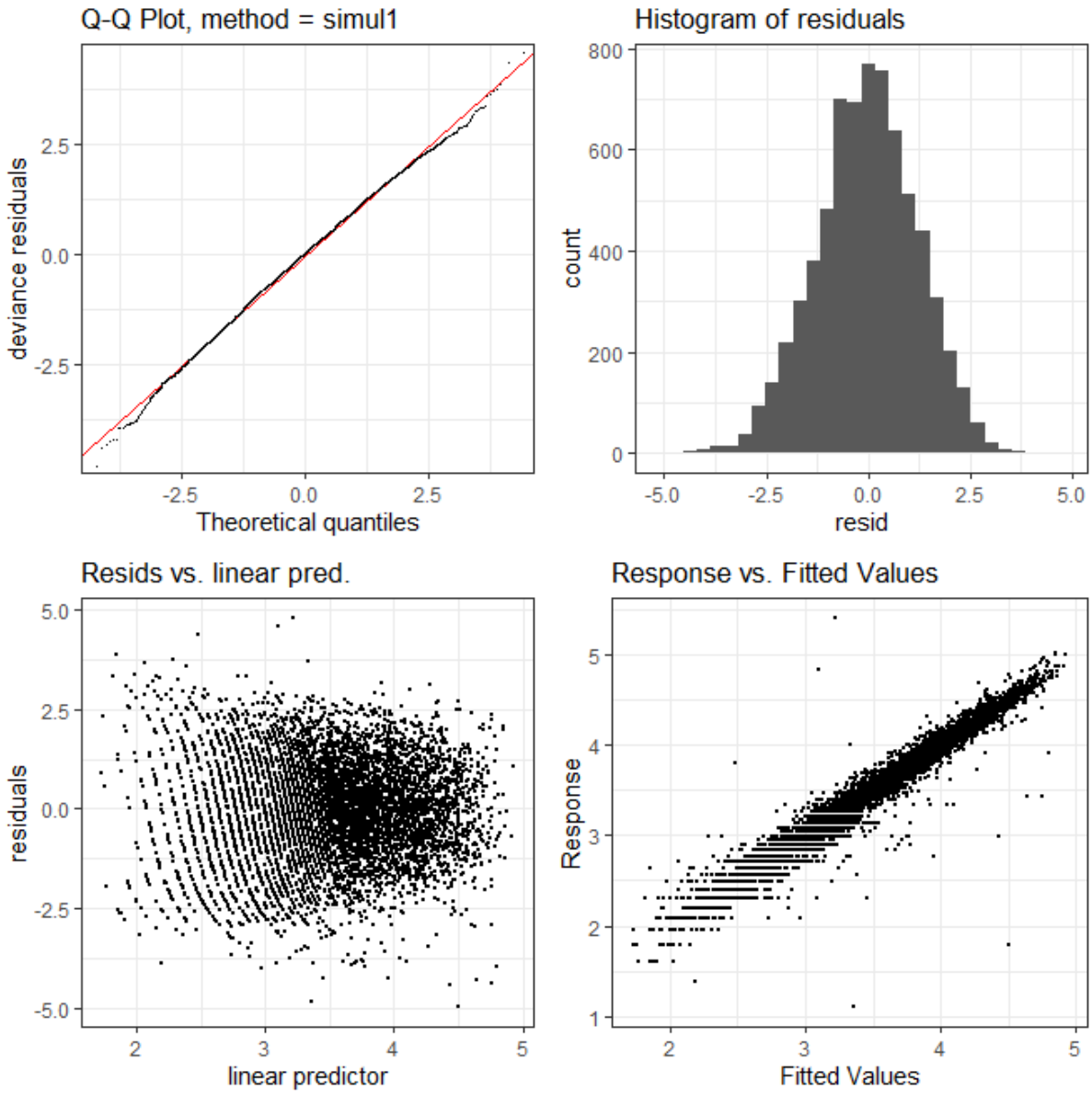

Figure 21: Diagnostic plots for best model of LW for males reported as process type RGG from 2009-2014.

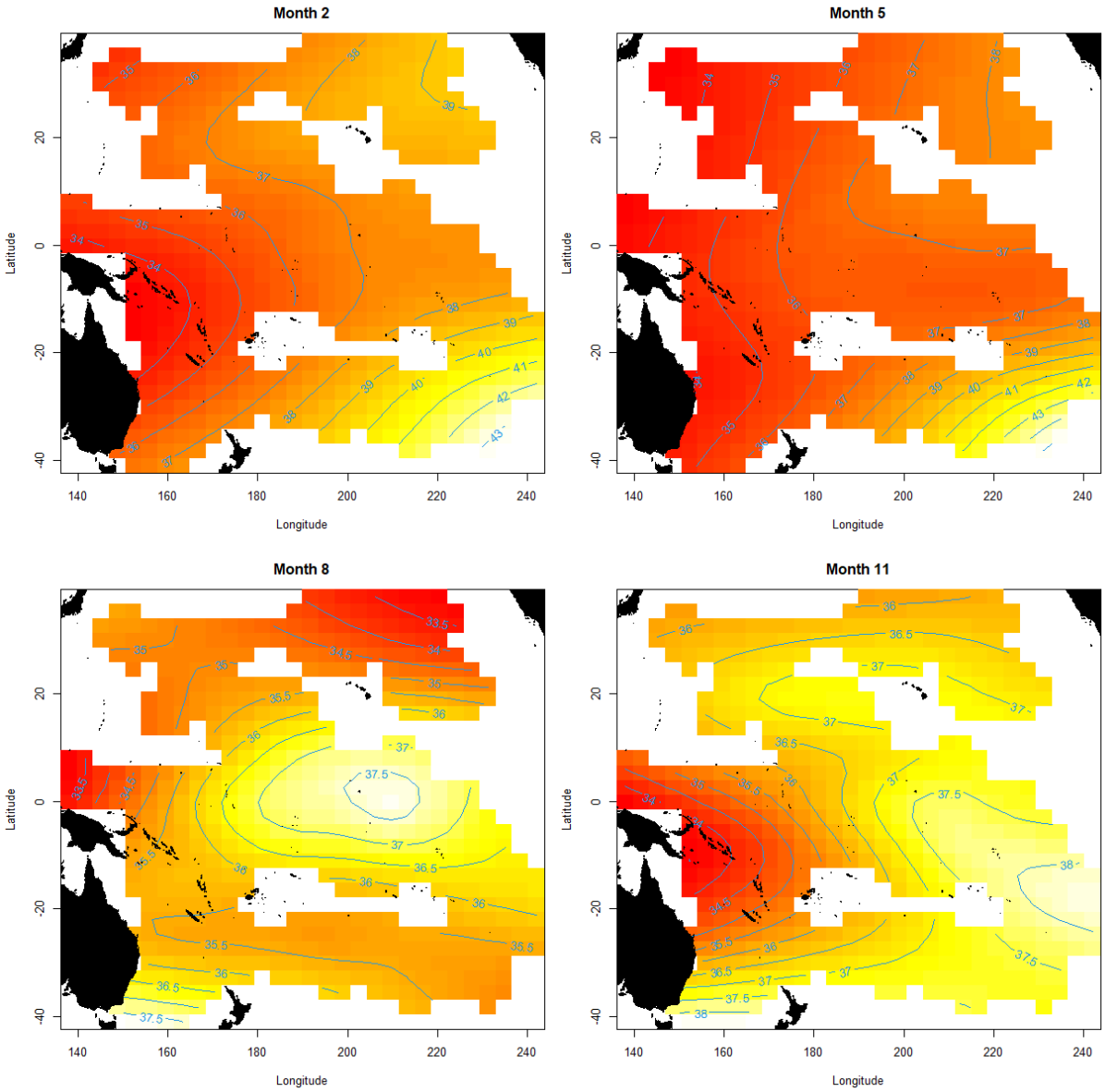

Figure 22: Predicted weight by location and month for length 130 cm caught using HBF of 20 at wave scale 2 in 2012, based on the best fitting model of data for males from 2009-2014.

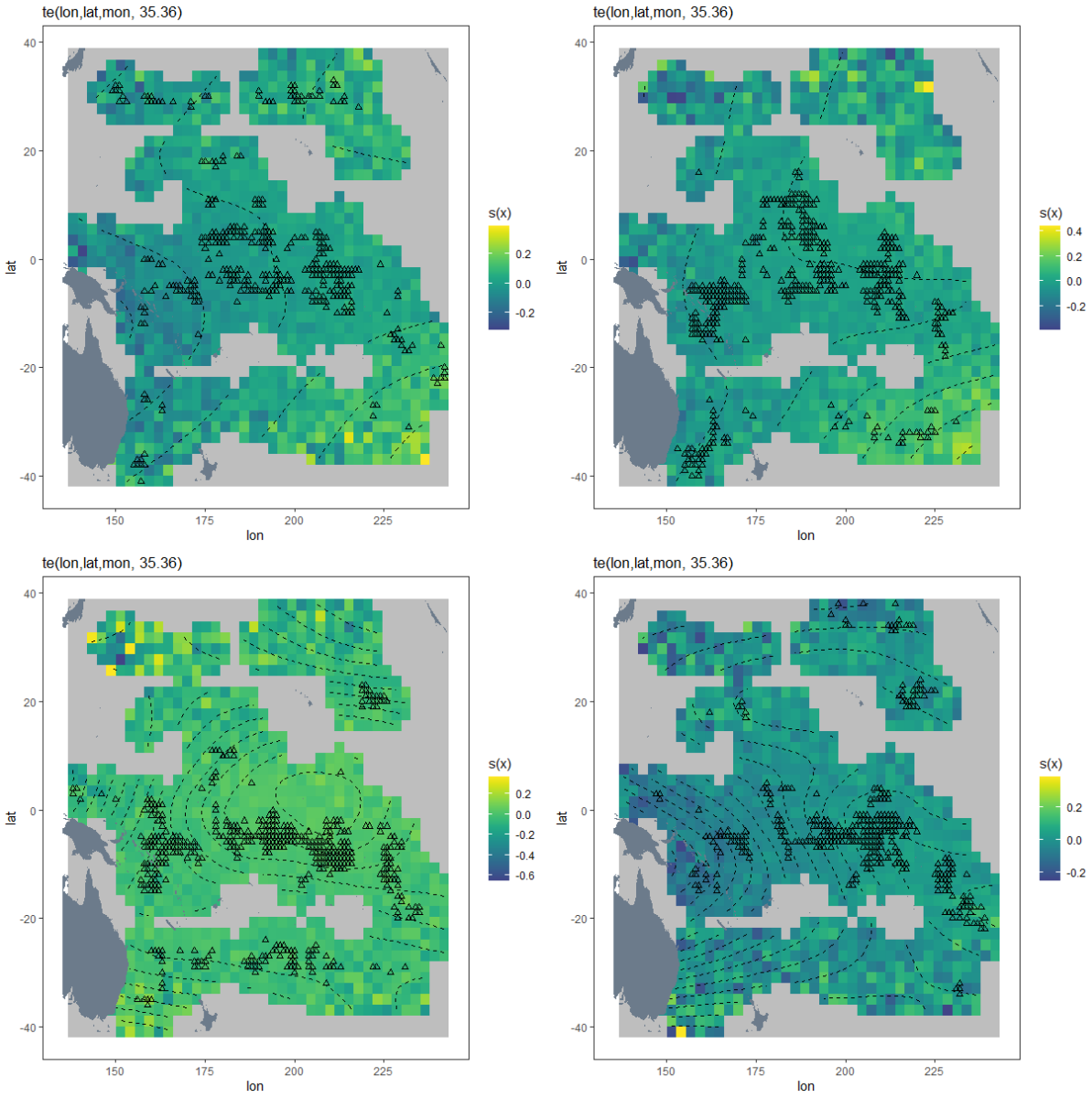

Figure 23: Effect plot by location and month (2, 5, 8, and 11) from the best fitting model of data for males from 2009-2014. The fitted effect is perturbed at each location by adding a random variable based on the local variance. Thus areas with more uncertainty appear more noisy. The triangles represent locations of observations closest to the month addressed by the plot.

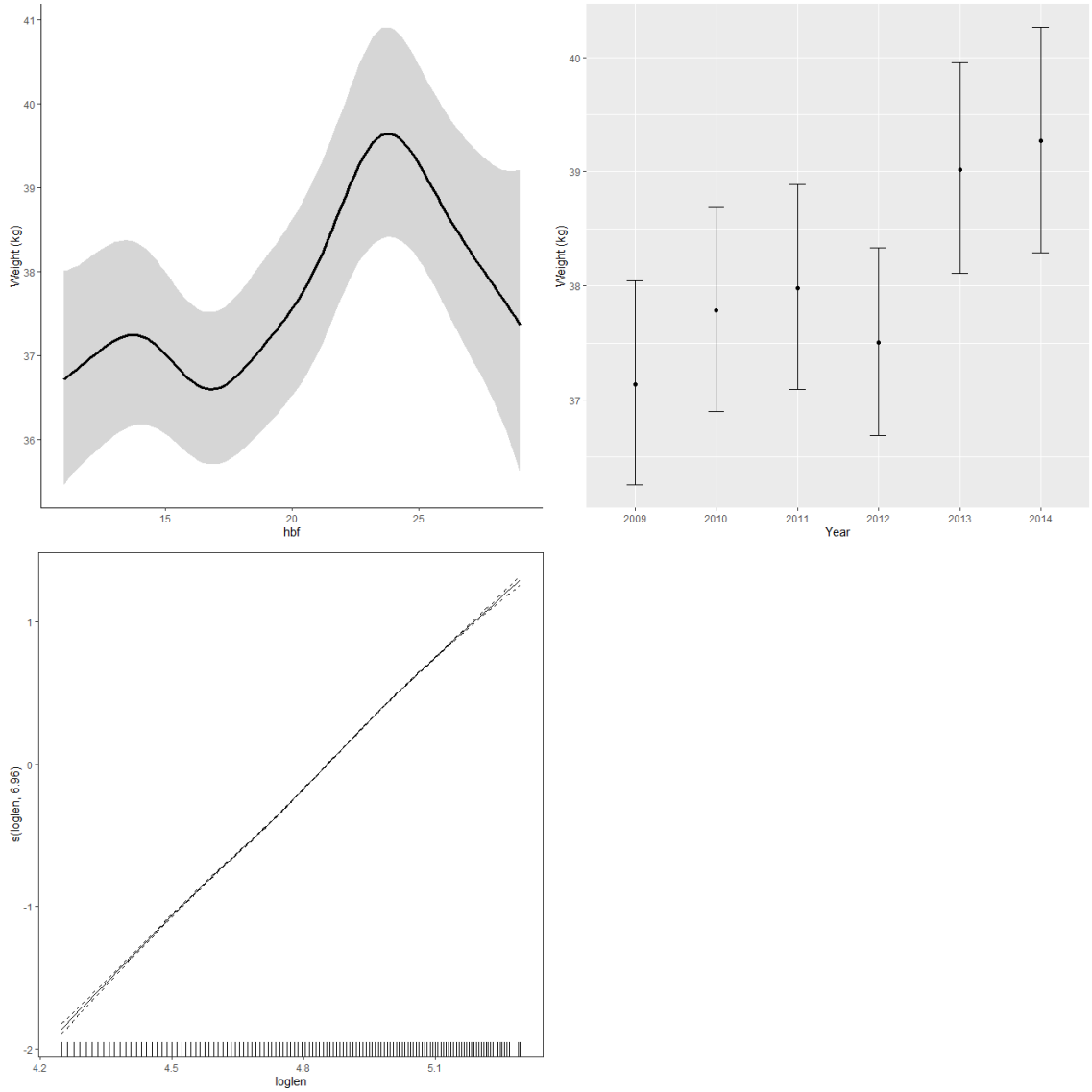

Figure 24: Predicted mean weight at length 130 cm by HBF (top left) and year (top right) based on the best fitting model of data for males from 2009-2014. In each case the variables latitude, longitude, month, and either hbf or year were excluded from the prediction, which resulted in the average effect being applied for these smooths. The partial effect of the log length smoother is shown at lower left.

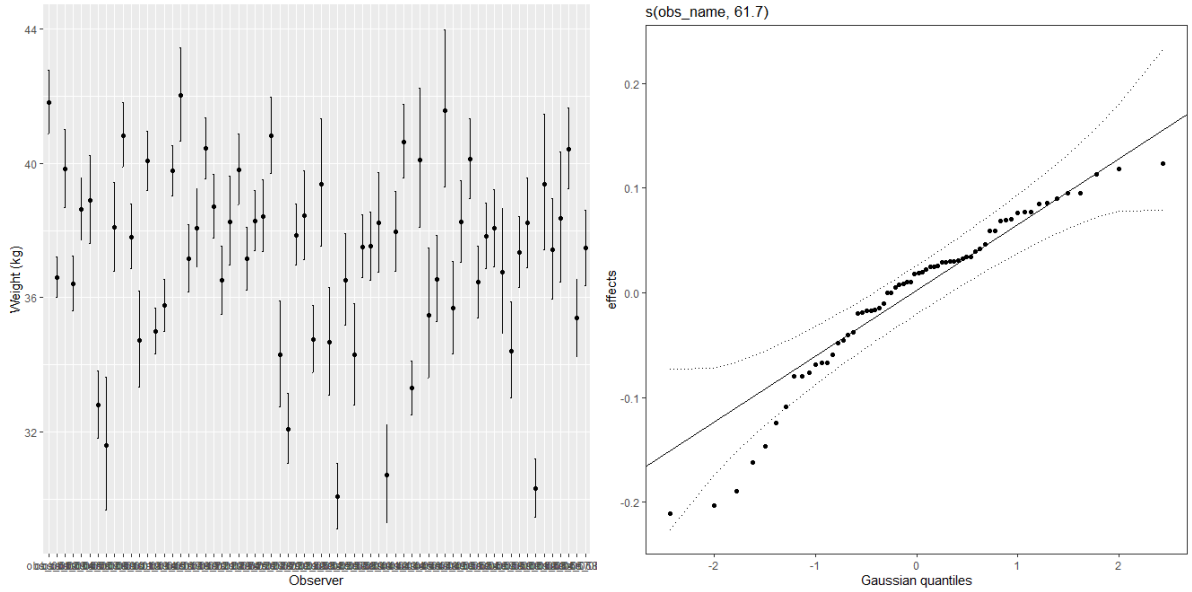

Figure 25: Predicted mean weight at length 130 cm by observer (left), based on the best fitting model of data for males from 2009-2014. In each case the variables latitude, longitude, month, hbf, and year were excluded from the prediction, which resulted in the average effect being applied for these smooths. The qq plot (right) shows the degree to which observer effects are normally distributed.

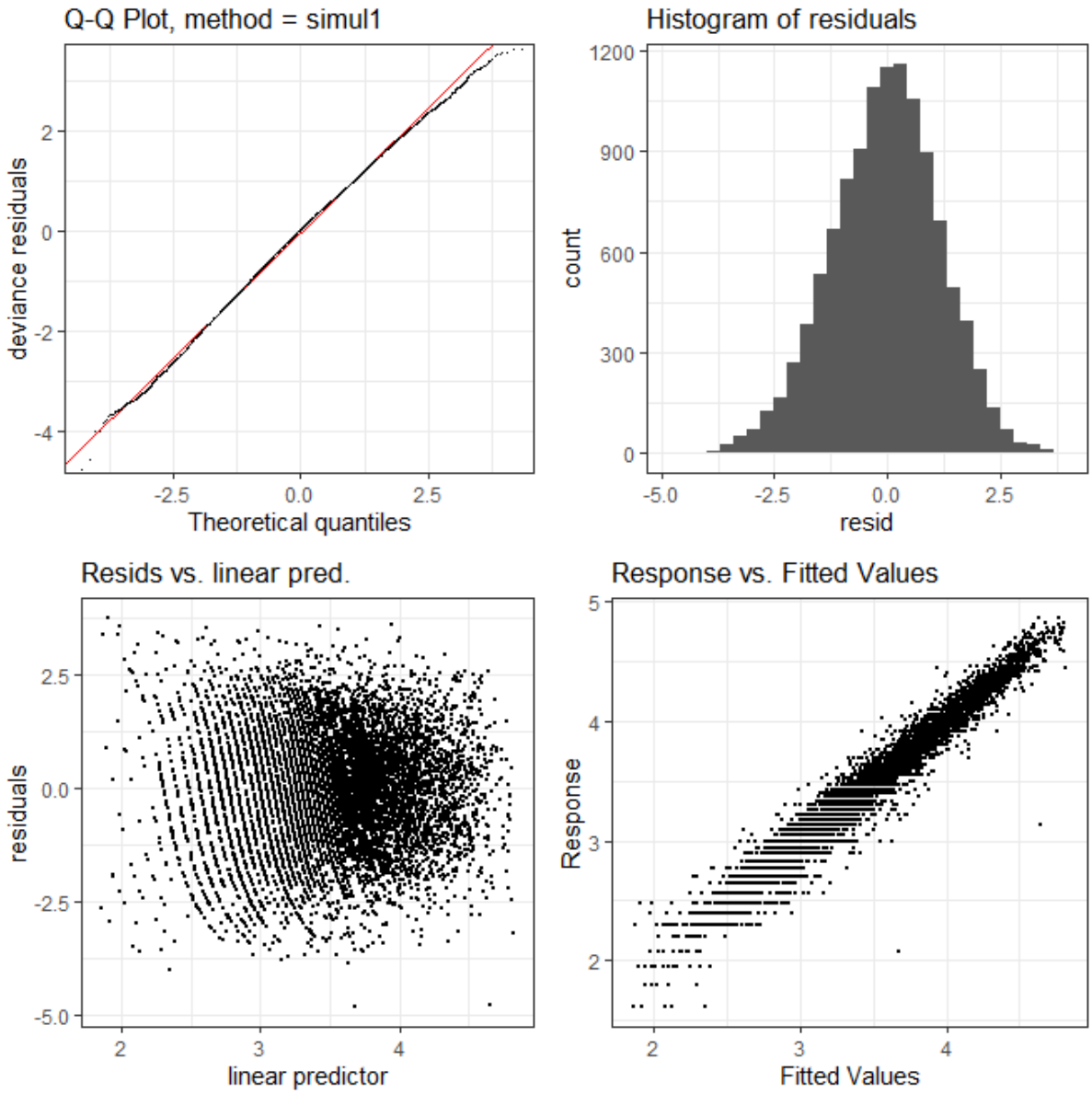

Figure 26: Diagnostic plots for best model of LW for females reported as process type RGG from 2015-2022.

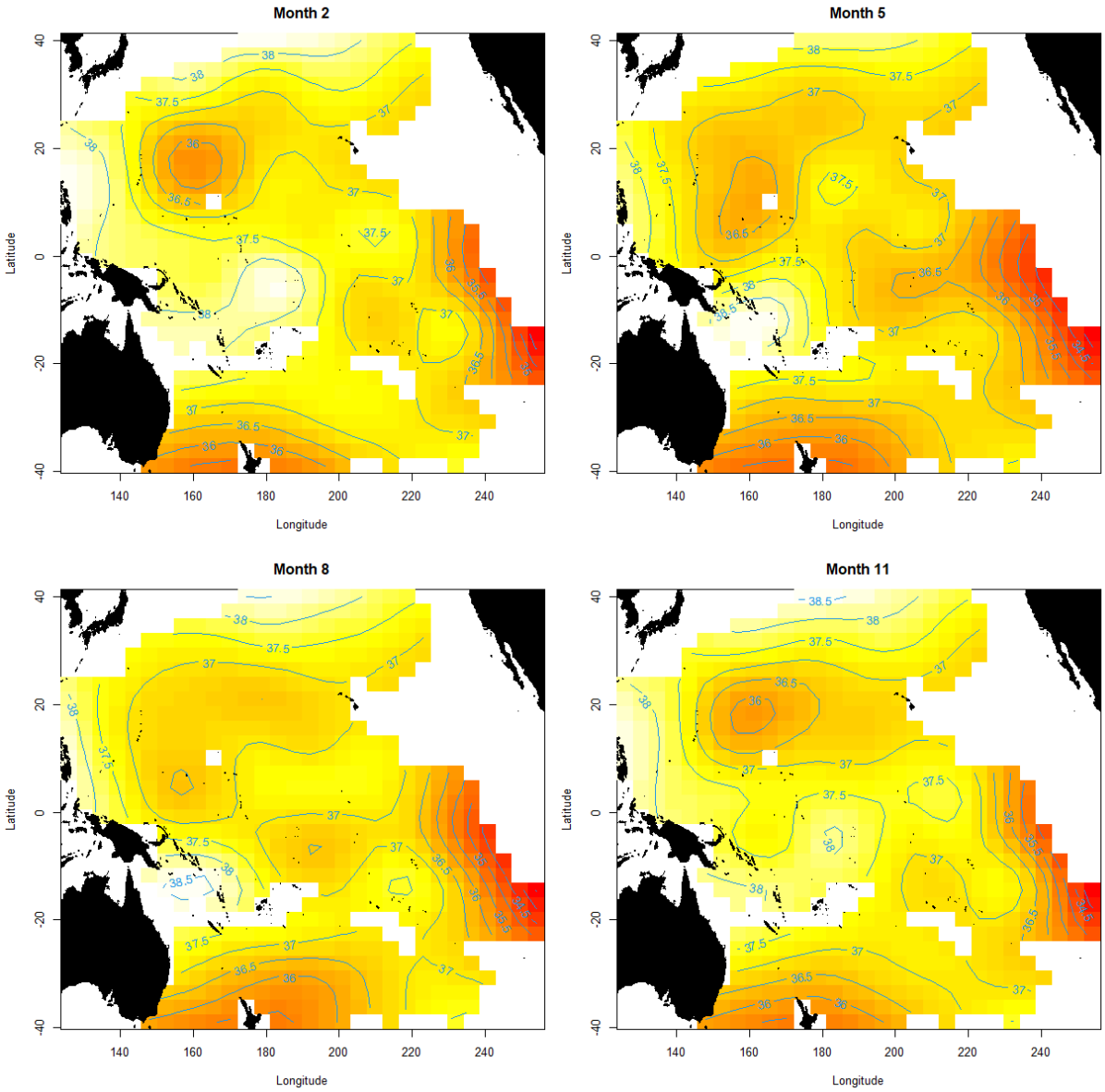

Figure 27: Predicted weight by location and month for length 130 cm caught using HBF of 20 at wave scale 2 in 2012, based on the best fitting model of data for females from 2015-2022.

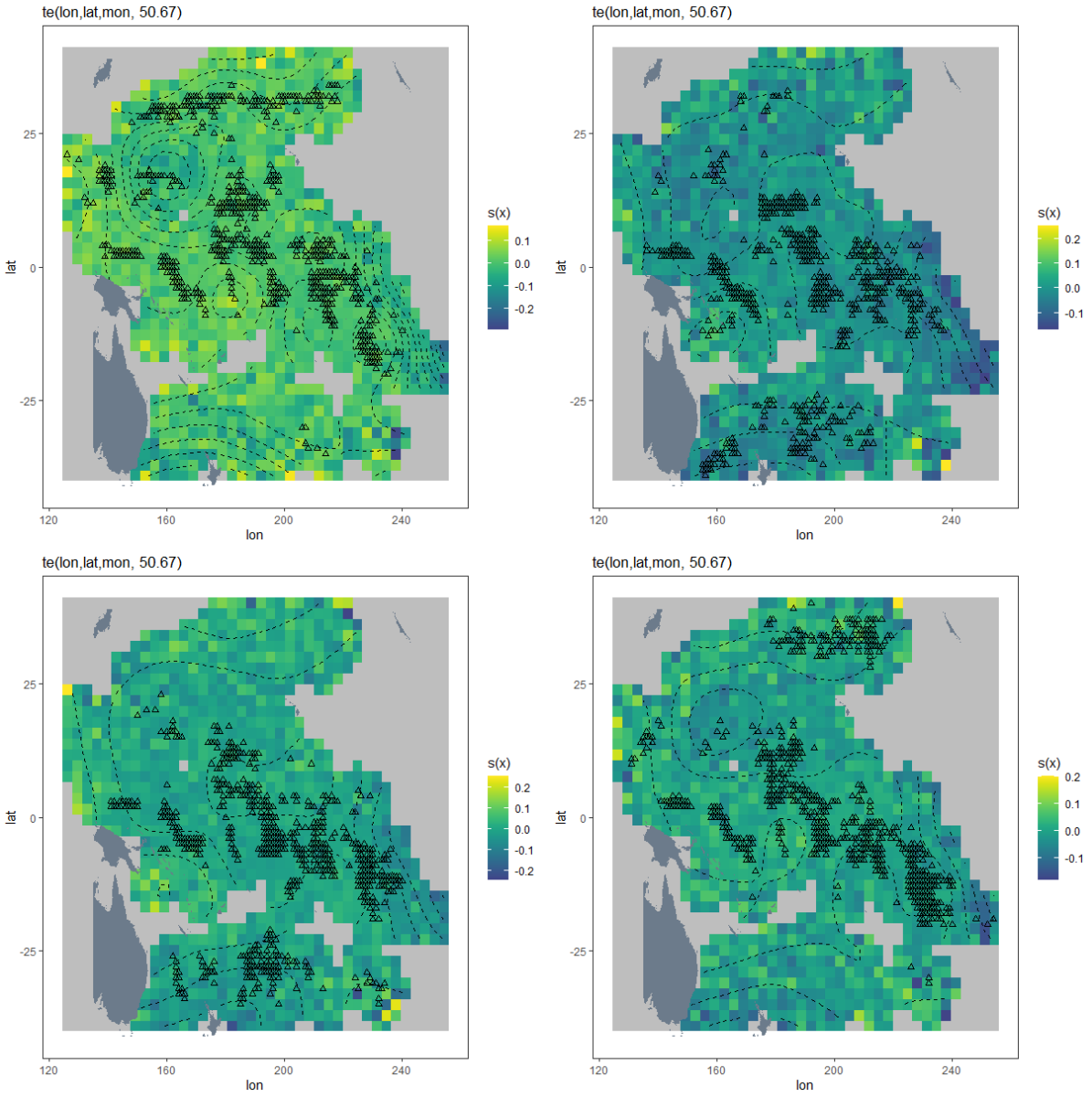

Figure 28: Effect plot by location and month (2, 5, 8, and 11) from the best fitting model of data for females from 2015-2022. The fitted effect is perturbed at each location by adding a random variable based on the local variance. Thus areas with more uncertainty appear more noisy. The triangles represent locations of observations closest to the month addressed by the plot.

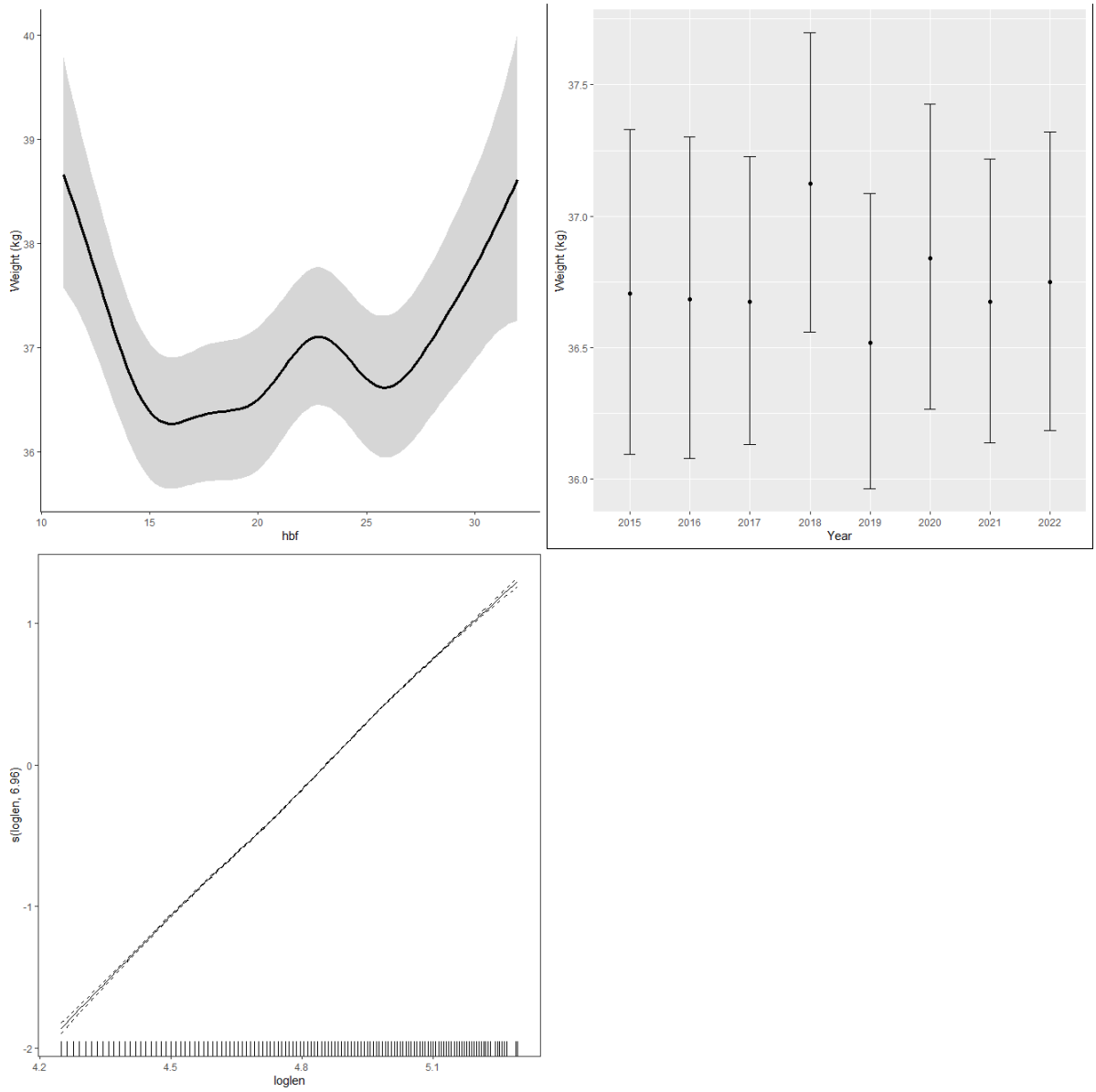

Figure 29: Predicted mean weight at length 130 cm by HBF (left), and year (right), based on the best fitting model of data for females from 2015-2022. In each case the variables latitude, longitude, month, and either hbf or year were excluded from the prediction, which resulted in the average effect being applied for these smooths. The partial effect of the log length smoother is shown at lower left.

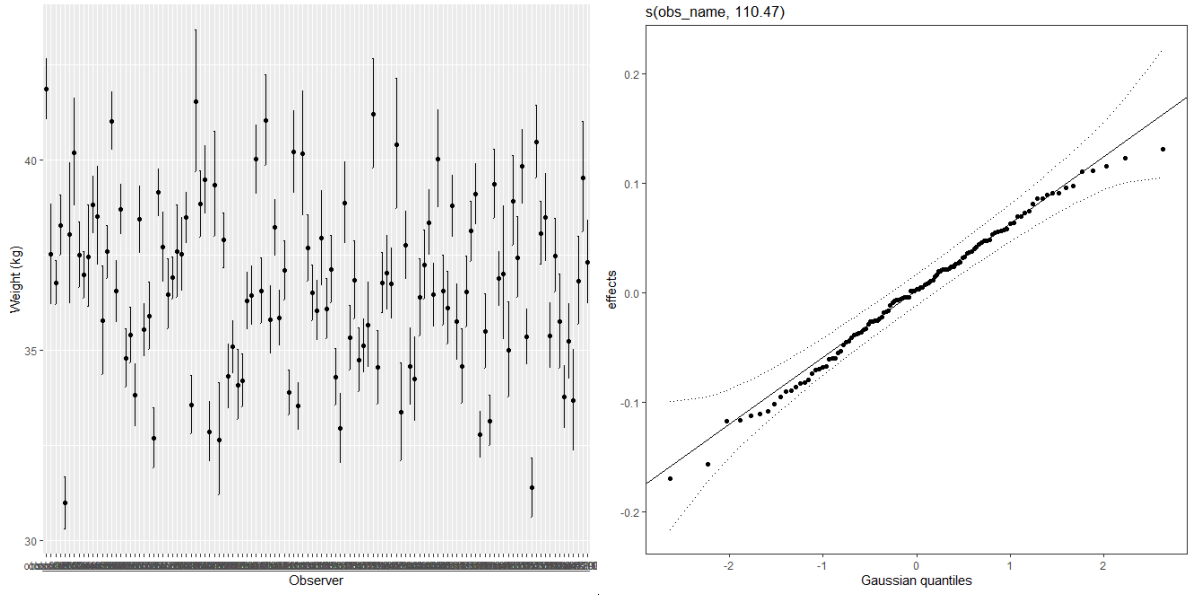

Figure 30: Predicted mean weight at length 130 cm by observer (left), based on the best fitting model of data for females from 2015-2022. In each case the variables latitude, longitude, month, hbf, and year were excluded from the prediction, which resulted in the average effect being applied for these smooths. The qq plot (right) shows the degree to which observer effects are normally distributed.

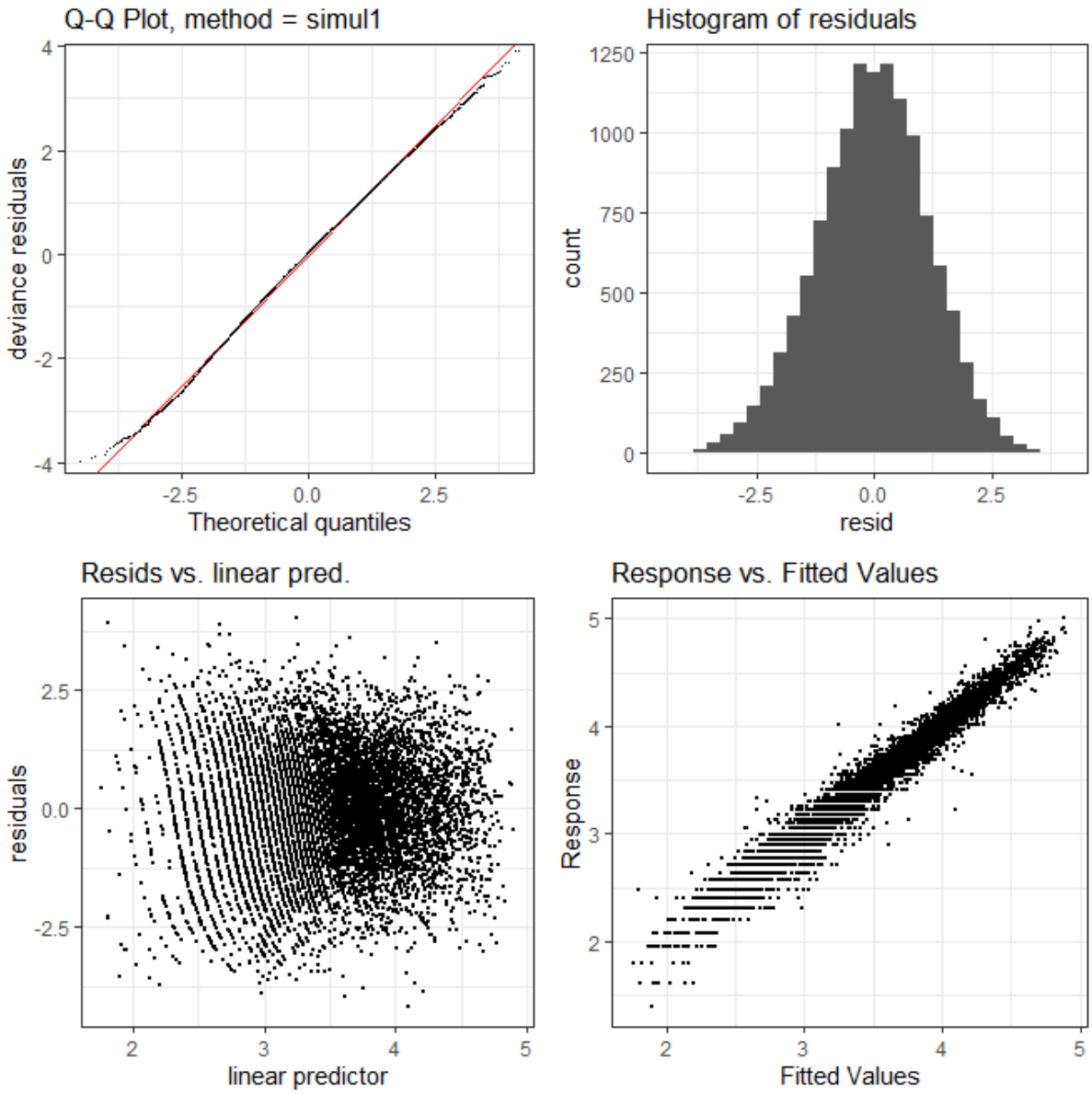

Figure 31: Diagnostic plots for best model of LW for males reported as process type RGT from 2015-2022.

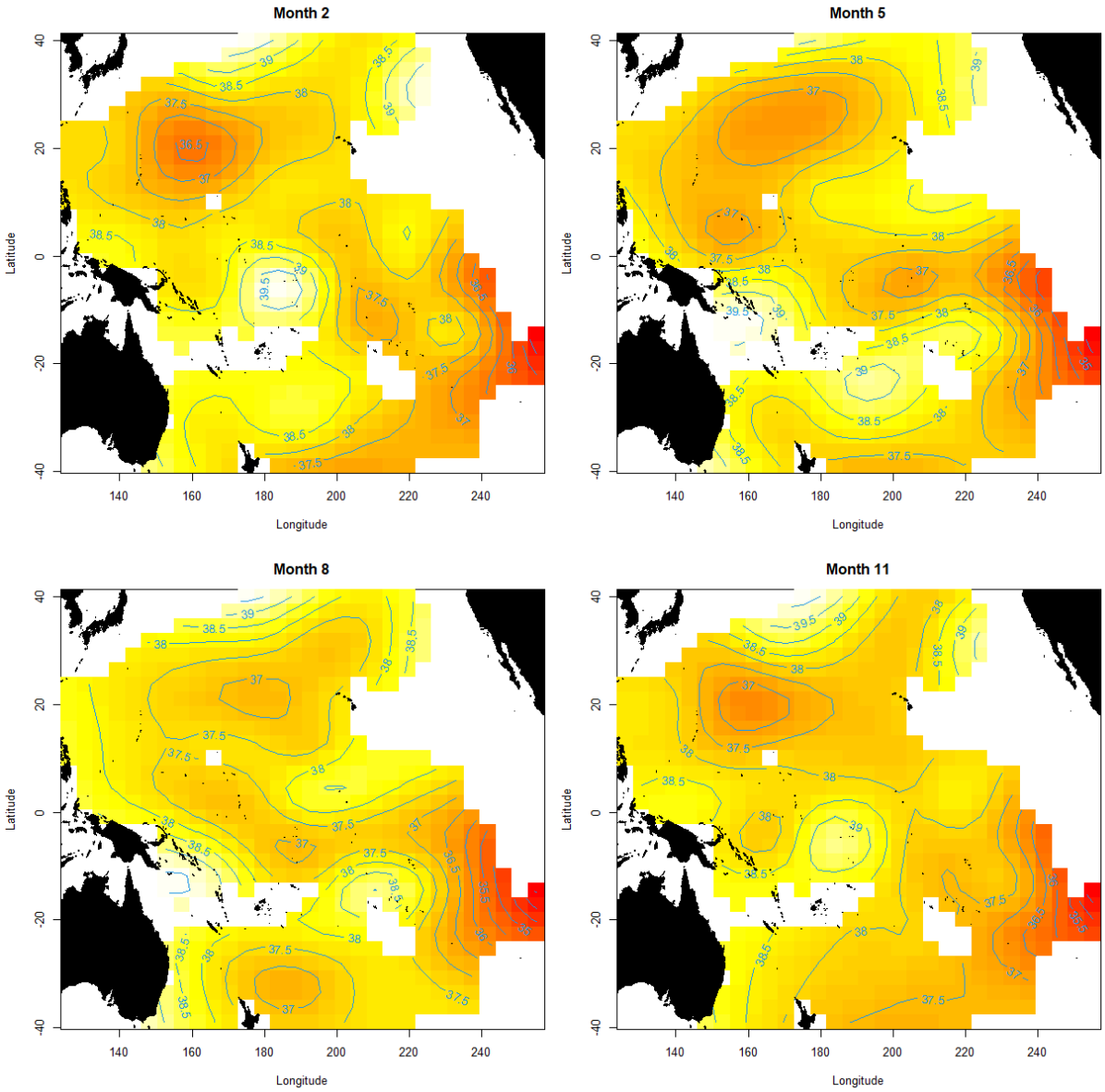

Figure 32: Predicted weight by location and month for length 130 cm caught using HBF of 20 at wave scale 2 in 2012, based on the best fitting model of data for males reported as process type RGT from 2015-2022.

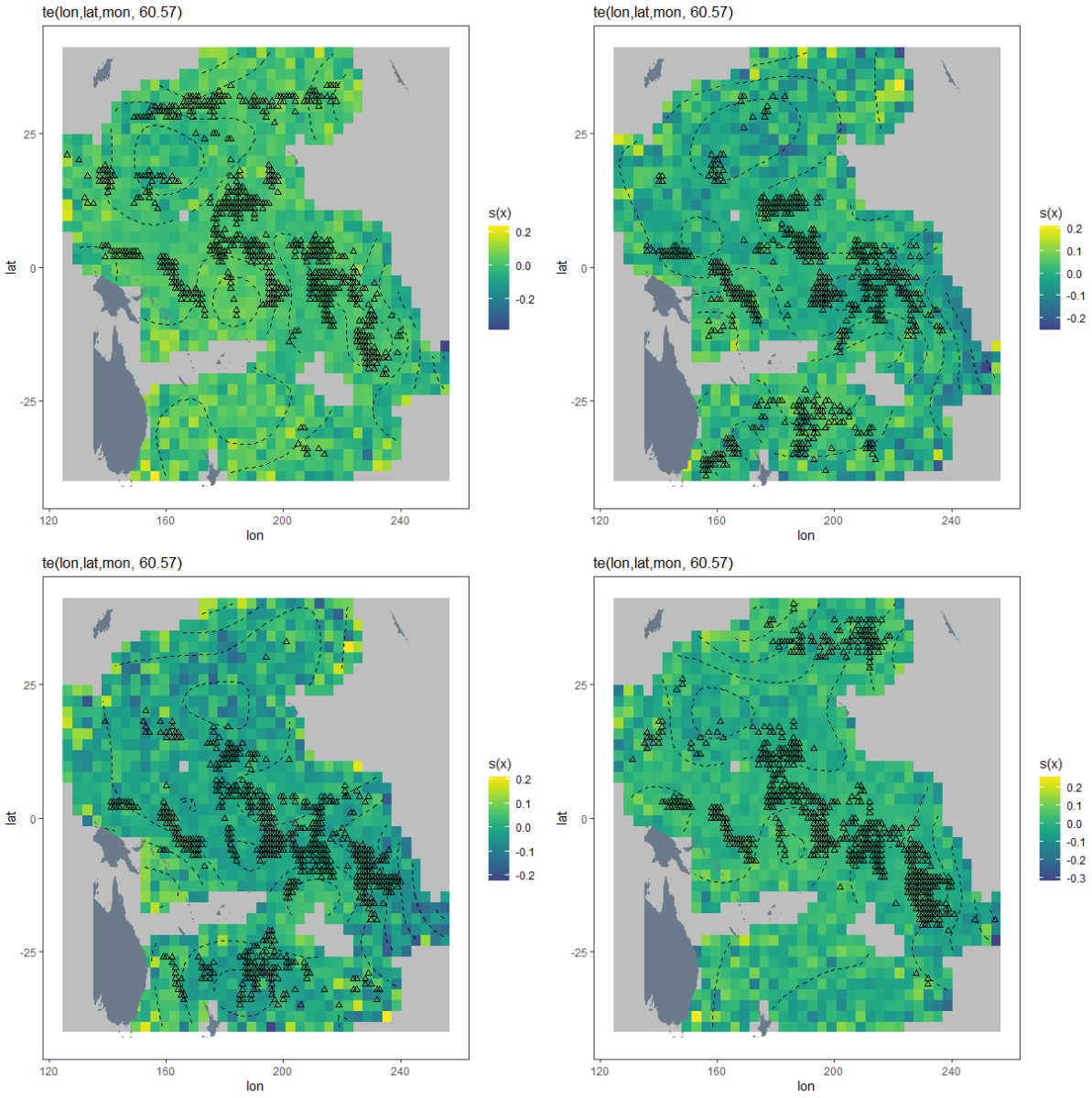

Figure 33: Effect plot by location and month (2, 5, 8, and 11) from the best fitting model of data for males reported as process type RGT from 2015-2022. The fitted effect is perturbed at each location by adding a random variable based on the local variance. Thus areas with more uncertainty appear more noisy. The triangles represent locations of observations closest to the month addressed by the plot.

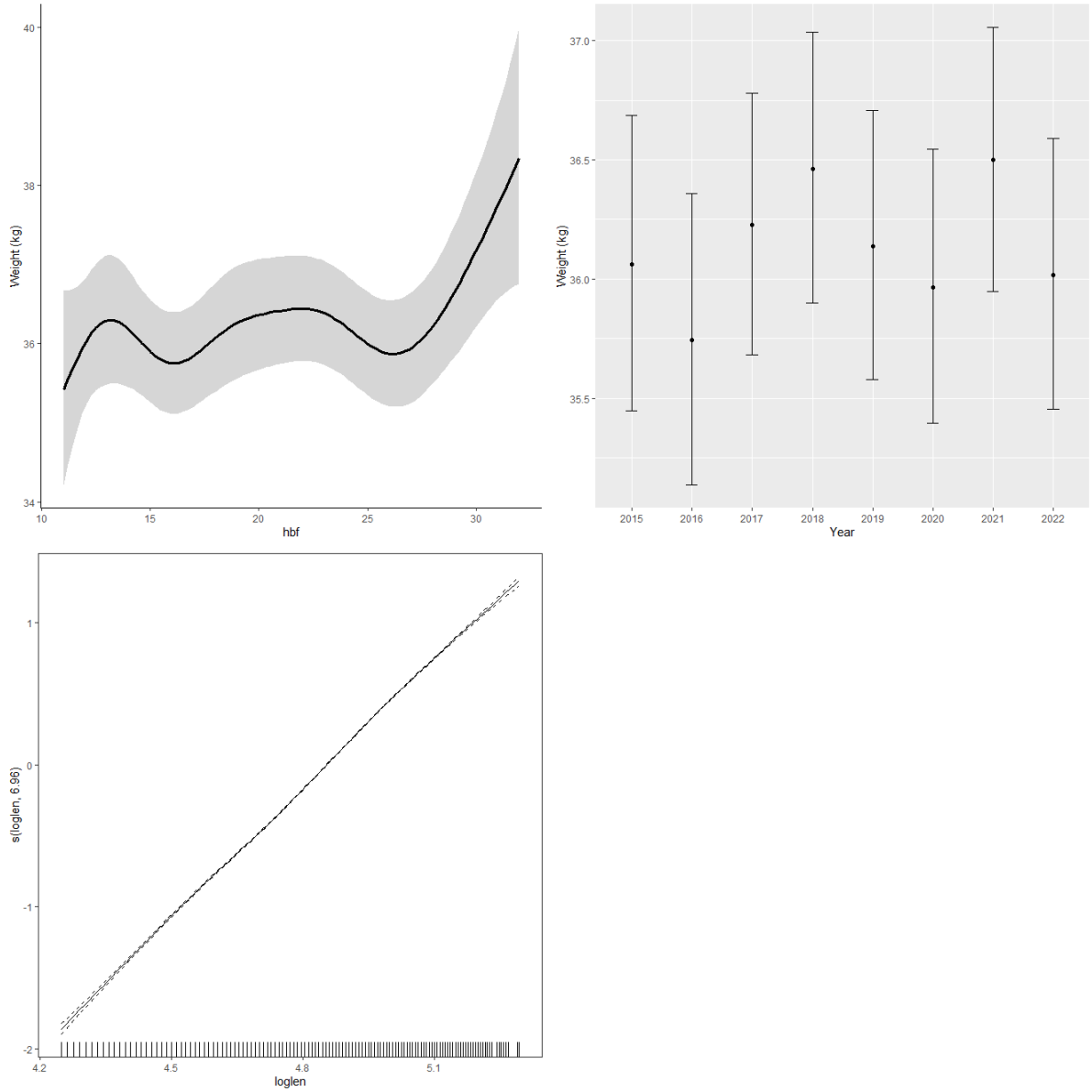

Figure 34: Predicted mean weight at length 130 cm by HBF (top left) and year (top right), based on the best fitting model of data for males reported as process type RGT from 2015-2022. In each case the variables latitude, longitude, month, and either hbf or year were excluded from the prediction, which resulted in the average effect being applied for these smooths. The partial effect of the log length smoother is shown at lower left.

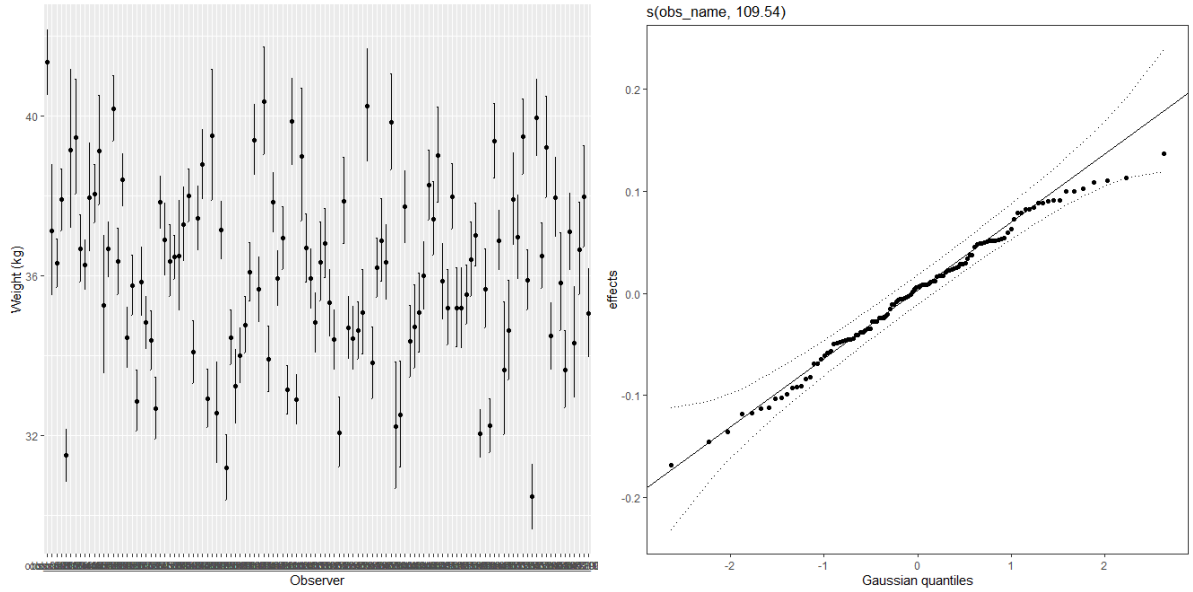

Figure 35: Predicted mean weight at length 130 cm by observer (left), based on the best fitting model of data for males reported as process type RGT from 2015-2022. In each case the variables latitude, longitude, month, hbf, and year were excluded from the prediction, which resulted in the average effect being applied for these smooths. The qq plot (right) shows the degree to which observer effects are normally distributed.

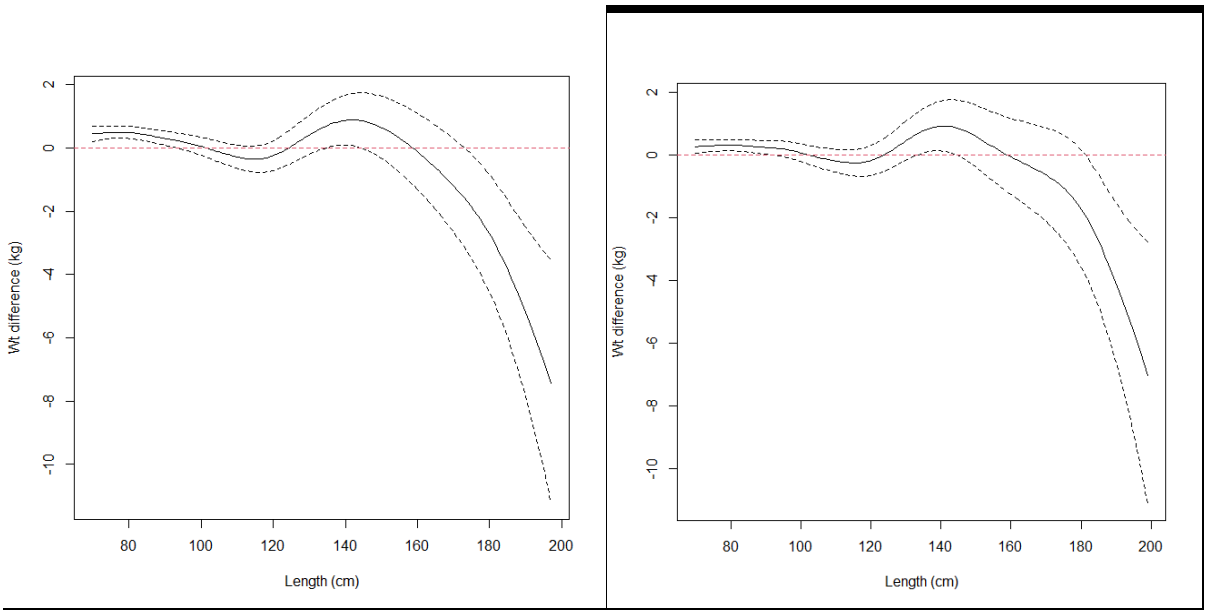

Figure 36: Comparison of predicted weights at length between the best fitting models for females (left) and males (right), and otherwise identical models that assumed a linear relationship between length and weight, based on data from fish reported as process type RGT from 2015-2022.

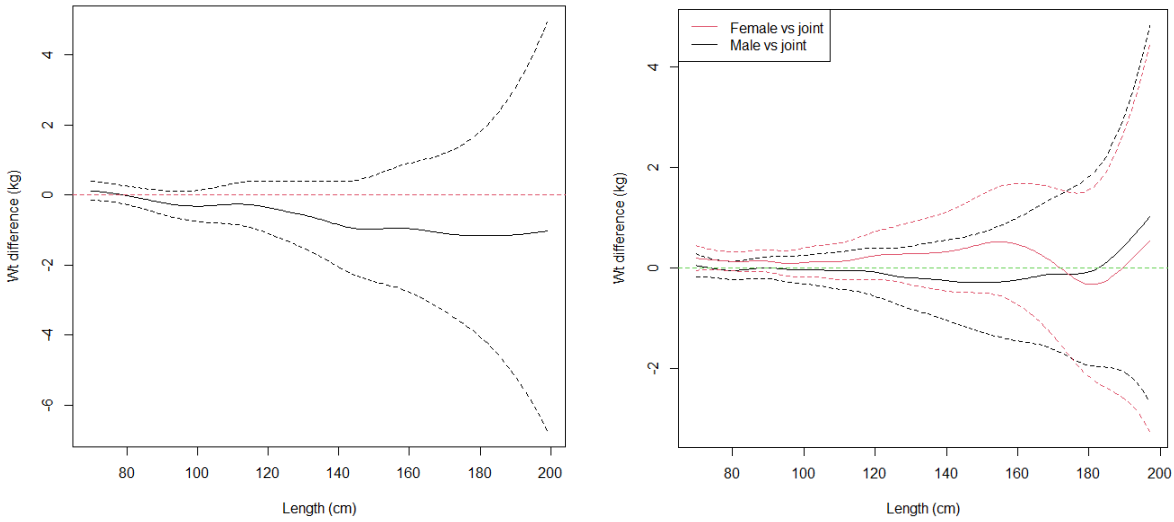

Figure 37: Comparisons of predicted weights at length from alternative models. Dashed lines represent 95% confidence intervals for individual predictions, but these should not be interpreted as confidence intervals on the differences.
1) Differences between models assuming residuals from the Gaussian versus the scaled-t distribution, showing the Gaussian model estimating lower weight at length (left). 2) Joint model versus individual models for males and females, based on data from 2015-2022 (right).

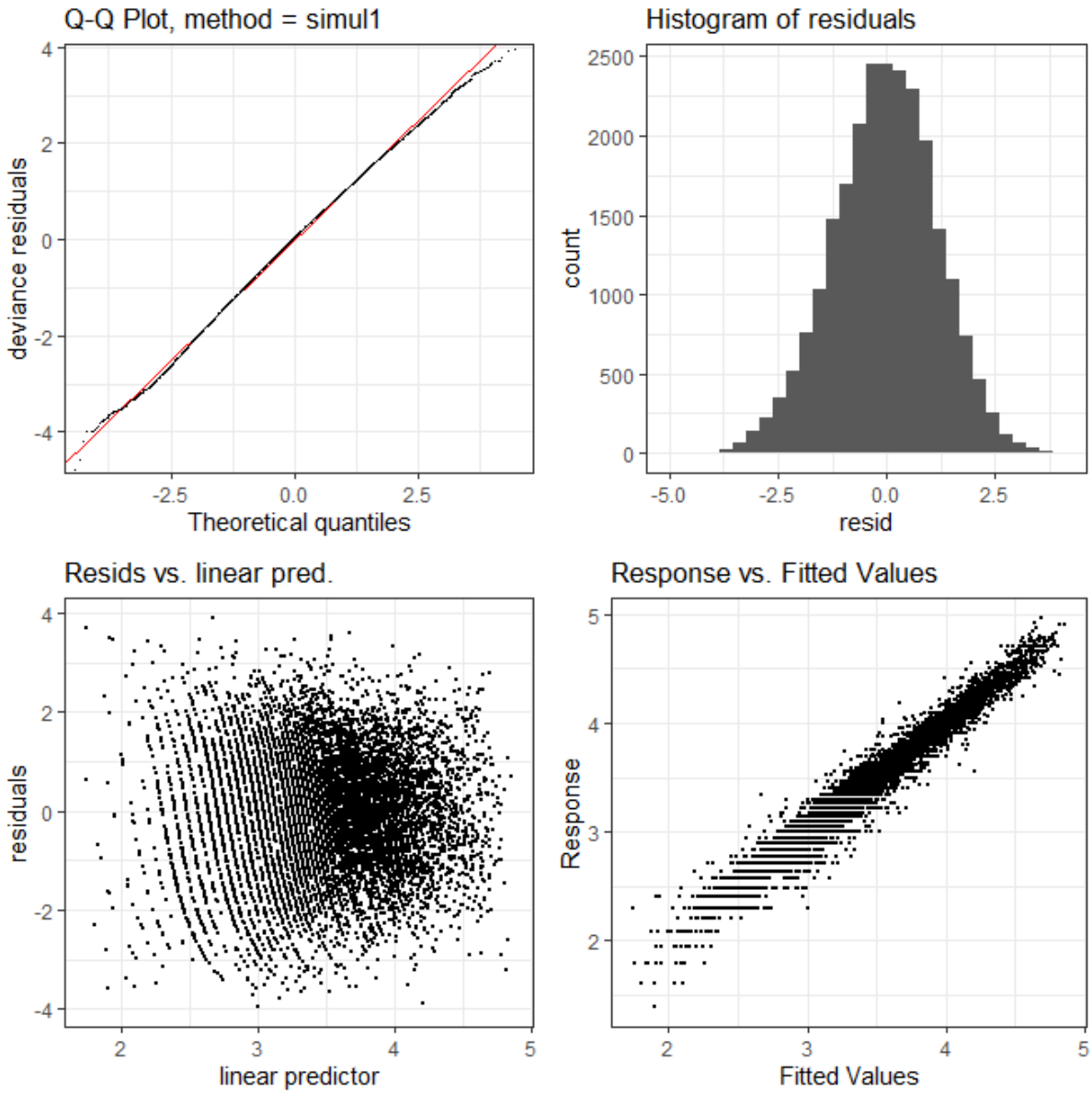

Figure 38: Diagnostic plots for best model of LW for a combined dataset of males and females reported as process type RGT from 2015-2022.

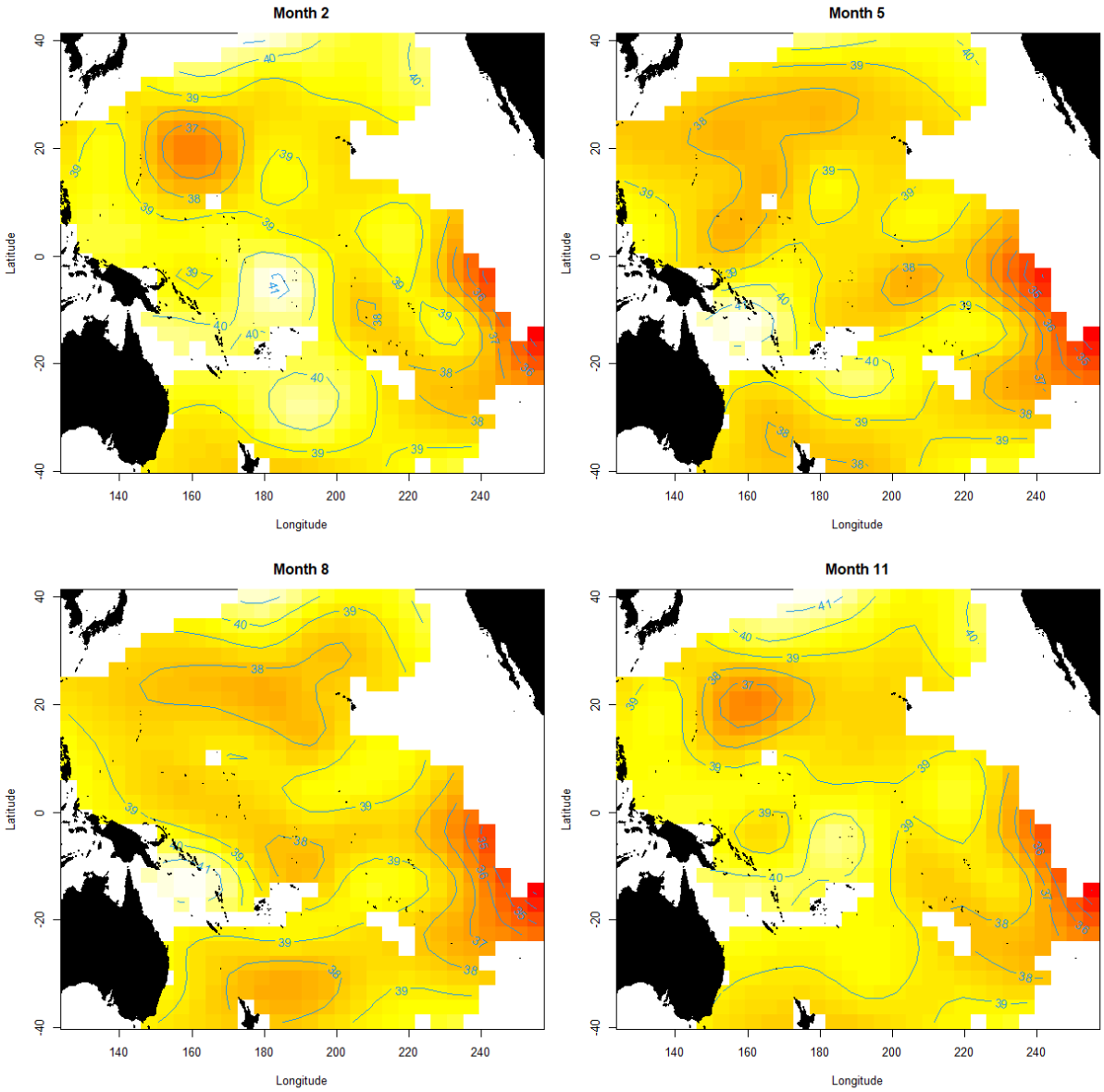

Figure 39: Predicted weight by location and month for length 130 cm caught using HBF of 20 at wave scale 2 in 2012, based on the best fitting model for a combined dataset of males and females reported as process type RGT from 2015-2022.

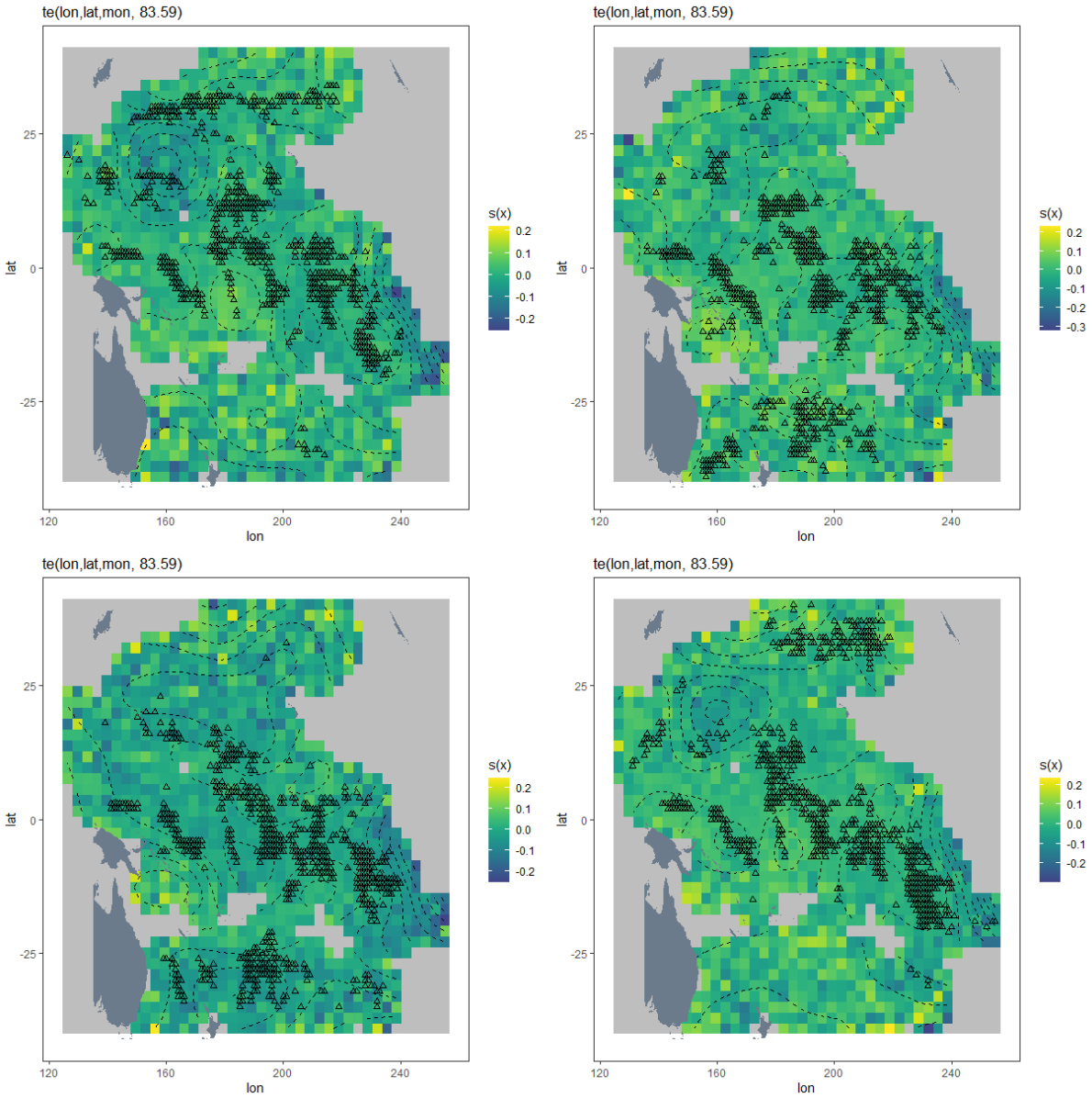

Figure 40: Effect plot by location and month (2, 5, 8, and 11) from the best fitting model to a combined dataset of males and females reported as process type RGT from 2015-2022. The fitted effect is perturbed at each location by adding a random variable based on the local variance. Thus areas with more uncertainty appear more noisy. The triangles represent locations of observations closest to the month addressed by the plot.

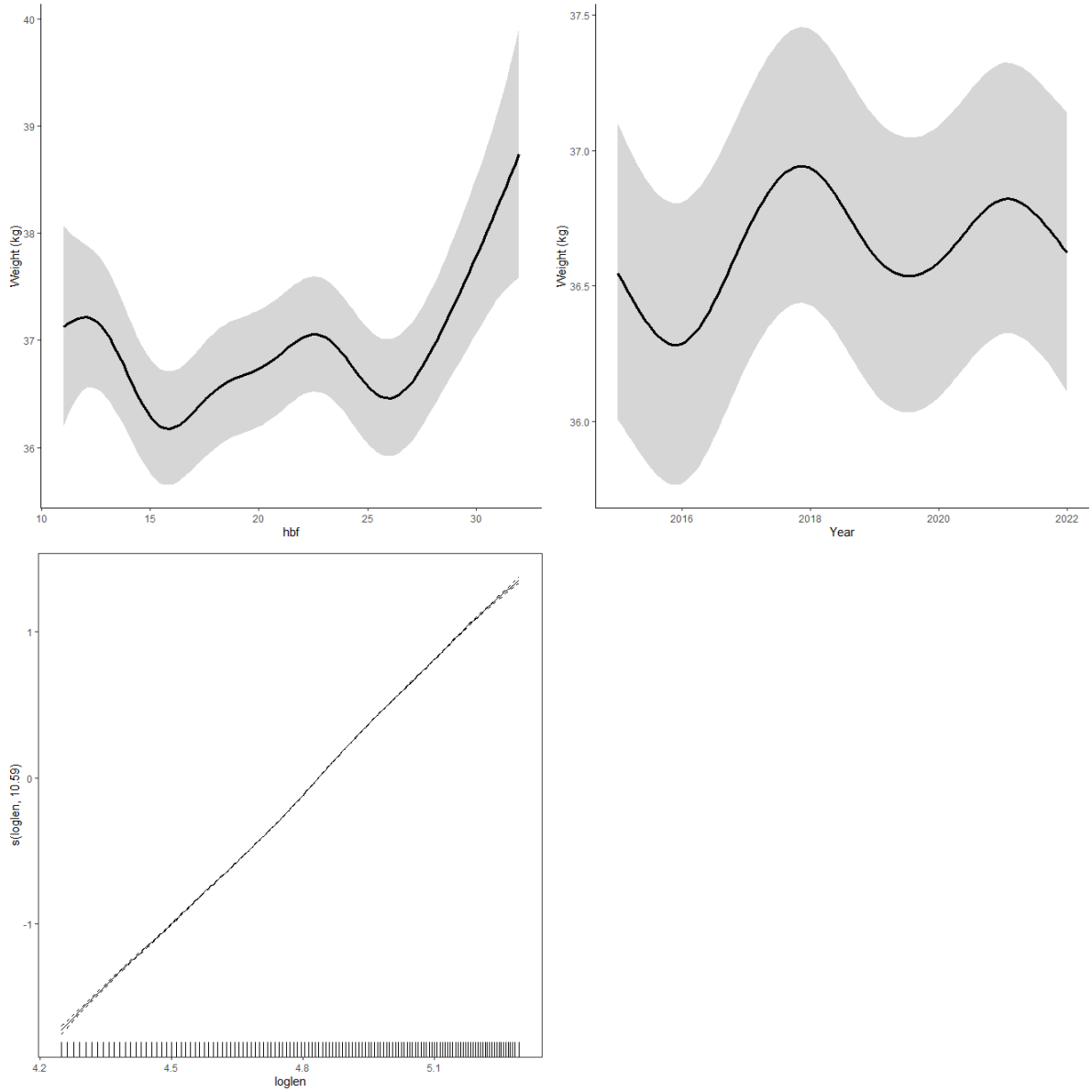

Figure 41: Predicted mean weight at length 130 cm by HBF (top left) and year (top right), based on the best fitting model for a combined dataset of males and females reported as process type RGT from 2015-2022. In each case the variables latitude, longitude, month, and either hbf or year were excluded from the prediction, which resulted in the average effect being applied for these smooths. The partial effect of the log length smoother is shown at lower left.

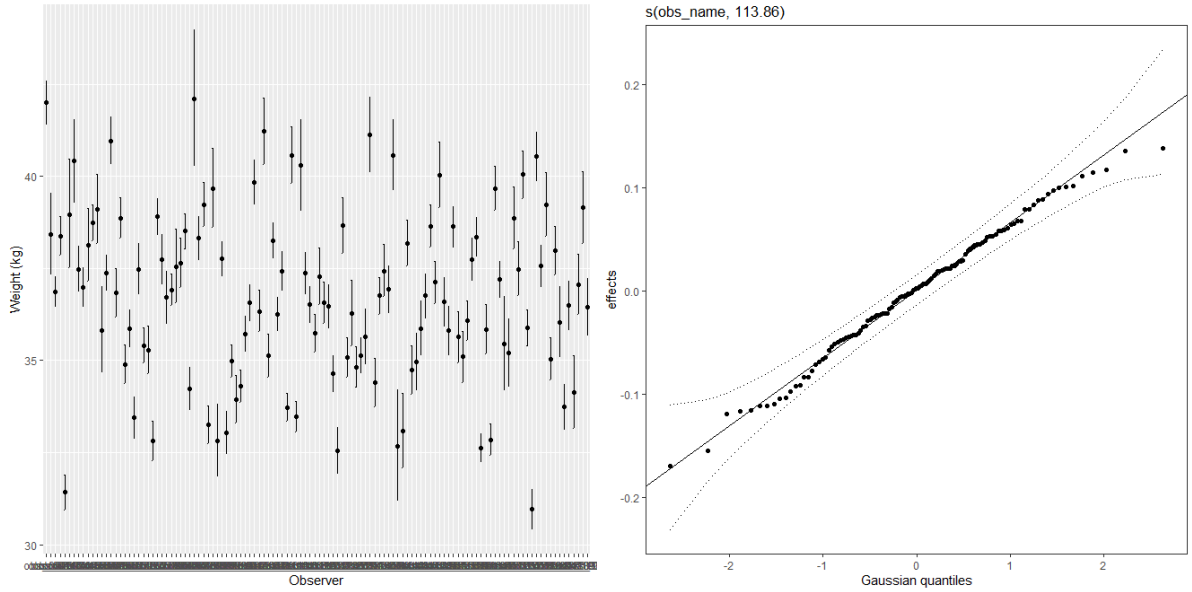

Figure 42: Predicted mean weight at length 130 cm by observer (left), based on the best fitting model to a combined dataset of males and females reported as process type RGT from 2015-2022. In each case the variables latitude, longitude, month, hbf, and year were excluded from the prediction, which resulted in the average effect being applied for these smooths. The qq plot (right) shows the degree to which observer effects are normally distributed.

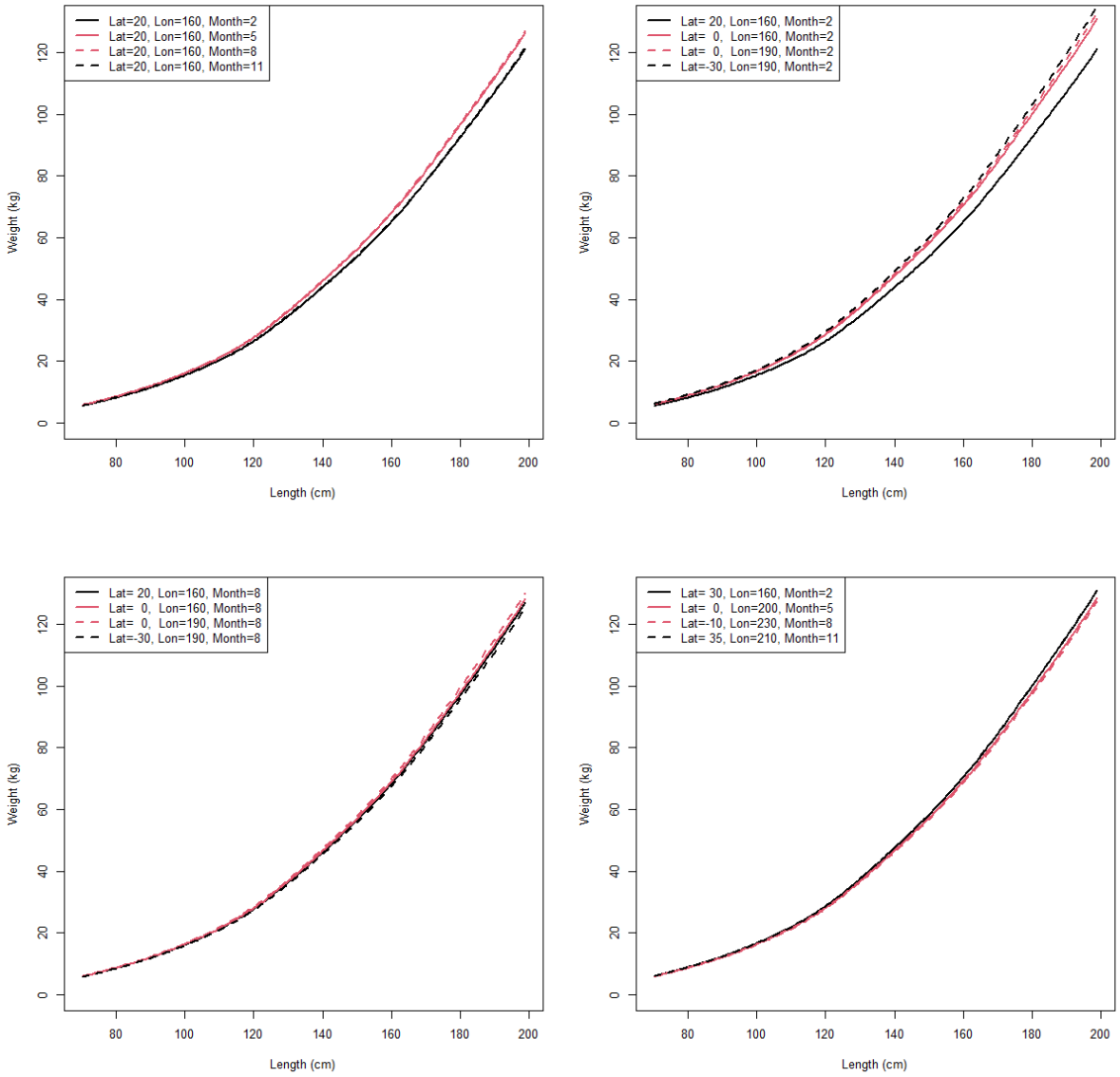

Figure 43: Predicted weight at length across a range of locations and months, based on the best fitting model to a combined dataset of males and females reported as process type RGT from 2015-2022. In each case the variables hbf, and year were excluded from the prediction, which resulted in the average effect being applied for these smooths.

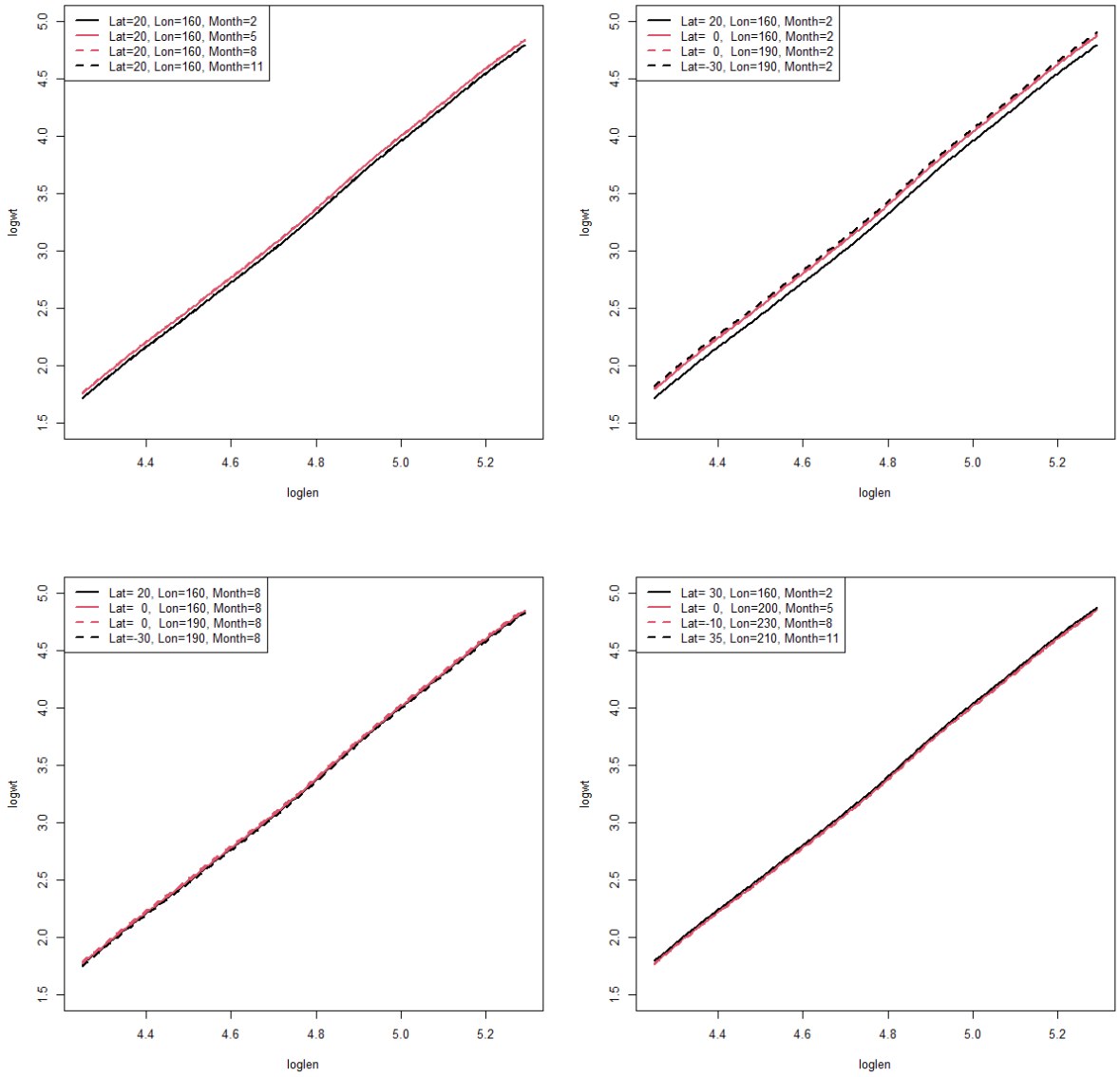

Figure 44: Predicted log(weight) at log(length) across a range of locations and months, based on the best fitting model to a combined dataset of males and females reported as process type RGT from 2015-2022. In each case the variables hbf, and year were excluded from the prediction, which resulted in the average effect being applied for these smooths.

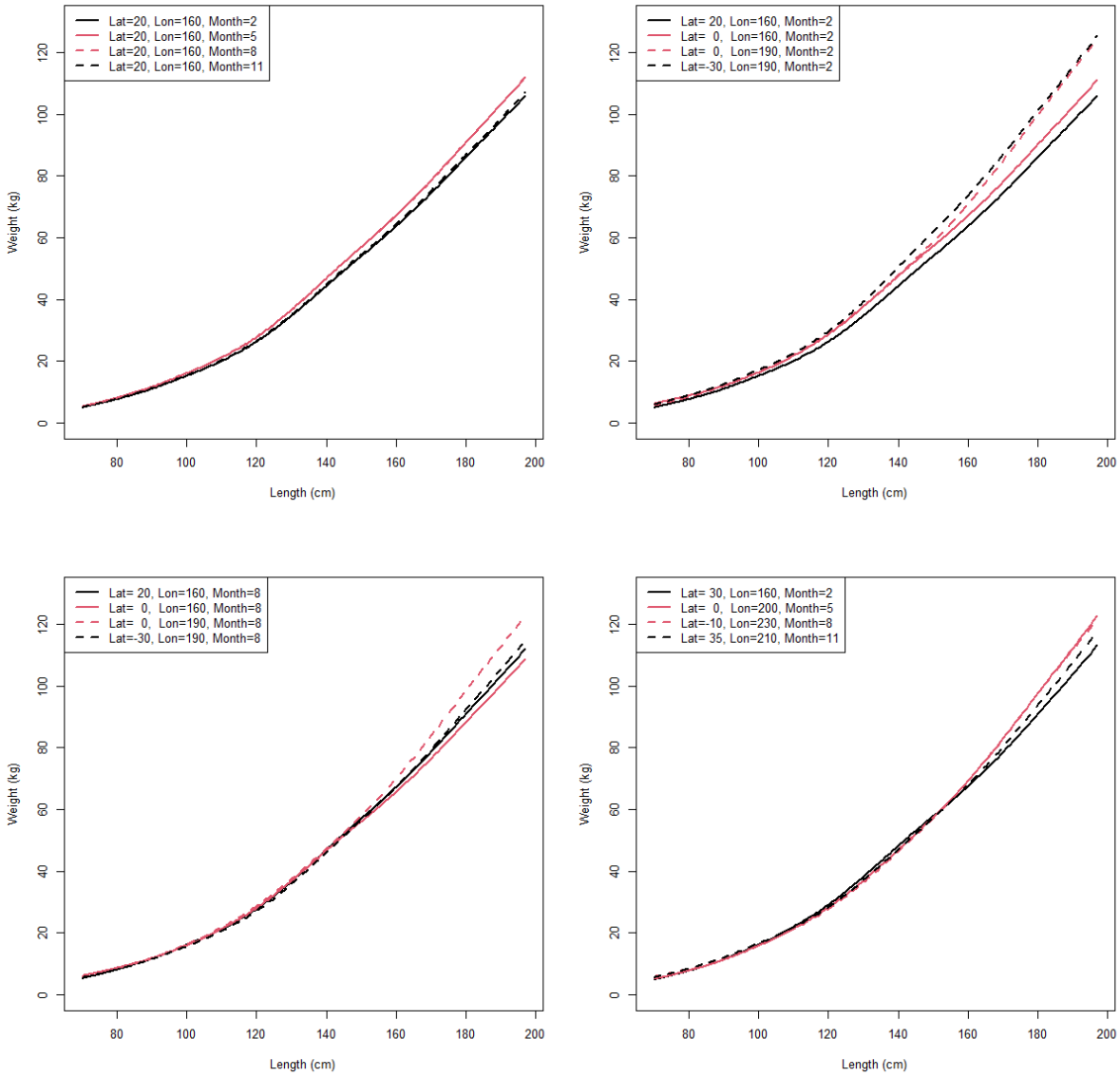

Figure 45: Predicted weight at length across a range of locations and months, based on a model with interactions between length and location and length and year, fitted to a combined dataset for females and males reported as process type RGT from 2015-2022. In each case the variables hbf, and year were excluded from the prediction, which resulted in the average effect being applied for these smooths.

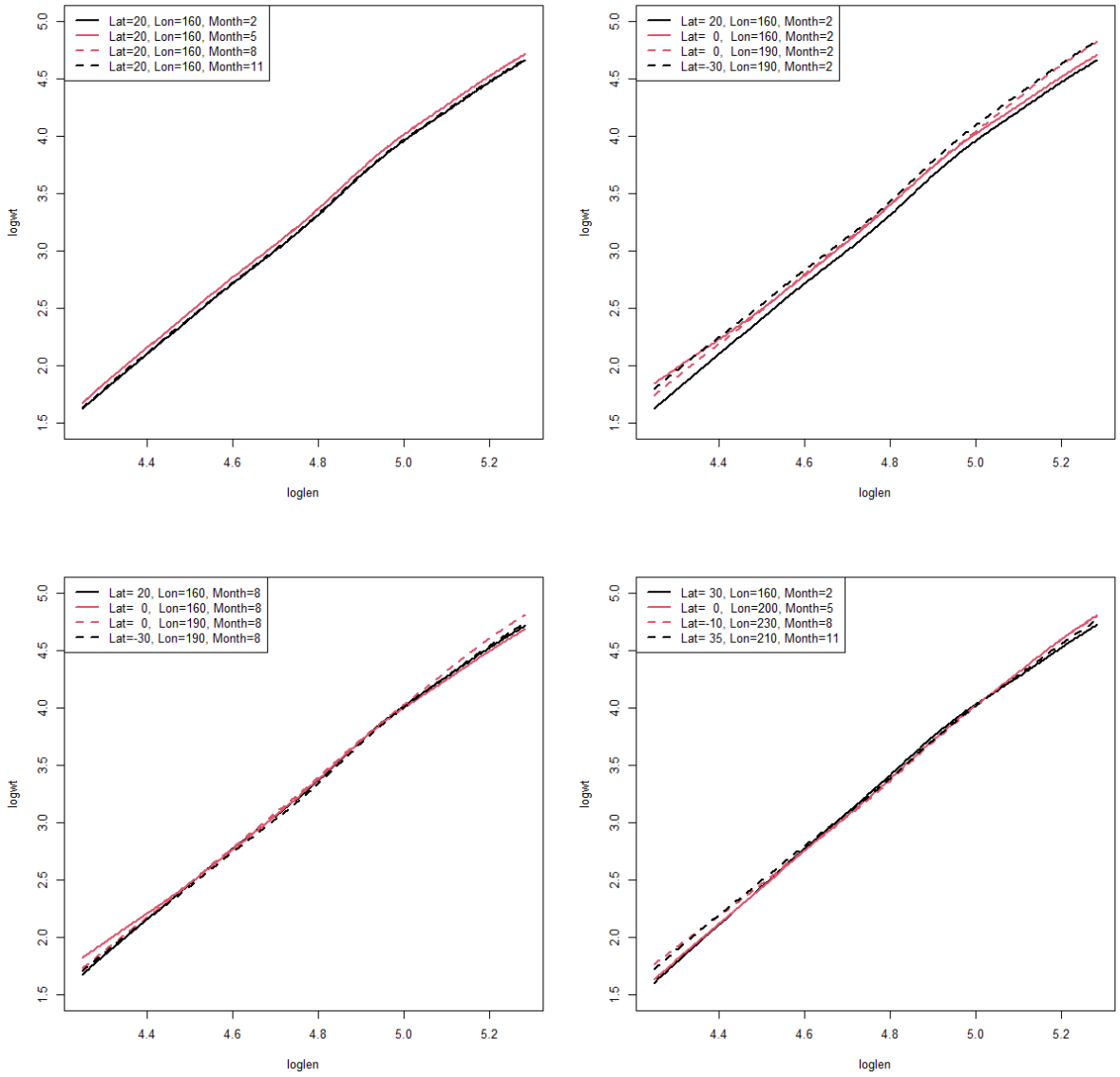

Figure 46: Predicted log(weight) at log(length) across a range of locations and months, based on a model with interactions between length and location and length and year, fitted to a combined dataset for females and males reported as process type RGT from 2015-2022. In each case the variables hbf, and year were excluded from the prediction, which resulted in the average effect being applied for these smooths.